IDENTIFICATION AND EVALUATION OF MOLECULAR BIOMARKERS IN URINE FOR THE DETECTION OF PROSTATE CANCER

PhD thesis presented by

Tamara Sequeiros Fontán

To obtain the degree of

PhD for the *Universitat Aut noma de Barcelona* (UAB)

PhD thesis done at the Research Unit in Biomedicine and Translational Oncology in the Vall d"Hebron Research Institute, under the supervision of Drs.

Andreas Doll, Marina Rigau Resina and Juan Morote Robles

Doctoral study in Cellular Biology; Universitat Aut noma de Barcelona, Faculty of Medicine, Department of Cellular Biology, Physiology and Immunology

Universitat Aut noma de Barcelona, 2014

Dr. Andreas Doll Dra. Marina Rigau Dr. Juan Morote

Tamara Sequeiros Fontán

This thesis has been supported by the grant “VHIR Predoctoral Fellowship (2013)” from “Vall d'Hebron Research Institute”.

This work was also supported in part with a grant for a short stay fellowship from “Ministerio de Ciencia e Innovación, Red Temática de Investigación Cooperativa en Cáncer” (RTICC), in VUmc Cancer Center Amsterdam, Amsterdam.

Finally, the financial support for the projects presented was granted by “Instituto de Salud Carlos III, Ministerio de Ciencia e Innovación” (FIS PI11/02486; FIS PI13/00173), by “Asociación Española Contra el Cáncer” (AECC-JB-2011-03; AECC-JB-2013), by “Fundación para la Investigación en Urología” (2011), and by the “Global Action on Urine-Based Detection of Biomarkers for Distinguishing Aggressive from Non-Aggressive Prostate Cancers” from Movember Foundation.

AGRADECIMIENTOS

Esta sección de la tesis es, generalmente, la primera (o única) que se lee pero la última que se escribe. O por lo menos en mi caso ha sido así. Mientras redactaba esta tesis me iba dando cuenta de la cantidad de personas que han colaborado, contribuido, aconsejado… o simplemente estado a mi lado o dejado huella en algún punto de mi desarrollo como científica y como persona. Esta lista es probablemente demasiado larga como para nombrarlos a todos, pero intentaré hacerlo lo mejor que pueda.

Por supuesto, la primera alusión ha de ser para mis directores. A vosotros, gracias por creer en mí y por darme la oportunidad y los medios necesarios para llevar a cabo este proyecto.

Me gustaría hacer una mención especial para Marina, que además guiarme en cuestiones de ciencia me ha dado infinitas lecciones de optimismo y de motivación para hacer un trabajo bien hecho.

Tampoco me puedo olvidar del equipo de clínicos del Servicio de Urología del Hospital Vall d'Hebron, así como de los patólogos, auxiliares y enfermeras, que han hecho posible el contacto con los pacientes y la recogida de muestras.

Como cualquiera que se dedique a la investigación sabrá, durante la realización de una tesis doctoral el laboratorio pasa a convertirse en tu segunda casa (¡y a veces casi parece que en la única!). Por eso, por hacer de estas cuatro paredes un lugar en el que me gusta estar, por haber compartido penas y glorias, lágrimas, frustraciones y muchas risas, quiero darle las gracias a las chicas que me han acompañado en este camino: Tati, Lucía, Irene, Elena, Blanca, Laura, Melánia, Eva, Mireia… También a mis ex-compis de oficina Marta y Núria, ¡os he echado de menos! Y a Tuğçe, que aunque hace tiempo que cambió de rumbo, nada de esto habría sido lo mismo sin ella.

Gracias al Dr. Michiel Pegtel, por acogerme como parte de su equipo y guiarme durante mi estancia. Gracias también a Rubina, Frederik, Niala, Monique y Danijela, por hacerme sentir como en casa, por vuestros consejos, y por todos los buenos ratos dentro y fuera del laboratorio.

También a todos los demás colaboradores que han participado en este proyecto. Especialmente a Alex Campos y Cristina Chiva por la gran labor de análisis de datos con la que han contribuido a la realización de esta tesis.

Por último, pero no menos importante, a todas las personas que, ajenas al ámbito laboral, han estado a mi lado durante esta etapa de mi vida. A los amigos que he encontrado en Barcelona y han hecho que mi paso por esta ciudad fuera todo lo que soñé y más; especialmente a Miguel y a Jose, que han aguantado todos mis desquicios sin rechistar, ¡nos vemos chicos! Por supuesto a mi familia, que aunque en la distancia, siempre han estado ahí para darme ánimo y para cebarme a base de marisco y otros manjares una vez cada seis meses; con mención especial a Diana, por su ayuda con la portada y por aguantar todas mis quejas. Y a Thijs, que es quizá el que más ha escuchado una y otra vez mis batallitas de laboratorio, gracias por tu apoyo y por hacerme ver cada día que siempre hay un motivo para sonreír.

Gracias a todos y todas.

Y ahora, ¡a leer el resto de la tesis!

INDEX

ABREVIATIONS

ADT - Androgen deprivation therapy

AFS - Anterior fibromuscular stroma

AJCC - American Joint Committee on Cancer

AMACR - Alpha-methylacyl-CoA racemase

ANXA - Annexin

AR - Androgen receptor

AUC - Area under the curve

AuTf - Colloidal gold-conjugated transferring

BPH - Benign prostatic hyperplasia

BRCA1 - Breast cancer 1

BRCA2 - Breast cancer 2

CAPB - Cancer of the Prostate and Brain

CDH1 - Cadherin 1, Type 1, E-Cadherin (Epithelial)

CRPC - Castration-resistant prostate cancer

CZ - Central zone

DRE - Digital rectal examination

DTT - Dithiothreitol

EAU - European Association of Urology

EGFR - Epidermal growth factor receptor

ELV - Exosome-like vesicle

EM - Electron microscopy

ENO1 - Alpha-enolase

EPCA - Early prostate cancer antigen

ERG - V-Ets avian erythroblastosis virus E26 oncogene homolog

ESCRT - Endosomal sorting complex required for transport

EV - Extracellular vesicle

FASN - Fatty acid synthase

FASP - Filter-aided sample preparation

FDA - Food and Drug Administration

fPSA - Free PSA

GOLM1 - Golgi membrane protein 1

H&E - Hematoxylin and eosin

HER2 - Epidermal growth factor receptor type 2

HGPIN - High grade prostatic intraepithelial neoplasia

HOXB13 - Homeobox B13

HPC1 - Hereditary Prostate Cancer 1

HPC20 - Prostate Cancer, Hereditary, 3

HPCX - Hereditary Prostate Cancer, X-Linked

HSP - Heat shock protein

ILV - Intraluminal vesicle

ISUP - International Society of Urological Pathology

ITGA3 - Integrin α3

ITGAV - Integrin αV

ITGB1 - Integrin β1

ITGB3 - Integrin β3

IUCC - International Union for Cancer Control

KLK3 - Kallikrein-3

LC - Liquid chromatography

LGPIN - Low grade prostatic intraepithelial neoplasia

MART-1 - Melanoma antigen recognized by T-cells 1

miRNA - microRNA

MRI - Magnetic resonance imaging

MS - Mass spectrometry

MV - Microvesicle

MVB - Multivesicular body

ncRNA - non-coding RNA

NTA - Nanoparticle tracking analysis

NUDT2 – Bis(5'-nucleosyl)-tetra-phosphatase [asymmetrical]

PAHs - Polycyclic aromatic hydrocarbons

PAP - Prostatic acid phosphatase

PB - Prostate biopsy

PCa - Prostate cancer

PCA3 - Prostate cancer antigen 3

PCAP - Predisposing for Cancer of the Prostate

PCBs - Polychlorinated biphenyls

PDCD6IP - Programmed cell death 6-interacting protein (Alix)

PGR - Periurethral glandular region

PHI - Prostate health index

PIA - Proliferative inflammatory atrophy

PIN - Prostatic intraepithelial neoplasia

PSA - Prostate-specific antigen

PSADT - PSA doubling time

PSAV - PSA velocity

PSGR - Prostate specific G-coupled receptor

PSMA - Prostate specific membrane antigen

PTOV1 - Prostate Tumor Overexpressed 1

PZ - Peripheral zone

qPCR - Quantitative PCR

ROC - Receiver operating characteristic

RP - Radical prostatectomy

RT - Radiation therapy

RTqPCR - Real time quantitative PCR

SCIN - Adseverin

SEER - Surveillance, Epidemiology, and End Results

SPINK1 - Serine protease inhibitor Kazal-type 1

SRM - Selected reaction monitoring

TEM - Transmission electron microscopy

TGM4 - Transglutaminase 4

THP - Tamm-Horsfall protein

TMPRSS2 - Transmembrane protease, serine 2

TNM - Tumour, node and metastasis

TRUS - Transrectal ultrasound

TSG101 - Tumor susceptibility gene 101

TURP - Transurethral resection of the prostate

TZ - Transition zone

WHO - World Health Organization

XPO1 - Exportin-1

INTRODUCTION

1 The prostate

1.1 Anatomy, morphology and function

The prostate gland belongs to the male reproductive system and is located in the subperitoneal compartment. It is positioned posterior to the symphysis pubis, anterior to the rectum, and inferior to the urinary bladder. Classically described as “walnut-shaped”, it is conical in shape and surrounds the proximal urethra as it exits from the bladder (Figure 1) (1).

In adult humans, the prostate is a small gland with ductal-acinar histology that lacks discernible lobular organization. During the 19th and part of 20th century, it was generally assumed that the prostate gland was composed of diverse lobes, by analogy with laboratory animals, even though no distinct lobes can be seen in the human (3). In his classic work, McNeal conceptualized the prostate as divided into distinct

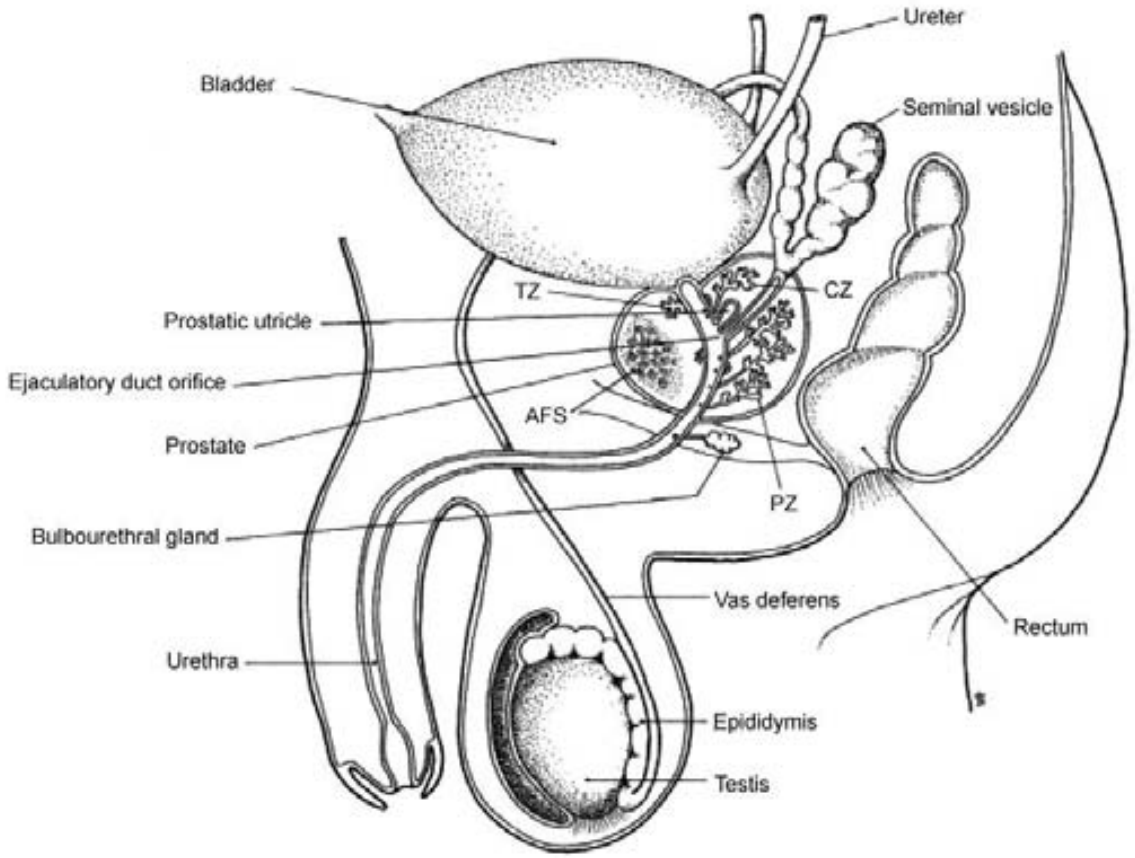

Figure 1. Schematic illustration of the anatomical position of the human prostate and associated structures. Adapted from (2).

morphological regions or zones, instead of lobes (4,5). The current and most widely accepted anatomical model of the prostate, in which this is divided into 4 zones, was eventually established in the early 1980s (6). According to this model, the anterior or ventral aspect of the gland, called anterior fibromuscular stroma (AFS), is almost entirely fibromuscular, while the glandular region occupies the posterior part of the tissue and surrounds the ejaculatory ducts as they enter the urethra. This glandular region can be divided in three zones: the peripheral zone (PZ), the central zone (CZ), the transition zone (TZ) (2,6).

Nearly 75% of the normal prostate gland is occupied by the PZ. It forms a disc of tissue that almost surrounds the prostate, forming a horseshoe shape with its thickest region at the back (7). The CZ constitutes 25% of the gland and is located behind the proximal prostatic urethra, surrounding the ejaculatory ducts. The TZ, which makes up approximately 5-10% of the prostate tissue, is located in the inner part of the prostate gland, surrounding the urethra. Both the PZ and TZ are derived from the urogenital sinus, while the histologically distinct CZ originates from the mesonephric duct (8). Some authors consider a last anatomically discrete area within the glandular prostate, called periurethral glandular region (PGR), representing less than 1% of the total volume of the gland (9). Nevertheless, nowadays it is mostly acknowledged as part of the TZ (3) (Figure 2).

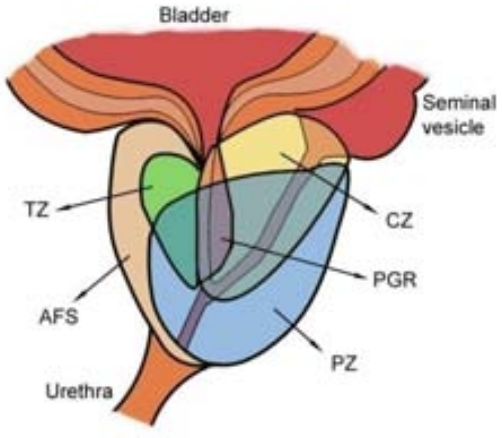

Figure 2. Anatomic representation of the prostate, indicating the location of MacNeal"s four zones AFS, TZ, PZ and CZ, as well as the PGR.

The significance of the described architecture is based upon the relationship of these glandular zones to prostatic disease (10). The TZ is the site of development of benign prostatic hyperplasia (BPH), whereas the PZ is where both prostatitis and prostate cancer (PCa) mainly occur (6). Today, McNeal"s CZ is considered merely a nonclinical curiosity, but it is clearly demonstrable both histologically and in whole-mount coronal section of the prostate using special stains to enhance duct-acinar architecture. On

sectioning of the prostate, this CZ is not readily grossly discernible or easily separable from the rest of the gland (11).

The histologic architecture of the prostate is that of a branched duct gland. Within the prostatic epithelium, there are diverse cell types that can be distinguished by their morphological characteristics, functional significance, and relevance for carcinogenesis. The cells that form this epithelium are arranged in two layers which line each gland or duct: a luminal secretory columnar cell layer and an underlying basal cell layer (Fig. 3) (12).

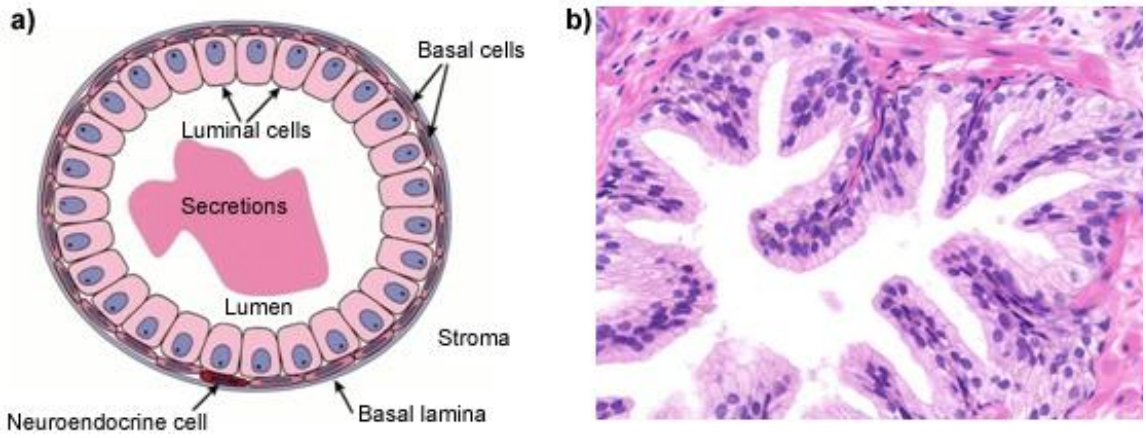

Figure 3. (a) Schematic depiction of the cell types within a human prostatic duct. Adapted from (10). **(b)** Hematoxylin & eosin stain of a normal prostate gland (image obtained from http://www.pathologyoutlines.com).

The predominant cell type is the secretory luminal cell, a differentiated androgen-dependent cell that produces and secretes prostatic proteins such as prostate-specific antigen (PSA) and prostatic acid phosphatase (PAP). This type of cells also expresses high levels of other characteristic markers such as the androgen receptor (AR) or the keratins 8 and 18 (13).

The second major epithelial cell type corresponds to the basal cells, which are found between the luminal cells and the underlying basement membrane, and which form a continuous layer in the human prostate. These cells conform the proliferative compartment of the normal prostatic epithelium and probably are involved in the epithelial renewal process (14). The basement membrane itself is a complex entity made up of a number of different structural proteins, adhesion molecules, and growth factors, and as such it provides a barrier between the epithelial layer and the underlying stroma (15).

Finally, the third prostatic epithelial cell type is the neuroendocrine cell, a minor population of uncertain embryological origin, which is believed to provide paracrine signals that support the growth and differentiation of luminal cells, among which they are located (10,16).

The prostate gland plays an important role in male reproduction. This organ is a fibromuscular exocrine gland that secretes a complex proteolytic fluid which constitutes one-third of the volume of the seminal fluid. In the prostatic secretions we can find enzymes, lipids, amines and metal ions essential for the normal function of spermatozoa (17).

1.2 Benign prostatic disorders

There are several benign diseases that can affect the prostate. They can be uncomfortable or painful but they are not life threatening, and they often can be treated with drugs or surgery. Accurate identification of these pathologies is central to a correct diagnosis and institution of therapy if necessary.

The most common benign conditions are discussed in this section, with the exception of high grade prostatic intraepithelial neoplasia (HGPIN). Due to its clinical significance and the relevance in the context of this thesis, it is discussed in its own section (section 2 of this introduction).

1.2.1 Benign prostatic hyperplasia

As previously commented, benign prostatic hyperplasia (BPH) is primarily found in the TZ. It begins its development as tiny glandular nodules that eventually coalesce, both in the smooth muscle stroma between the bladder and prostate and within the smooth muscle wall of the urethra (11).

Histologically, BPH is classically characterized by a mixed hyperproliferation of both stromal and epithelial elements to form nodules (Fig. 5). There are, however, individual variations, with some patients developing a predominantly stromal version of the disease and others showing mainly epithelial overgrowth. The luminal-to-basal cell relationship is retained in HBP, which is not considered to be a pre-malignant condition (18).

BPH is a highly prevalent disease, suffered by 80% of male population by age 80, severely affecting the quality of life. Men with BPH present with lower urinary tract

symptoms (due to bladder outlet obstruction) which include storage and voiding disorders (19).

The exact etiology of BPH is unknown; however, several mechanisms may be involved in the pathogenesis and progression of the disease. Aging is a well-established risk factor for the development of BPH. In ageing men, an interference in growth factors pathway occurs and a significant tissue-remodeling process takes place, leading to prostatic enlargement (20). It is also known that AR signaling plays a key role in development of BPH, and BPH tissue has higher dihydrotestosterone activity than normal prostate gland tissue (21). Blockade of this signaling decreases BPH volume and can relieve lower urinary tract symptoms, but the mechanisms of androgen/AR signaling in BPH development remain unclear, and the effectiveness of current drugs for treating BPH is still limited (22). Finally, in the last few years the role of prostatic inflammation as a crucial part of BPH pathogenesis and progression has emerged. Interestingly, it has been hypothesized that inflammatory infiltrate leads to tissue damage and to a chronic process of wound healing that might subsequently determinate prostatic enlargement (23).

Several strategies have been suggested in the past for the management of BPH. Currently, only α-blockers and 5-α-reductase (an enzyme responsible for the conversion of testosterone to 5-α-dihydrotestosterone) inhibitors are in clinical use (24), whereas transurethral resection of the prostate (TURP) remains the "gold standard" for surgical treatments (25).

In the last years, several minimal invasive treatments are emerging with promising outcomes. These techniques aim to obviate the complications of open surgery while ensuring durability of outcomes. As an example, laser-based prostatectomy for BPH causing obstruction has emerged over the past decade as a treatment alternative to TURP and open prostatectomy. Enucleation, which mimics open prostatectomy in that the whole prostate adenoma is removed, and vaporization, which involves ultra-rapid heating of superficial tissue layers and subsequent ablation, are the most often used surgical techniques in laser prostatectomy (26).

As personalized medicine continues to grow, the options for targeted therapy increase. Promising developments in the application of new techniques in genomics, proteomics and epigenetics, grant us the ability to risk stratify patients with symptomatic BPH, to identify those at higher risk of progression, and seek alternative therapies for those likely to fail conventional options (27).

1.2.2 Prostatitis

For reasons not fully understood, the prostate seems especially prone to chronic inflammation, and prostatitis is a common cause of visits to primary care physicians and urologists (28). Whatever the cause of the inflammatory process of prostatitis, once initiated, the disorder tends to become chronic in nature. Activation of complement and the involvement of macrophages are both central to this ongoing inflammatory process (18).

Chronic prostatitis affects the PZ more often than the other zones of the gland. This can be explained by the fact that urine might reflux into the prostatic ducts during micturition, being important both as a route of infection in bacterial prostatitis and as a cause of the inflammatory process in abacterial prostatitis (29).

In approximately 10% of the cases prostatitis is the result of a bacterial, chlamydial or other microorganism infection. For the remaining 90% of the cases, however, no definite etiological cause is usually identified (18). Various potential sources exist for the initial inciting event, when it is not a direct infection, including urine reflux inducing chemical and/or physical trauma, dietary factors, hormonal imbalances, or a combination of two or more of these factors (30).

Pain, predominantly in the groin or pelvic area, is the most common symptom of chronic prostatitis (31). Due to the generally unidentified etiological agent causing this condition, the optimal management for chronic prostatitis is unknown. Standard treatment usually consists of prolonged courses of antibiotics, even though well-designed clinical trials have failed to demonstrate their efficacy. Recent treatment strategies with some evidence of efficacy include: alpha-blockers, anti-inflammatory agents, hormonal manipulation, phytotherapy (quercetin, bee pollen), physiotherapy and chronic pain therapy (32).

There is emerging evidence that prostate inflammation may contribute to prostatic carcinogenesis. Chronic inflammation has been associated with the development of malignancy in several other organs such as esophagus, stomach, colon, liver and urinary bladder. Inflammation is thought to incite carcinogenesis by causing cell and genome damage, promoting cellular turnover, and creating a tissue microenvironment that can enhance cell replication, angiogenesis and tissue repair (33).

1.2.3 Proliferative inflammatory atrophy

The term proliferative inflammatory atrophy (PIA) was coined in 1999, to designate regions of hyperproliferative glandular epithelium, occurring in association with inflammation. In response to unknown stimuli, regions of prostatic atrophy (which are generally associated with inflammatory cell infiltrates) start developing at a very high frequency to encompass large regions of the prostate in some men (34). Morphologically, this proliferative glandular epithelium retains the appearance of simple atrophy (35) (Fig. 5).

The frequent location of PIA in the periphery of the gland near to PCa or even showing direct transition to malignant or pre-malignant epithelia suggests a connection between PIA and PCa. Other characteristics of PIA, such as imbalance between proliferation and apoptosis and detection of molecular-biological abnormalities specific for oxidative stress or malignancy, support this hypothesis (36). Morphological transitions between PIA, prostatic intraepithelial neoplasia (PIN) and PCa have also been described (37,38). The proposed progression process leading from normal epithelia to PCa is depicted in Fig. 4.

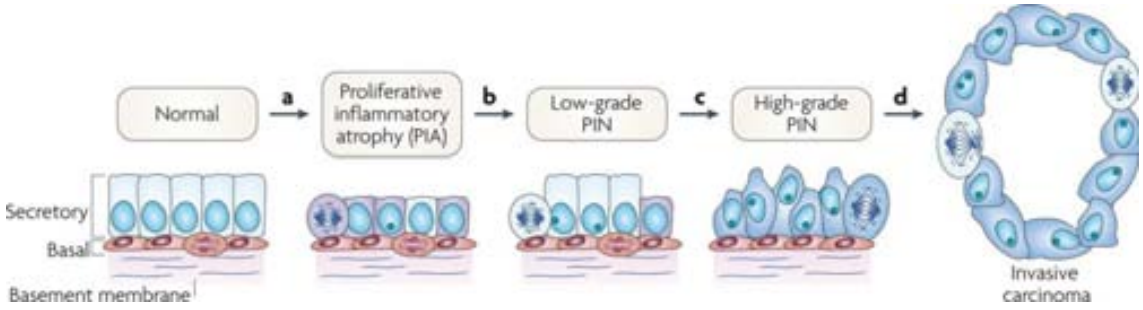

Figure 4. Model of early prostate neoplasia progression. Changes in morphology are represented. In the last stage, PCa **(d)**, the basement membrane is disrupted and the epithelial cells invade the surrounding tissue. Adapted from (30).

Moreover, in the transition from PIA to PIN, cellular detoxification function is gradually lost by silencing of glutathione-S transferase, a detoxifying enzyme. This cellular feature leads to an increased susceptibility of the prostatic epithelial cells to genomic damage by inflammatory oxidants or nutritional carcinogens. Consecutive somatic genome damage might then arise which modulates the further pathogenesis of PCa (39,40).

2 High grade prostatic intraepithelial neoplasia

Prostate intraepithelial neoplasia (PIN) is defined histologically by the presence of nuclear and cytoplasmic features similar to those of PCa, but in glands with a normal architecture (41) (Fig. 5). Notable cytological changes include (i) prominent nucleoli in at least 5% of the cells, (ii) nuclear enlargement, (iii) nuclear crowding, (iv) an increased density of the cytoplasm and (v) a variation in the nuclear size (42). In addition, PIN lesions generally display a marked elevation of cellular proliferation markers within the pre-existing secretory epithelium, ducts and acini (43).

However, unlike in cancer, in PIN the basal cell layer is not disrupted and the process is confined to the epithelium (hence the name intraepithelial) (44).

This prostate disorder is classified into a two-tier classification, based in the cytological characteristics of the secretory cells: low grade PIN (LGPIN) and high grade PIN (HGPIN) (45) (Table 1).

Table 1. Characteristics of the two types of PIN lesions (44,46).

PIN	Nucleoli of the cells	AMACR staining	Basal cell layer
LGPIN	Enlarged, vary in size, have a normal or little increase in the chromatin content and possess small or inconspicuous nucleoli	Negative	Intact
HGPIN	Large nucleoli rather uniform in size, an increased chromatin content and prominent nucleoli that are similar to those of PCa cells	Positive in the cytoplasm	Highly disrupted

HGPIN is considered most likely to represent a forerunner of PCa, based on several lines of evidence: (i) the incidence and extent of HGPIN on the prostate increase with advancing age (47,48); (ii) HGPIN lesions are usually found in the PZ, where most prostate tumors occur (49); (iii) the frequency, severity and extent of HGPIN increase in the presence of PCa; (iv) the appearance of HGPIN lesions generally precedes the appearance of carcinoma by at least 10 years, which is consistent with the idea of cancer progression; (v) rates of cell proliferation and death are elevated in HGPIN and PCa when compared to the rates for normal prostates, (vi) chromosomal abnormalities and allelic imbalance analyses have shown that HGPIN lesions are multifocal, as is the case with carcinomas (50); (vii) the architectural and cytological features of HGPIN closely resemble those of invasive carcinoma, including a disruption of the basal layer and the presence of prominent nucleoli (Figure 5); (viii) differentiation markers that are commonly altered in early invasive carcinoma are also altered in HGPIN lesions (42);

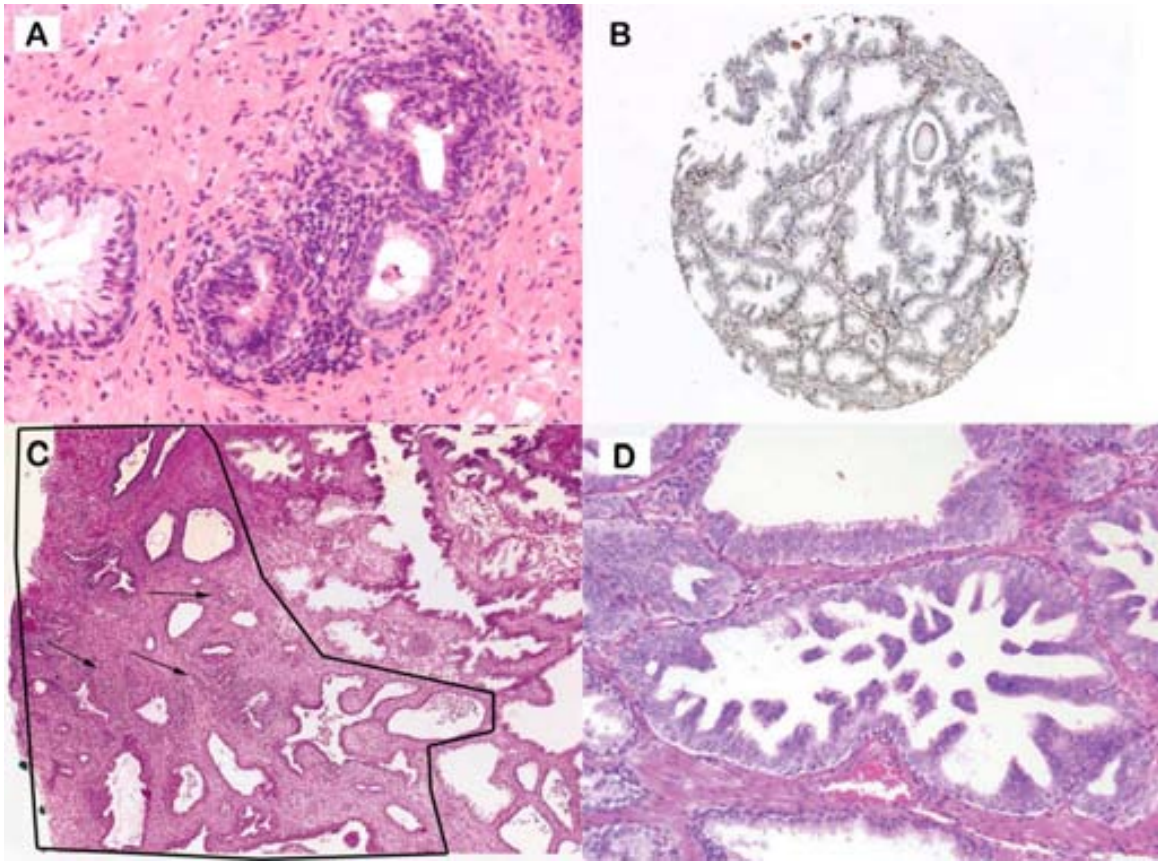

Figure 5. Architecture of the main disorders affecting the prostate. (A) Prostatitis (52), **(B)** BPH, from human tissue microarray (53), **(C)** PIA (outlined area) occurring adjacent to benign normal appearing glands (lower right). Arrows indicate collections of chronic inflamatory cells (predominantly lymphocytes) (34) and **(D)** HGPIN (52).

and, (ix) the rate of neovascularization is raised in HGPIN and in PCa when compared to the rate found in normal prostates (51).

Nevertheless, recent studies suggest that the majority of alterations that occur in the progression to PCa take place in the transition from benign epithelium to HGPIN, rather than from HGPIN to PCa (54). On the other hand, HGPIN differs from invasive carcinoma in that it normally retains the basal cellular membrane and does not invade the stroma. In addition, HGPIN lesions do not produce high levels of PSA and, consequently, HGPIN can only be detected by biopsy and not through serum PSA testing.

Bostwick and Brawer (55) described a progression model of PIN to carcinoma in which the transition from benign to LGPIN, to HGPIN, and then to PCa is continuous. Nevertheless, Putzi and de Marzo (37) found that LGPIN often coexists with HGPIN,

suggesting that both forms arise concomitantly. However, due to the fact that LGPIN is not documented in pathology reports, these data remain controversial.

2.1.1 Clinical significance of HGPIN

The only clinical importance of a diagnosis of HGPIN, at present, is when it is diagnosed without associated malignancy in prostate biopsy PB specimens (8). The reported incidence of HGPIN diagnosis on needle biopsies varies greatly between studies, ranging from 0.6 to 25%, with a median incidence of ~4% (56).

Finding of HGPIN in PB is a frequent indication for repetition of the biopsy (57). After repeated PBs with LGPIN, a 16% incidence of PCa was reported (47), whereas it has been estimated that around a 30% of the patients diagnosed with HGPIN in the first PB will present PCa in consecutive PBs (58–60).

Nevertheless, the magnitude of the risk of PCa in men with HGPIN and the optimal follow-up strategies remain controversial. In early studies, using limited biopsy schemes, HGPIN was associated with high rates of PCa and it was suggested that its presence indicated an immediate need for repetition of the biopsy (61). However, when a more extensive biopsy scheme was initially used, the cancer detection rate was considerably lower. This was due to the fact that the number of cores sampled during the initial biopsy affected the likelihood of detecting PCa in subsequent biopsies (48). For this reason, some researchers believe that repeat PBs might be unnecessary in the current era and that follow-up for these men can be accomplished using serial digital rectal examinations (DREs) and PSA measurements (62). HGPIN does not contribute to the serum concentration of PSA or modify the percentage of free PSA (fPSA) (57); however, PSA velocity (PSAV) helps to identify those men who possess a high likelihood of suffering from PCa and who have a real need for repeating the biopsy (63).

Several attempts have been made in the past to improve the current management of HGPIN patients. For instance, the number of positive HGPIN cores at the moment of diagnosis has been associated with the risk of cancer, suggesting that patients with unifocal HGPIN should be managed expectantly, whereas those with multifocal HGPIN could benefit from a more aggressive surveillance including re-biopsy (64,65).

Overexpression of certain molecules in HGPIN tissue has been found to correlate with the likelihood of finding a PCa in subsequent biopsies. One of these predictors is the *TMPRSS2*:*ERG* gene fusion. Park *et al*. assessed the presence of this molecular rearrangement through the measurement of ERG expression levels by

immunohistochemistry on biopsies from 461 patients, showing that patients with ERG expression were more likely to develop PCa (66). Alpha-methylacyl-CoA racemase (AMACR) expression has been found to be negative to weakly positive in biopsy specimens containing HGPIN without carcinoma and weakly positive in radical prostatectomy specimens, while its expression was highly positive in HGPIN lesions adjacent to adenocarcinoma (67). Similar results were obtained with the immunohistochemical study of GSTP1 expression (68). Finally, Prostate Tumor Overexpressed 1 (PTOV1) may be linked to PCa in detecting the risk of carcinoma in repeat biopsies following diagnosis of HGPIN (69).

Markers in biological fluids have also been described. For example, an increased serum level of early prostate cancer antigen (EPCA) has been associated with a higher cancer risk in men with isolated HGPIN (70). In urine, *PCA3* has been suggested as a candidate diagnostic marker with a good performance before the first repeat biopsy. In one study, *PCA3* predicted PCa well in HGPIN cases (AUC=0,80) and would have avoided 72.2% of repeat biopsies, compared to serum PSA (71). However, this study presented the limitation of a small sample size and Chin *et al*. have shown, in a larger cohort, that the efficacy of the *PCA3* score to rule out PCa in men with HGPIN is lower than in men with milder pathological conditions (e.g. prostatitis, BPH) (72).

In summary, the recognition of this HGPIN is clinically important because of its association with PCa. Although the relationship between both has not yet been conclusively demonstrated, HGPIN has been widely accepted as a precursor lesion to PCa and, consequently, men with a first PB positive for HGPIN usually undergo a close clinical follow-up over several years, comprising the measurement of serum PSA, DRE, ultrasound and repeat PBs (73). Evidently, many of these patients will have consistently negative results year after year, thus many of these biopsies could be avoided if clinicians were provided with better tools to predict the presence of PCa in this specific set of cases. Clearly, there is still a need for new biomarkers that could differentiate between indolent HGPIN cases and those who actually present PCa.

3 Prostate cancer

3.1 Epidemiology

PCa is the second most frequently diagnosed cancer and the sixth leading cause of cancer death in male world population, accounting for 14% (903,500) of the total new cancer cases and 6% (258,400) of the total cancer deaths in males, according to data from 2008 (74). Incidence rates vary by more than 25-fold worldwide, with the highest rates recorded primarily in the developed countries of Oceania, Europe, and North America (for 2014, there was an estimation of 233,000 new cases and 29,480 deaths in the United States only) (75), largely because of the wide utilization of PSA testing that detects clinically important tumors as well as other slow-growing cancers that might otherwise escape diagnosis. In contrast, males of African descent in the Caribbean region have the highest PCa mortality rates in the world, which is thought to reflect in part a difference in genetic susceptibility (74).

In countries with a frequent use of PSA screening such as the United States, Australia, Canada and North European countries, PCa rates rose rapidly in the early 1990s -soon after the introduction of this testing method- as a result of the increasing detection of tumors (Fig. 6). This epidemic of PCa was quickly followed by a sharp decline due to a smaller pool of prevalent cases. In other high-income countries with a low and gradual increase in the prevalence of PSA testing, such as Japan and the United Kingdom, PCa rates continue to increase slightly (74,76).

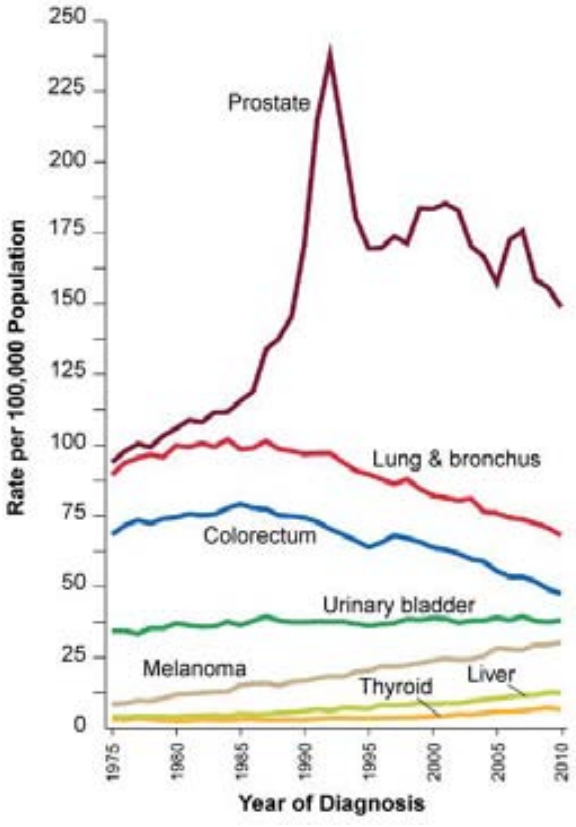

Figure 6. Trends in incidence rates for selected cancers (including PCa) in the United States male population, 1975 to 2010. Adapted from (77).

Death rates for PCa have been decreasing in many western countries, in part because of the improved treatment with curative intent. In contrast to these trends, incidence of metastatic PSA and mortality rates in most native Asian populations have gradually increased, and is substantially higher (even in the more developed Asian countries) than in migratory Asian populations residing in Western countries. Lower exposure to PSA screening in Asian individuals might be a major contributing factor to this effect (74,78).

3.2 Risk factors

3.2.1 Correlation with aging

Increasing age is, clearly, the most significant risk factor for PCa. Median age at diagnosis and PCa-related death is 66 years and 80 years, respectively (79).

The prostate is exposed to environmental and endogenous stress that may underlie this remarkable incidence. DNA methylation, genomic imprinting, and histone modifications are examples of epigenetic factors known to undergo change in the aging and PCa (80).

3.2.2 Race

It is also well established that men with an African American ancestry have higher PCa incidence rates than White American men. According to data from the Surveillance, Epidemiology, and End Results (SEER) program, age-adjusted PCa incidence rates from 2002 to 2006 for White and African American men were 153.0 and 239.8 per 100,000 persons, respectively. Incidence rates have decreased over the last few years along both groups, but the large disparity between them remains prominent. Furthermore, a higher percentage of PCa are diagnosed at advanced stages among African American (6% at distant stages) compared to White American men (4% at distant stages) (81).

Worldwide, the incidence of PCa in African American men is possibly exceeded only by rates in men of sub Saharan African descent in other countries, notably Jamaica and Trinidad and Tobago (82).

3.2.3 Familial inheritance

Genetic predisposition and familial aggregation of PCa have been demonstrated in numerous studies. Men with one affected first-degree relative have a two-fold increased risk of PCa and even higher risk for an early onset of PCa compared to those without such a relative (83).

Linkage studies have been performed on large collections of PCa pedigrees and several candidate familial loci have been identified. The most convincing locus is the Homeobox B13 (*HOXB13*), which is known to bind to the AR and to play an important role in prostate development. Recently, a nonsynonymous mutation in *HOXB13* has been described, resulting in a substitution of glutamic acid for glycine in the codon 84 (G84E) (84). This G84E mutation is significantly associated with disease in men with a family history and/or early disease onset (85). Other loci implicated in familial studies include *HPC1* (Hereditary Prostate Cancer 1), *PCAP* (Predisposing for Cancer of the Prostate), *HPCX* (Hereditary Prostate Cancer, X-Linked), *CAPB* (Cancer of the Prostate and Brain) and *HPC20* (Prostate Cancer, Hereditary, 3) (86).

There is also a recognized association of breast cancer with PCa in families. The contribution of the breast cancer susceptibility genes Breast Cancer 1 (*BRCA1*) and Breast Cancer (*BRCA2*) to male cancer has been extensively studied, since families with these mutations show clustering of cancer in men. Recent studies reported an 3.5-fold and 8.6-fold increase in the risk of PCa for *BRCA1* and *BRCA2* mutation carriers by age 65, respectively (87).

3.2.4 Environmental factors

The most well recognized risk factors for the development of PCa are those described above: advanced age, race and family history. However, there is also a distinct geographic distribution to PCa incidence, and an apparent increase in risk with the adoption of a „westernized" lifestyle, suggesting the involvement of environmental factors in addition to hereditary factors (88).

For many years, studies have been conducted to investigate potential occupations with a high risk of PCa. For example, farmers have been consistently found to be at increased risk for this illness (89,90). The exposure to pesticides and other agricultural chemicals including toxic metals, polychlorinated biphenyls (PCBs) and polycyclic aromatic hydrocarbons (PAHs), have been postulated as the agents responsible for such increases (91,92).

In addition, animal model studies implicate dietary carcinogens, such as the heterocyclic amines from over-cooked meats and sex steroid hormones, particularly estrogens, as candidate etiologies for PCa. Each of them acts by causing epithelial cell damage, triggering an inflammatory response that can evolve into a chronic or recurrent condition (93). Bad diet habits, together with lack of physical activity, are also linked to obesity, what has been shown to be associated with many cancer types, including PCa (94). On the contrary, for other dietary components, such as soy isoflavones, an association has been demonstrated with reduced risk of PCa in Asian populations, which traditionally consume large amounts of soy food (95).

3.3 Morphological characteristics and classification

More than 95% of PCas are adenocarcinomas that arise from prostatic epithelial cells (96). According to the 2004 World Health Organization (WHO) scheme, variants of the usual acinar adenocarcinoma include, atrophic, pseudohyperplastic, foamy, colloid, signet ring, oncocytic and lymphoepithelioma-like carcinomas. These variants have a wide incidence range, from exceedingly rare, such as the lymphoepithelioma-like and oncocytic carcinomas, to fairly common, such as foamy gland features in acinar adenocarcinoma (97).

Non-acinar carcinoma PCa variant account for only a small amount of carcinomas that are primary in the prostate. These histological variants or types include, according to the WHO, sarcomatoid carcinoma, ductal adenocarcinoma, urothelial carcinoma, squamous and adenosquamous carcinoma, basal cell carcinoma, neuroendocrine tumors, including small-cell carcinoma, and clear cell adenocarcinoma. Recently described variants not present in the 2004 WHO list include PIN-like adenocarcinoma, large-cell neuroendocrine carcinoma, and pleomorphic giant cell carcinoma (97).

As discussed above, the normal prostate luminal cells are physically separated from the stroma by a layer of basal cells and basement membrane, which constitute a continuous sheet encircling luminal cells. Thereby, the epithelium is normally devoid of blood vessels and lymphatic ducts, and totally relies on the stroma for its metabolic needs. Due to these structural relationships, the disruption of both the basal cell layer and the basal membrane is a pre-requisite for PCa invasion (98). The demonstration of this invasion is essential for the diagnosis of actual PCa rather than other pre-neoplasic lesion such as HGPIN, which may have an intact or intermittent basal cell layer.

Once invasion has occurred, the histological grading of the malignancy is accomplished by use of Gleason"s system, named after Donald Gleason, the pathologist who devised it in the 1970s (99). Gleason score grading system is based entirely on the histologic pattern of arrangement of carcinoma cells in hematoxylin and eosin (H&E)-stained sections. Five basic grade patterns are used to generate a histologic score, which can range from 2 to 10, by assigning a grade to the most and second most common tumor pattern and adding these two numbers up (100). These patterns are illustrated in a standard drawing that can be employed as a guide for recognition of the specific Gleason grades (Fig. 7).

Gleason grade of PCa is a well-established prognostic indicator that has stood the test of time. Increasing Gleason grade has been linked to a number of clinical end points, including clinical stage, progression to metastatic disease, and survival, and it is routinely used to plan patient management (100). However, one of the major drawbacks of the Gleason grading system is that it is partly subjective, and therefore associated with significant interobserver variability (101,102).

3.3.1 Staging of prostate cancer

The tumor, node and metastasis (TNM) system is the most widely used staging system for PCa. The American Joint Committee on Cancer (AJCC) and the International Union for Cancer Control (IUCC), the organizations responsible for the TNM cancer staging system, update it periodically. The most recent revision is the 7th edition, effective for cancers diagnosed on or after January 1, 2010 (Fig. 8) (103).

Once the T, N, and M categories have been determined, this information is combined, along with the Gleason score and PSA levels. The overall stage is expressed in Roman numerals from I (the least advanced) to IV (the most advanced) (Table 2). This is done to help determine the prognosis for the patients, as well as the best treatment options (104).

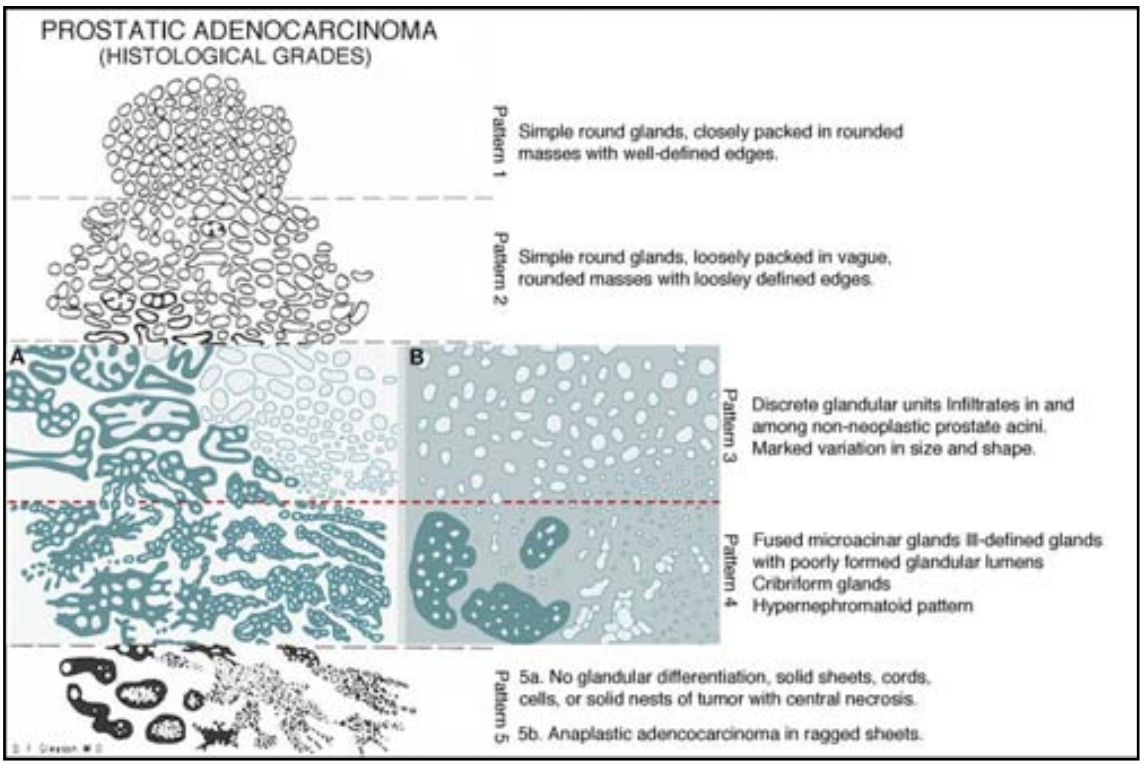

Figure 7. Original simplified drawings of the five Gleason grades of PCa. Grade 1 appears on the top and grade 5 on the bottom of the drawing (99). The color image shows a comparison of the original Gleason and the International Society of Urological Pathology (ISUP) 2005 modified systems for patterns 3 and 4, **(A)** Gleason"s original and **(B)** ISUP modified system, adapted from (104).

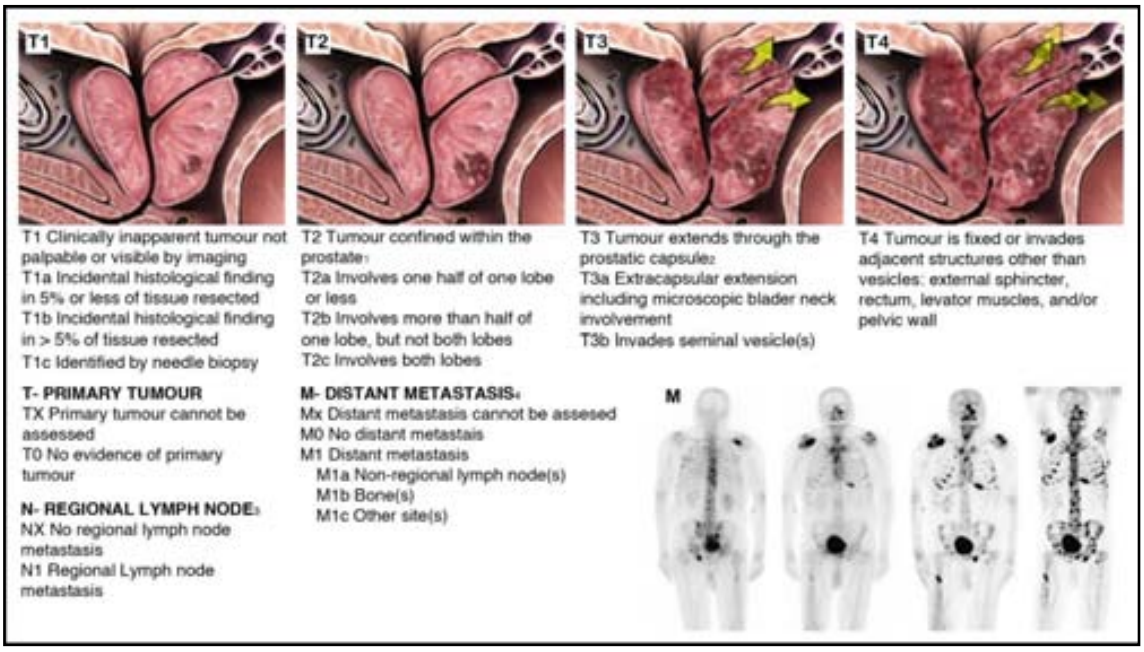

Figure 8. Tumor Node Metastasis (TNM) classification of PCa. Adapted from (105).

Table 2. American Joint Committee on Cancer (AJCC) stage grouping of PCa (106).

Stage	T	N	M	PSA (ng/mL)	Gleason score
I	T1a-c	N0	M0	<10	≤6
	T2a	N0	M0	<10	≤6
	T1-2a	N0	M0	X	X
IIA	T1a-c	N0	M0	<20	7
	T1a-c	N0	M0	≥10 and <20	≤6
	T2a	N0	M0	<20	7
	T2b	N0	M0	<20	≤7
	T2b	N0	M0	X	X
IIB	T2c	N0	M0	Any PSA	Any Gleason
	T1-2a	N0	M0	≥20	Any Gleason
	T1-2a	N0	M0	Any PSA	≥8
	T3a-b	N0	M0	Any PSA	Any Gleason
III	T4	N0	M0	Any PSA	Any Gleason
IV	Any T	N1	M0	Any PSA	Any Gleason
	Any T	Any N	M1	Any PSA	Any Gleason

M, metastasis; N, node; T, tumor; X, unknown.

3.4 Metastatic spread of prostate cancer

As evidenced in the TNM classification of PCa presented in the previous section, lymph nodes adjacent to the primary tumor are often the first site of metastases. Although lymph node metastases are themselves rarely life threatening, their detection is of major prognostic significance, since these patients exhibit a poor prognosis with significantly decreased survival rates (107).

Like most other solid tumors, if not detected early PCa can also metastasize to distant organs, such as the liver, lungs and brain, having an unusually high propensity for metastasizing to the bone. In patients with localized PCa, the 5-year survival approximates 100%; however, in patients in whom distant metastases have occurred, the 5-year survival drops to 31% (108).

Skeletal metastases occur in up to 90% of patients with advanced PCa (109). Bone metastatic disease, usually incurable, also has serious clinical manifestations, such as severe pain, pathologic fractures, hypercalcemia and spinal cord compression, which have a strong detrimental effect on patients' quality of life (109–111).

3.5 Current screening and diagnosis methods

The current screening method to diagnose PCa is based on the measurement of serum PSA levels and a digital rectal examination (DRE), whereas the decisive diagnosis is based on the result of the transrectal ultrasound-guided PB.

3.5.1 Serum PSA

PSA is a serine protease that was first identified in 1966 in seminal fluid, originally called γ-seminoprotein. Its relevance as a tumor marker was not established until 1979, when its prostate tissue specificity became apparent. Some years later, it was approved by the U.S. Food and Drug Administration (FDA) for monitoring the disease status of recurrence after definitive treatment in men with PCa, and it is now widely used for diagnosis (112). Currently, PSA serum level of 4.0 ng/mL is the established cutoff for recommending biopsy (113).

It is clear that the introduction of serum PSA testing in the late 1980s resulted in an increased detection of new PCa cases and a marked stage shift to early stages. Nevertheless, serum PSA has some well-recognized limitations, as it lacks diagnostic specificity and prognostic value, not being able to distinguish between indolent PCa, aggressive PCa, and certain benign conditions (e.g., prostate inflammation is characterized by increased levels of PSA) (114). This lack of specificity is associated with an increased percentage of negative PB and an over-diagnosis of many indolent tumors, linked with an over-treatment of these patients (115).

Moreover, the effect of mass PSA screening on PCa mortality remains debated, despite decades of clinical experience and several randomized trials (116,117). Still, the current strategy of the European Association of Urology (EAU) recommends that a baseline serum PSA level should be obtained at 40-45 years of age, intervals for early detection of PCa should be adapted in accordance to the baseline PSA serum concentration and early detection should be offered to men with a life expectancy ≥ 10 years (118).

Several modifications to PSA biomarker detection have been suggested to improve its sensitivity and selectivity including PSA density, ratio of free:total PSA, PSA velocity (PSAV) or PSA doubling time (PSADT) and different PSA isoforms, but they all present their own limitations and further research needs to be done to evaluate their performance (119).

3.5.2 Digital rectal examination

DRE was for a long time the primary means of diagnosis of PCa, until the popularization of the PSA test in the 1990s. The technique consists in the palpation of the prostatic gland by inserting a lubricated, gloved finger through the rectum. It allows a fairly accurate estimate of the gland volume, as well as a description of the character of the tissue with respect to the known pathologic conditions that can affect the prostate (e.g. a hard, irregular prostate is typical of a PCa) (120).

The sensitivity of DRE is limited because the cancer might not have a different “feel” from the surrounding benign tissue or may be beyond the reach of the examining finger. The DRE also has limited specificity, producing a large proportion of false-positive results (121). Additionally, it has low accuracy in localizing PCa, and it is subject to wide interobserver variability, even among experienced urologists (122–124).

3.5.3 Prostatic biopsy

Gray scale transrectal ultrasound (TRUS)-guided PB using local anesthesia remains the standard approach to the definitive diagnosis of PCa. Although there is intense controversy concerning PCa screening, when a decision is made to perform a diagnostic PB, based on abnormal DRE or increased PSA level, TRUS-guided PB is the preferred and standard-of-care technique. TRUS has many advantages over other medical imaging modalities, such as the lack of ionizing radiation, low cost, and the proximity of the prostate to the rectal wall (125).

PB techniques have significantly changed since the original Hodge's „sextant scheme“ (six cores, three from each side of the prostate: apical, middle and basal) described in 1989, which should now be considered obsolete. As a result of the great improvement and efficacy of local anesthesia, nowadays it is feasible to carry out a biopsy scheme with a high number of cores in an outpatient setting (126).

Evidence supports the inclusion of at least four additional laterally directed cores (typically a total of 12 cores) during PB, which significantly improves cancer detection without a demonstrable increase in morbidity. These data indicate that such PB templates, known as extended PB, represent the optimal template in initial PB intended to detect clinically significant PCa (127). On the contrary, it has been suggested that repeat PB should be based on saturation biopsies (number of cores ≥ 20) and should include the TZ, especially in patients with an initial negative biopsy (128).

3.6 Treatment

The management of the diagnosed PCa is crucially dependent on the presentation of the disease (stage and grade of the cancer), as well as patient comorbidity, age, and personal preferences (129).

By nature, PCa progresses slowly and in many cases it can be treated effectively by radical prostatectomy (RP) when it is detected early. Excellent cancer-specific survival is seen when specimen-confined PCa is found at final histopathology, even for high-risk PCa patients (130). Active surveillance rather than immediate treatment is also a reasonable and commonly recommended approach, especially for older men and men with less aggressive tumors and/or more serious comorbid conditions (131). Nonetheless, the best treatment for localized PCa remains controversial. This controversy is highlighted by a recent specialist survey on the “optimal” treatment of a hypothetical patient with localized PCa: approximately 29% favored expectant management, 33% favored radiation therapy (RT) and 39% chose RP (132).

On the other hand, for patients with a more advanced stage, presenting lymph node or bone metastases, current evidence suggests a survival benefit to multimodality therapy, which combines local therapies, such as surgery and RT, with systemic androgen deprivation therapy (ADT) (133).

Most men with advanced PCa initially respond to various types of androgen ablation, but a considerable portion of them eventually progress to castration-resistant PCa (CRPC). Among patients with non-metastatic CPRC, about one-third will develop bone metastasis within 2 years (134).

To help clinicians choosing the best treatment approach in each particular case, it is critical to identify markers that distinguish those PCa that will progress and metastasize, from those with indolent PCa.

4 Urine as source of biomarkers for prostate cancer

In recent years, the interest in new biomarkers obtainable by non-invasive means has increased significantly. A promising source for these, not only for PCa but also for many other diseases, is urine.

As stated before, the main function of the prostate gland is the secretion of prostatic fluid, which on ejaculation is combined with fluid from the seminal vesicle to promote sperm activation. The gentle massage of the gland during DRE stimulates the movement and release of prostatic fluids and detached epithelial cells into the urethra, which can be collected in voided urine post-exam (135). The greatest advantage of urine as source of biomarkers is that its collection can be accomplished without a disruption of standard clinical practice and can be sampled multiple times throughout the course of prostatic disease in a non-invasive manner (136).

4.1 RNA biomarkers

RNA-based biomarkers include coding as well as non-coding transcripts. Thanks to recent improvements in RNA microarray platforms, quantitative PCR (qPCR), and the development of new high-throughput technologies, such as next-generation sequencing, it is possible nowadays to perform accurate comparisons between specimens of different pathological conditions. In recent years, a wide range of promising PCa biomarkers that are not only prostate-specific, but also differentially expressed in prostate tumors, have been identified (136).

Although several of the recently described markers are promising -often showing increased specificity for PCa detection compared to that of PSA- their clinical application is limited. Currently, only Prostate Cancer Antigen 3 (*PCA3*) is used in clinical practice, and always in combination with serum PSA measurements.

4.1.1 PCA3

PCA3 was first described as DD3 in 1999 by Bussemakers *et al*., as a mRNA overexpressed in PCa *versus* normal prostate tissue (137). *PCA3* is a non-coding RNA (ncRNA), which functional role remains unknown (138). It has been found to be over-expressed in more than 95% of all primary PCa tumors (139).

The feasibility of a *PCA3* gene-based molecular assay based on the detection of PCa cells in urine has been demonstrated and it is currently utilized in a commercially available test under the name PROGENSA® *PCA3*, approved by the U.S. FDA in 2012 (140). The PROGENSA® *PCA3* assay is specially indicated for use in conjunction with other patient information to help determine the need for PB in men who have had one or more previous negative PBs (141–143).

4.1.2 RNA marker panels

In an effort to improve the sensitivity of using single gene analysis, some groups have assessed the usefulness of panels of RNA markers, usually combining those commented above (*PCA3* and *TMPRSS2:ERG*) with more recently discovered markers. Some recently published studies on RNA marker panels are presented in Table 4.

Despite the effectiveness of multiplex RNA-based platforms, the high costs of using multiple RNA assays simultaneously may slow their widespread clinical application (144).

Table 4. Representative examples of proposed mRNA marker panels.

Study	mRNA panel	No. of patients	Sens.	Spec.	Limitations
Leyten et al., 2014 (145)	*PCA3*, *TMPRSS2*:*ERG*	443	88%	50%	Low specificity
Nguyen et al., 2011 (146)	*TMRPSS2*:*ERG* subtypes	101	35%	100%	Low sensitivity
Rigau et al., 2011 (147)	*PCA3*, *PSMA*, *PSGR*, serum PSA	154	96%	50%	Requires use of serum PSA
Rigau et al., 2010 (148)	*PCA3*, *PSGR*	215	96%	34%	Low specificity
Salami et al., 2013 (149)	*PCA3*, *TMPRSS2*:*ERG*, serum PSA	48	80%	90%	Small sample size, requires use of serum PSA
Laxman et al., 2008 (150)	*GOLPH2*, *SPINK1*, *PCA3*, *TMPRSS*:*ERG*	138	66%	76%	Inconvenience of using 4 RNA markers in the clinical setting
Jamaspishvili et al., 2011 (151)	*PCA3*, *AMACR*, *TRPM8*, *MSMB*	104	72%	71%	Use of markers that are unpredictive of PCa when used alone

PSMA, prostate specific membrane antigen; PSGR, prostate specific G-coupled receptor; GOLPH2, Golgi phosphoprotein 2; SPINK1, serine protease inhibitor Kazal-type 1; AMACR, alpha-methylacyl-CoA racemase; TRPM8, transient receptor potential cation channel subfamily M member 8; MSMB, microseminoprotein β.

4.2 miRNA biomarkers

MicroRNAs (miRNAs) are short, single-stranded RNA molecules of ~22 nucleotides in length that bind to complementary sequences in the 3′ UTR of multiple target mRNAs and regulate their expression at the transcriptional level, usually resulting in their silencing (152).

In PCa, most of the studies on circulating miRNA which have found associations between miRNA populations and disease have been conducted using serum or plasma. In this setting, two promising miRNAs, miR-141 and miR-375, have emerged as diagnostic and prognostic markers across independent studies (153–155).

In urine, some attempts have been made to establish new miRNA biomarkers or signatures, including miR-1825 and miR-484 (156), miR-187 (157), miR-888 (158), miR-205 and miR-214 (159). However, to date the majority of miRNA studies were addressed in relatively small patient cohorts limiting the validity and the clinical application of these potential biomarkers (160). Clearly, the analysis on miRNAs for PCa is still in its infancy.

4.3 Protein biomarkers

Thanks to the availability of proteomic platforms, allowing the analysis of hundreds of peptides simultaneously, protein-based urinary marker research has evolved enormously during the last decade (161).

Nowadays, annexin A3 (ANXA3) is one of the most generally accepted markers of non-invasive PCa in urine. ANXA3 is a calcium-binding protein with decreased production in PCa cells. It is been reported as a complementary marker to serum PSA. It has huge potential to avoid unnecessary biopsies with a particular strength in the clinically relevant large group of patients who have a negative DRE and PSA in the lower range of values (2 to 10ng/mL) (162).

More recently proposed urinary protein markers like delta-catenin (163), the receptor tyrosine kinase c-met (164), thymosin β15 (165) and zinc α2-glygoprotein (166) have been evaluated in different pilot studies, but none of these have yet been validated in independent cohorts.

4.4 Biomarkers in exosomes

Exosomes, also known as extracellular vesicles (EVs), are small tissue-derived vesicles that are shed by many mammalian cell types, including malignant cells. Recently, they have been pointed out as a promising source of biomarkers, since their content (including proteins, mRNA and miRNA) is thought to represent their tissue of origin (167).

The next section (section 5, “Exosomes and exosome-like vesicles”) will fully discuss the potential advantages of exosome-derived biomarkers, as well as the current status of research in the field, including the main drawbacks such as the vesicles handling difficulties the lack of standardized protocols.

4.5 Current state of the art of urine PCa biomarkers

While many novel PCa biomarkers have shown promise, none seem currently poised to replace the utility of PSA. It must be noted that PSA has been one of most successful tumor markers to date and remains the single most predictive marker for identifying men at increased risk for PCa. Many of the current proposed alternatives modestly increase the operating characteristics relative to PSA; however, no individual marker is ideal. In order to move forward, further validation of promising markers and continued discovery of novel markers is needed. While it will be determined which of these markers will play an important role in screening, the fundamental goal is to decrease the number of unnecessary biopsies, and differentiate between indolent and aggressive PCa (168).

5 Exosomes and exosome-like vesicles

5.1 A brief history of extracellular vesicles

Intercellular communication is an essential hallmark of multicellular organisms and can be mediated through direct cell-cell contact or transfer of secreted molecules. In the last three decades, a third mechanism for intercellular communication has emerged that involves intercellular transfer of extracellular vesicles (EVs).

Although the release of apoptotic bodies during apoptosis has been long known, the fact that also perfectly healthy cells shed vesicles from their plasma membrane has only recently become appreciated (169). These vesicles fall mainly into two groups, depending on their size, origin, and the mechanism of their release: the endosome-derived vesicles, named exosomes, and the vesicles shed from plasma membranes, referred to as ectosomes, microparticles, or microvesicles (MVs) (170).

The number of reviews on shedding vesicles are few, dealing mostly with single cell types, and are often published in specialized journals and addressed to restricted audiences (171).

Exosomes are the vesicles that have, by far, received the most attention over the past recent years, and are also the main interest of this work. These vesicles were first described in sheep reticulocyte maturation in 1983, as small (50-150 nm) membranous vesicles involved in the externalization of the transferrin receptor, released during reticulocyte differentiation as a consequence of multivesicular body (MVB) fusion with the plasma membrane (172). At the very same time, in an independent study, Harding and colleagues published the first images of MVB externalization event (173) (Fig. 9). The two simultaneous papers nicely complemented each other and, together, these findings laid the foundations of a compelling model for a vesicle shedding pathway. Nevertheless, it took some time for the appreciation of the general significance of exosomes to extend beyond the reticulocyte/transferrin receptor model. Considered to be some kind of cellular garbage cans at the time, which role was to discard unwanted molecular components, exosomes remained little studied for the next 10 years.

However, interest in these vesicles has increased dramatically over the last three decades, when evidence has begun to accumulate that the vesicles are like signaling payloads containing cell-specific collections of proteins, lipids, and genetic material that are transported to other cells where they alter function and physiology (174). This nearly explosive growth in the field of exosome biology resulted in over two thousand publications on exosomes, to date (175).

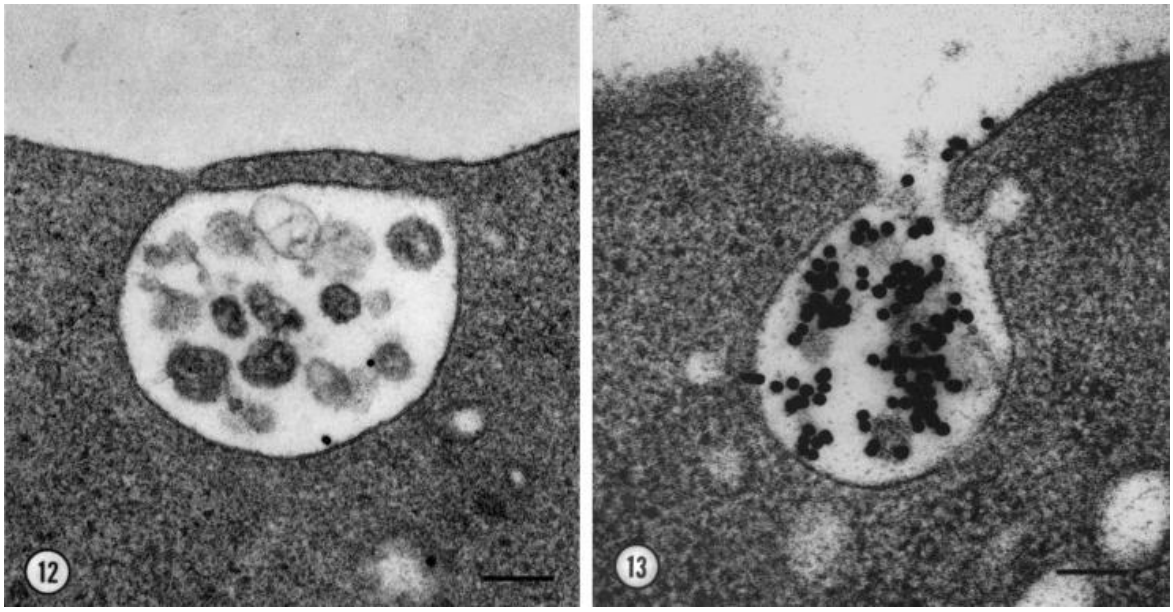

Figure 9. Exocytosis of MVBs releases exosomes containing transferrin receptor. (Left) View of an MVB from a fixed reticulocyte sparsely labeled with colloidal gold-conjugated transferring (AuTf). The apparent fusion of the MVB and the plasma membrane may represent incipient MVB exocytosis. Bar, 100 nm. **(Right)** View of MVB exocytosis in a reticulocyte labeled with AuTf, quick frozen without prior fixation, and freeze substituted. Bar, 200 nm. From (173).

5.2 Nomenclature and classification

Despite of the intense general interest in the field in recent years, because of the EVs isolation and detection difficulties, the multidisciplinary research field, and different ways of classification, there is currently no consensus about the correct nomenclature of cell-derived vesicles.

Researchers have invented dozens of different names for secreted vesicles, most of which reflect specific functions (e.g. *calcifying matrix vesicles* that initiate bone formation and *tolerosomes* that induce immunological tolerance to dietary antigens) or their cell of origin (e.g. *dust* released by platelets and *prostasomes* released by prostate epithelium). Although such terms can be useful within a specialized field, more generic terms, such as “exosome” and “microvesicle”, have broader utility. Unfortunately, these generic terms mean different things to different investigators. For example, exosome can be used in 3 different ways, with some investigators preferring a biogenetic definition (i.e. vesicles that bud into endosomes and are released when the resulting MVB fuses with the plasma membrane), others preferring the original, broad definition (i.e. secreted vesicles that

"may serve a physiologic function") and still others employing an empirical definition based on differential centrifugation (i.e. vesicles that sediment only after centrifugation at ~70,000-100,000xg). A similar range of definitions is evident for the term MV, which some define as vesicles that bud from the plasma membrane, while others mean all secreted vesicles and still others define based on the differential centrifugation (i.e. vesicles that sediment at ~10,000xg) (176).

Important criteria for classification with regard to the type of cell-derived vesicles are size, density, morphology, lipid composition, protein composition, and subcellular origin, which are summarized in Table 5.

Table 5. Physicochemical characteristics of different types of secreted vesicles. Adapted from (177).

Feature	Exosomes	Microvesicles	Apoptotic bodies
Size	50–100nm	100–1,000nm	50–500nm
Density in sucrose	1.13–1.19g/ml	ND	1.16–1.28g/ml
Appearance by electron microscopy*	Cup shape	Irregular shape and electron-dense	Heterogeneous
Sedimentation	100,000xg	10,000xg	1,200xg , 10,000xg or 100,000xg
Lipid composition	Enriched in cholesterol, sphingomyelin and ceramide; contain lipid rafts; expose phosphatidylserine	Expose phosphatidylserine	ND
Main protein markers	Tetraspanins (CD63, CD9), Alix and TSG101	Integrins, selectins and CD40 ligand	Histones
Intracellular origin	Internal compartments (endosomes)	Plasma membrane	ND

* Appearance by electron microscopy is only an indication of vesicle type and should not be used to define vesicles, as their microscopic appearance can be influenced by te fixation and phase contrast techniques used. ND, not determined; TSG101, tumor susceptibility gene 101.

The listed features of vesicles secreted by live cells are based on observation of preparations of 100% pure vesicles. However, in daily practice, all vesicle preparations are heterogeneous, with different protocols allowing the enrichment of one type over another. This type of preparations can be classified according to the presence of several (but not necessarily all) of the listed features (177).

5.2.1 Nomenclature in this thesis

Following the trend of the latest publications, in this study the term “exosome” will be used when referring to vesicles that are released from the cells as a consequence of MVB fusion with the plasma membrane, and “microvesicle” when referring to the larger vesicles budding directly from the plasma membrane. Since the fractions obtained after centrifugation 100,000xg, enriched in exosomes, may also contain other types of vesicles with similar physicochemical characteristics, for this particular case we prefer to use the term “exosome-like vesicles” (ELVs).

5.3 Characteristics and composition

5.3.1 Size

The reported size range of ELVs varies notably between studies. Most findings have focused on vesicles sized between 50 and 100 nm, while others employ a lower (30 nm) or higher (150 or 200nm) cutoff value (178–180). These differences can be explained by the influence of several variables, such as the isolation procedure and the detection limit of the applied detection technique.

It is lately becoming apparent that they might actually have a slightly larger size than previously thought. The classical size estimation (50-100 nm) was generally based on transmission electron microscopy (TEM) measurements but, with the appearance of new technologies (such as nanoparticle tracking analysis (NTA), which allow to analyze the ELVs directly in suspension) it has been noted that shrinkage artifacts during fixation for TEM may have been leading to an under-sizing of the vesicles (181).

5.3.2 Morphology

The morphology of ELVs has traditionally been described as “cup-shaped” after fixation, adhesion, negative staining, and visualization by TEM (182). Nevertheless, newer techniques (such as cryo-electron microscopy; cryo-EM) led to the finding that this “cup-shaped” morphology of ELVs was in fact an artifact related to fixation for TEM, and that their actual shape is perfectly rounded (Fig. 10) (183).

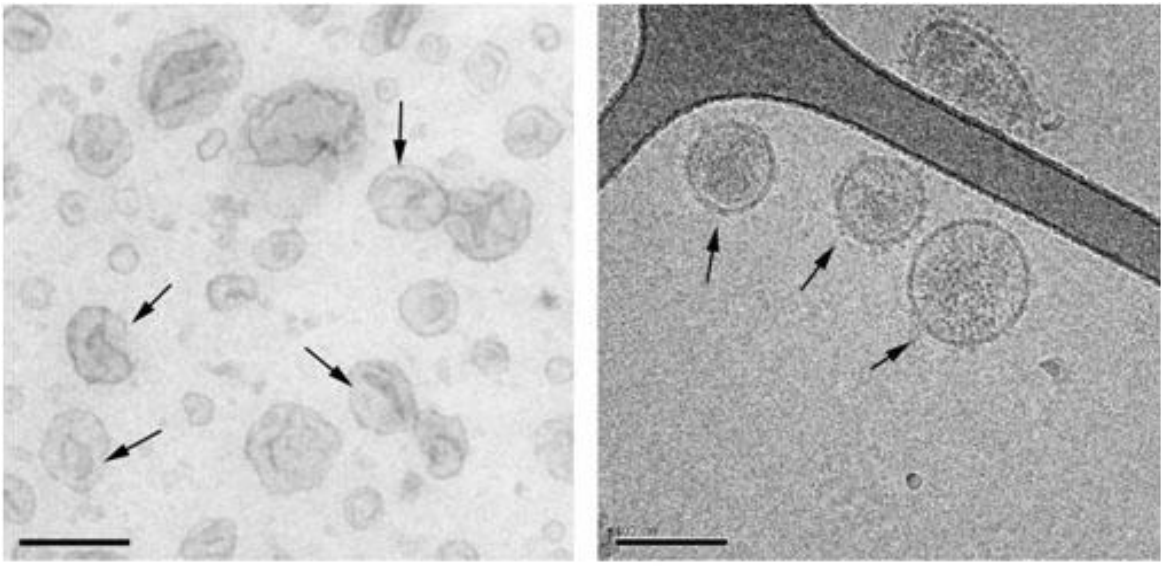

Figure 10. Ultrastructure of exosomes. (Left) Exosomes isolated from melanoma cells were contrasted with uranyl-acetate and embedded as whole mount preparations in methylcellulose. Note their artificial cup-shape appearance (examples are indicated with arrows). **(Right)** Exosomes from prostate epithelial cells were directly frozen and observed by cryo-EM without chemical fixation or contrasting. Exosomes appear round and are visualized with improved resolution (arrows). The elongated structure (top right of the micrograph) is the Formvar film on the EM grid. Bars, 100 nm. From (169).

5.3.3 Composition

During the last 20 years, the ELV protein content has been extensively investigated by mass spectrometry (MS)-based proteomic analysis, Western blotting, fluorescence-activated cell sorting, and immuno-EM. Recently, MS-based proteomic tools have played a particularly important role in improving our understanding of the protein compositions of EVs from various cell types and body fluids (184).

Exosomes are characterized by the presence of proteins involved in membrane transport and fusion, such as Rab, GTPases, Annexins (ANXA), and Flotillin-1 and -2 (FLOT1, FLOT2), components of the endosomal sorting complex required for transport (ESCRT) complex such as Alix, tumor susceptibility gene 101 (TSG101), heat shock proteins (HSPs), integrins, and tetraspanins, including CD63, CD81, and CD82 (182).

Beyond their repertoire of characteristic markers, exosomes also feature a wide range of surface and internal proteins specific to their origin source (185). As an example, it has been shown that glioblastoma-derived exosomes express the specific mutation of the

epidermal growth factor receptor (EGFR) EGFRvIII (186), while the tumor antigens epidermal growth factor receptor type 2 (HER2) and melanoma antigen recognized by T-cells 1 (MART-1) were found in samples from patients with breast cancer and melanoma, respectively (187).

Thanks to the development of high-throughput techniques for nucleic acid analyses, in recent years there has been an ever-increasing number of studies reporting sequences of the RNA in exosomes. Such studies show that not all messenger RNAs present in a cell end up in exosomes, and apparently there is specific targeting of some mRNA sequences into the released vesicles. In addition, Valadi *et al*. showed that the mRNA stored in the exosomes can be delivered to another cell, where it can be translated into full-length, entirely functional proteins (188). However, it is still unclear from the few published studies whether one can (as for exosomal proteins) find a set of exosomal mRNA that would be consistently targeted to exosomes in any cell type (Théry, 2011).

In the same paper from 2007, Valadi and colleagues also demonstrated for the first time the presence of miRNA in the exosomes (188). Later, it has been shown that these molecules, like the mRNA, can be transferred to acceptor cells where they can act on repressing target mRNAs (189). The miRNAs loaded into exosomes are protected from degradation and therefore remain highly stable, which render them very interesting as biomarkers for cancer and other diseases (190).

Finally, a few investigators have performed lipidomic profiling of EVs. It is currently known that exosomes are surrounded by a phospholipid membrane containing relatively high levels of cholesterol, sphingomyelin, and ceramide and containing detergent-resistant membrane domains (lipid rafts) (182).

In summary, exosomes are phospholidid bilayer-enclosed vesicles that contain proteins, mRNAs and miRNAs. A part of these molecules is tissue specific, while others are related to the exosomes biogenesis and therefore common to all exosome populations, independently from their source (Fig. 11).

Currently, in 146 investigations compiled in the ExoCarta database, over 4500 proteins, 1600 mRNAs, 760 miRNAs and 190 lipids have been linked with exosomes (http://www.exocarta.org).

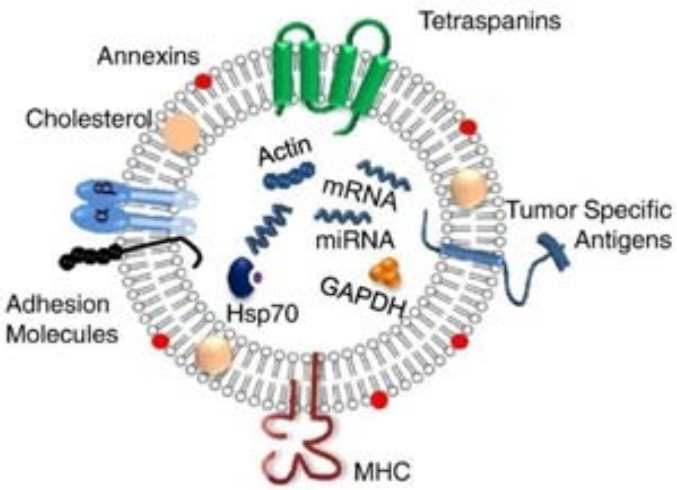

Figure 11. Typical molecular composition of an exosome. Adapted from (191).

5.4 Biogenesis

As stated before, in contrast with the direct budding from the plasma membrane of MVs, exosomes biogenesis involves their formation as intraluminal vesicles (ILVs) inside MVBs in a more complex process.

The first function of MVBs to be identified was the sorting of proteins into the lysosome. More recently it has become clear that MVBs can have alternative fates, including fusion with the cell surface to release the ILVs as exosomes. The extent to which MVBs with different destinations exist as entirely separate entities or, by the contrary, mechanisms of ILV formation and sorting operate within the same MVB, is unclear (192).

The ILVs, which progressively accumulate during MVB maturation, are formed by inward budding and scission of vesicles from the limiting membrane into the endosomal lumen. During this process, transmembrane and peripheral membrane proteins are incorporated into the invaginating membrane, maintaining the same topological orientation as at the plasma membrane, while cytosolic components are engulfed and enclosed into the small vesicles (193).

The best characterized MVB sorting mechanism is the ESCRT machinery, which is composed of four protein complexes (ESCRTs-0, -I, -II, -III). In this system, ubiquitinated cargos are first recognized and bound by the ESCRT-0 complex, and subsequently passed to later ESCRT components, which also mediate ILV formation (194). This

pathway has been clearly described for MVB cargo destined for degradation in the lysosome (195); however, its implication in the biogenesis of ILVs destined for secretion as exosomes is more controversial.

Interestingly, ESCRT-independent ILV formation has also been described. It has been reported that, in mammalian cells, depletion of components of all four ESCRT complexes does not abolish MVB formation, suggesting the existence of an alternative mechanism (196). Later, a study conducted in melanocytes proposed the requirement for the tetraspanin CD63 in the ESCRT-independent mechanism and, more importantly, showed that the involvement of the different sorting complexes has important implications for distinct fates of ILVs (i.e., secretion or degradation) (197).

Finally, lipid components have also been implicated in the process. Exosomes present lipid-raft microdomains on their surface, enriched in sphingolipids, that might be involved in concentration of cargo (proteins present in these subdomains have a low lateral diffusion) and in the initiation of vesicles formation (lipid-rafts are weak points on the membrane surface, prone to outward bending) (198,199).

Taken all together, the existence of ESCRT-dependent and independent mechanisms for the loading of proteins into exosomes is not necessarily contradictory, but rather points to the presence of heterogeneous populations of MVB and exosomes (Fig. 12). Accordingly, it has been shown in multiple studies that cancer cell lines secrete several types of exosomes, which share morphological characteristics and contain stereo-typical exosome markers (TSG101, Alix and Hsp70), but differ on their miRNA composition and are differently enriched in specific markers, including CD63 (200).

After vesicle accumulation, fusion of the MVBs with the plasma membrane releases ILVs (which from then on are defined as exosomes) into the extracellular space. This process of directed transport relies on several components of the endocytic machinery such as the Rab GTPases Rab11, Rab27a and Rab27b, cytoskeleton regulatory proteins, molecular motors such as myosins, and SNAREs (SNAP (soluble NSF attachment protein) receptor) for targeted fusion (192,202).

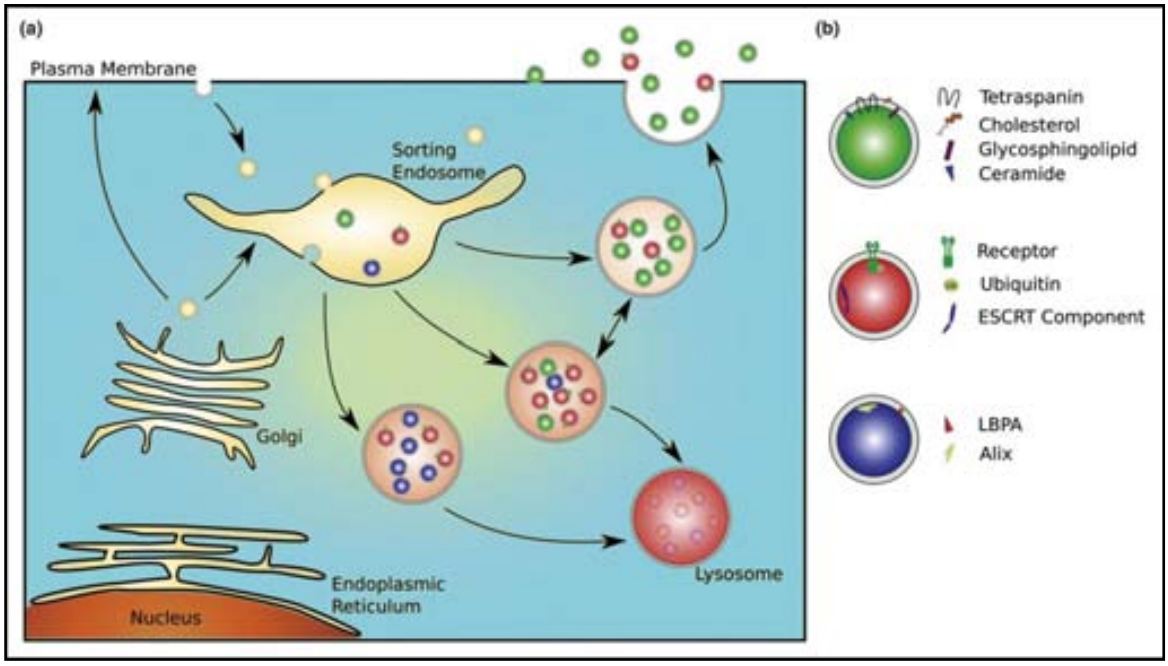

Figure 12. Model for sorting of cargo into different MVB subpopulations. (a) Different hypothetical MVB subclasses with distinct populations of ILVs (red, green and blue) are shown. The putative compositions of these ILVs are shown in the right panel. Whether the MVBs contain a mixture of different ILVs as depicted in the figure is not known. **(b)** At least three different subclasses of ILVs may coexist. The molecules shown represent a selection of protein and lipids that define different classes of ILVs. From (201).

5.5 Functions

Exosomes are nowadays considered to be an integral part of the intercellular microenvironment and are believed to participate in cell-to-cell communication. It is worth noting that, after being released, exosomes can both locally influence the behavior of target cells as well as enter a body fluid to reach distant sites to exert their function.

In healthy individuals, they can contribute to the regulation and maintenance of physiological conditions, acting as immune-modulators (with immunosuppressive or immune-activating effects), or intervening in other processes such as programmed cell death, angiogenesis, inflammation and coagulation (203,204). These vesicles have also been depicted as morphogen transporters implicated in cell polarity and developmental patterning of tissues (205).

Over the last decade, a number of studies have revealed that exosomes can influence major tumor-related pathways such as hypoxia-driven epithelial-to-mesenchymal transition, cancer stemness, stromal remodeling, induction of angiogenesis, modulation

of response to therapy and metastasis (191,206). Indeed, *in vitro* functional assays demonstrated that these vesicles can influence cancer microenvironment and promote cancer progression (207), and that they may play a role in pre-metastatic niche formation (208).

5.6 Isolation methods

Because of their small size, EVs are below the detection range of conventional detection methods. Consequently, recovery and contamination in the separation process cannot be reliably quantified, and isolation protocols have not been standardized. The inter-related difficulties of the detection and isolation of vesicles partly explains the differences in classification criteria and clearly exposes one of the main issues still to be solved by the research field (182).

The most widely applied method for isolating EVs -in particular exosomes- is the isolation by differential centrifugations. This method involves a number of centrifugations, which sequentially increase in speed and time, and thus sequentially pellet smaller particles. The pellets are discarded from each run and subsequent centrifugations are performed on the supernatant from the prior ones until the last centrifugal run, which aims to pellet exosomes (209). Improvements proposed for this method include the addition of an extra step to increase the purity of the isolated urinary exosomes; specifically, the incorporation of an additional ultracentrifugation step with a 30% sucrose cushion or a pre-processing of the sample through a 0.22μM filter just before ultracentrifugation (210).

Although ultracentrifugation based methods allow researchers to efficiently isolate EVs from body fluids and cell culture media, they are time consuming and require the use of expensive equipment. In an attempt to make exosomes isolation possible in a clinical setting, several alternative methods have been suggested; these include immunoaffinity capture (211), polymer-mediated precipitation (212) and filtration-based protocols (213). These methods are faster and easier than ultracentrifugation, but are not devoid of their own limitations, such as a decreased purity of the vesicles, as they are commonly co-purified with a high quantity of protein complexes. Furthermore, most of them have only been tested in a very limited range of sample types and their performance in different fluids is yet to be studied.

In the specific case of urine samples, even thought EVs are abundant, they are difficult to cleanse from the most common urinary protein, Tamm-Horsfall protein (THP; also known as uromodulin). THP, which can reach concentrations of 1.5mg/mL, has a role in protecting the urinary tract from pathogens by acting as a decoy receptor, and it may also inhibit stone formation in supersaturated urine (214). THP molecules oligomerize into long, double-helical strands several microns long, forming a three-dimensional gel which traps and sequesters the exosomes in any centrifugation-based protocol (215). For this reason, modified protocols, including treatments with the denaturing agent dithiothreitol (DTT), have been proposed to increase the purity and yield of vesicles isolated from urine (210,214).

5.7 Exosomes as source of biomarkers

Nowadays, the discovery of new biomarkers in body fluids such as serum and urine remains a challenge. Since a few high-abundance proteins (albumin, THP) make up 97% of body fluids, they hinder the detection of the low-abundance proteins, which are generally the most promising candidates for biomarker discovery (216). This dynamic range problem could be solved by the specific enrichment of the desired fraction, but obviously during a discovery phase the protein marker of interest is not known.

Urine is a particularly complicated sample for the discovery of biomarkers, due to its extremely high dynamic range. The dynamic range is defined as the ratio between the largest and smallest possible values of a changeable quantity, in this case, protein quantity. Plasma samples exhibit tremendous variations in individual protein abundances, typically of the order of 10^{10} or more, with the result that only the high-abundance proteins are usually detected (217). In the case of urine, the problem is further aggravated by its very low protein content, requiring a concentration step of 100- to 1000- fold (218). It is believed that, within “deep proteome” (the hidden or low abundance urine proteins), a few, potential novel biomarkers for the disease may be represented (219). Exploring the exosomes fraction allows us to reveal part of this deep proteome.

Indeed, the possibility of using EVs as source of PCa biomarkers as a means to overcome the dynamic range problem has generated considerable interest in the last years. The contents of these vesicles include a tumor-enriched repertoire of biomolecules dependent on their cellular origin, strongly related to the stimulus that triggers their release. For that reason, the discovery of a disease-specific protein, lipid, or

RNA associated with EVs could make it possible to use them as novel biological markers for prognostic and diagnostic purpose and for monitoring of the disease. Indeed, a number of studies in this direction have been already conducted in several cancer diseases (Table 6) (220).

Analyzing the content of exosomes harvested from urine has a number of advantages: (i) it is non-invasive, (ii) data is informative with regards to PCa diagnosis and potentially the status of overall tumor malignancy, (iii) the genetic and proteomic material within exosomes is protected from enzyme degradation by the exosomal lipid bilayer (221), and (iv) exosomes are stable after long-term storage at -80ºC, which makes prospective studies feasible (222).

On the other hand, the main drawbacks of exosomes use for the discovery of biomarkers are (i) the lack of fast, reliable and low-cost isolation methods, and (ii) the lack of an appropriate standardization method, such as creatinine standardization for the general urine proteome, to overcome the wide variation of urine content between samples, mostly due to differences in the patient"s daily intake of fluid (223).

Table 6. Summary of some studies in which tumor EVs have been assessed for their potential clinical use in disease monitoring and diagnosis of cancer patients.

Cancer type	Sample type	Biomarker	Biomarker type	Study
Ovarian cancer	Plasma	Claudin-4	Protein	Li *et al*., 2009 (224)
Glioblastoma	Serum	EGFRvIII, miR-21	Protein / miRNA	Skog *et al*., 2008 (225)
Mucinous adenocarcinoma	Blood	TF activity, MUC1	Protein	Tesselaar *et al*., 2009 (226)
Bladder cancer	Urine	*LASS2*, *GALNT1*, *ARHGEF39*, *FOXO3*	RNA	Perez *et al*., 2009 (227)
Renal cell carcinoma	Urine	MMP9, CP, PODXL, DKK4, CAIX, AQP1, EMMPRIN, CD10, Dipeptidase 1, Syntenin-1	Protein	Raimondo *et al*., 2009 (228)

TF, tissue factor; MUC1, mucin; *LASS2*, ceramide synthase 2; *GALNT1*, UDP-N-acetyl-alpha-D-galactosamine:polypeptide N-acetylgalactosaminyltransferase 1 (GalNAc-T1); *ARHGEF39*, rho guanine nucleotide exchange factor (GEF) 39; *FOXO3*, Forkhead Box O3; MMP9, Matrix metalloproteinase 9; CP, Ceruloplasmin; PODXL, Podocalyxin; DKK4, Dickkopf related protein 4; CAIX, Carbonic anhydrase IX; AQP1, Aquaporin-1; EMMPRIN, Estracellular matrix metalloproteinase inducer; CD10, Neprilysin.

5.7.1 RNA biomarkers for PCa

There are very few reports on RNA present in PCa-derived exosomes. However, it has been proved that known markers for PCa, such as the *TMPRSS2:ERG* fusion gene and *PCA3*, could be detected in urine-derived and PCa cell line-derived exosomes by PCR, showing the potential for diagnosis and monitoring cancer patients status (229,230).

5.7.2 miRNA biomarkers for PCa

To date, there is only one article published where the different expression profiles of miRNAs in EVs have been compared between PCa and control samples. In this particular study, using serum samples, it was confirmed that the putative PCa markers miRNA-141 and miRNA-375 levels in EVs are associated with metastatic PCa. In the same study but using urine samples, miR-107 and miR-574-3p were quantified at significantly higher concentrations in PCa cases compared with controls (154).

5.7.3 Protein biomarkers for PCa

So far, most of the studies aimed at the discovery of new exosome-related protein biomarkers for PCa have been conducted in cell lines derived exosomes, rather than in actual patient samples.

For example, based on comparative protein profiling by MS-based proteomics of LNCaP and PC3 exosomes, the integrins α3 (ITGA3) and β1 (ITGB1), involved in migration/invasion, have been proposed as potential biomarkers. Indeed, in this same study they have shown that ITGA3 might be involved in cancer invasion, since its inhibition reduced the migration and invasion of non-cancerous prostate epithelial cells almost completely. Finally, in a small set of samples, these integrins were found to be more abundant in urine exosomes of metastatic patients, compared to BPH or PCa (231).

In another recent study, a comparison of exosomal proteins from different PCa cell lines using high performance MS resulted in the discovery of Alix, Fatty acid synthase (FASN), Exportin-1 (XPO1) and Alpha-enolase (ENO1) as new candidate biomarkers for PCa. These results have not been further validated in human samples (232).

Nonetheless, some reports have indicated urinary exosomes to be an excellent source of urinary PCa biomarkers. Mitchell and colleagues analyzed, by Western blot, urinary exosomes from 10 healthy donors and 10 PCa patients who were undergoing hormonal

therapy. PSA and prostate-specific membrane antigen (PSMA) were found to be present in almost all of the PCa specimens, but not in the healthy donor specimens (233). Another study characterized pooled urine exosome preparations using a shotgun proteomics procedure, and they were able to identify ~900 proteins. Among these, they found prostate-related proteins such as PSA, PAP, PSMA and Transglutaminase 4 (TGM4) as well as several exosomal markers, such as CD9, CD63, CD81, Alix, TSG101, FLOT1, FLOT2, ANXA2 and ANXA5 (234).

However, to our knowledge, to date no high-throughput technique has been used to analyze the protein content of urinary exosomes for PCa biomarker discovery in individual patient samples.

OBJECTIVES

Working hypothesis

We hypothesize that the use of targeted genomic and proteomic techniques on urine samples from patients suspected of having PCa can provide a pattern of biomarkers able to efficiently distinguish between the presence or absence of a carcinoma, both in a first biopsy setting and in patients with a previous diagnosis of HGPIN.

General objective

The main objective of this work is to develop a non/minimally-invasive method, using protein or mRNA biomarkers, for the early and accurate diagnosis of PCa in urine obtained after DRE.

This could, in the future, help to improve the detection and management of PCa, avoiding the over-diagnosis and over-treatment associated with the currently used screening methods.

In the long term this will help to reduce the number of unnecessary biopsies practiced (both first and repeat PB) and, therefore, reduce unwanted secondary effects and health care costs. Furthermore, this will help to increase the survival of patients diagnosed with PCa.

Specific objectives

1 Identification of new protein biomarkers for PCa in urinary exosome-like vesicles

1a. Establishment of a suitable protocol for the isolation of ELVs from urine

The gold-standard method for vesicles isolation remains the differential centrifugation-based protocol. The first objective of this project will be to improve it and to and adapt it to the specific requirements of this type of study.

In this scenario, the desired parameters are: vesicles purity, reproducibility of the method and time/cost effectiveness.

1b. To characterize at morphological and molecular level urinary ELVs

The isolated ELVs will be visualized, measured, counted and studied at the molecular level, to verify the enrichment in exosomes in our vesicles population.

This objective is comprised of two parts:

(i) Structural characterization: Electron microscopy, Nanoparticle Tracking Analysis
(ii) Molecular characterization: mRNA, miRNA and protein level

1c. To identify, by label-free quantitative mass spectrometry, highly PCa specific urinary ELV-derived proteins

This point forms the core of the project. By LC-MS/MS, we will determine the differential molecular profiles in urine ELVs of patients with PCa, as compared to age matched controls.

This objective is comprised of three parts:

(i) Optimization of the methods for protein extraction and digestion.
Due to the extremely low amount of protein recovered in the urinary ELVs fraction, it is necessary to carefully set up the workflow and to utilize specifically designed methods (such as filter-aided sample preparation (FASP)), in order to minimize sample loss and increase the reproducibility.

(ii) Comparison of the proteomic profile of urinary ELVs isolated from PCa patients *vs*. ELVs isolated from benign samples by label-free LC-MS/MS.

(iii) High- throughput proteomics data analysis; label-free quantitative proteomics analyses generate a huge amount of data that needs to be processed using sensitive and complicated algorithms. To date, there is no consensus about the best way to proceed, and therefore we assayed different methods of quantification.

1d. To verify the candidate proteomic profile of ELVs by targeted proteomics

The most promising candidate biomarkers found in objective 3 will be verified by a targeted proteomics approach, such as Selected Reaction Monitoring (SRM).

To increase the reliability of the results, in this phase we analyzed a new and larger and independent cohort of samples, including PCa patients in all the stages of the malignancy, as well as benign prostatic conditions as controls.

1e. To characterize, *in vitro*, selected biomarker candidates

Based on biological significance, some new marker candidates will be chosen for further characterization, seeking to confirm their intracellular location in endosomes.

2 Evaluation of the performance of RNA-based PCa biomarkers in HGPIN patients referred for repeat biopsy

2a. To establish the best urinary mRNA data normalization strategy

Currently, there is no consensus on the best way to normalize gene expression data from urine samples, due to the lack of reliable endogenous control genes. Therefore, the first step of our project will be focused in the selection of a suitable gene for use as a reference control.

2b. To identify, by RTqPCR, highly specific mRNA biomarkers able to differentiate between HGPIN and PCa cases

The main body of the project will be the differential expression analysis, by RTqPCR, of a panel of selected genes in urine samples of isolated HGPIN patients (n=90) as compared with PCa patients (detected in second or subsequent repeat biopsy) (n=24).

MATERIALS & METHODS

1 Human samples

All samples (except for the healthy donors) were obtained from males undergoing the standard procedure for PCa detection at the Urology Service of the Vall d'Hebron University Hospital. Written informed consent was obtained from all the study participants and samples were coded to ensure sample tracking and confidentiality on patient/donor identity.

Patients were asked to urinate after DRE, a procedure included in the standard process for detection of PCa. DRE involves applying severe digital pressure to the prostate, what stimulates the release of products contained in the gland, as well as the desquamation of cells from the prostatic epithelia, thus enriching the urine with prostate-derived molecules (135).

Urine (30-50mL) was collected in urine collection cups, kept on ice, transported to the lab and processed within 2h of their collection. The urine samples were centrifuged at 2500xg for 10min at 4 C. From this point pellet and supernatants were processed separately. Cellular pellets were washed twice with cold PBS and finally resuspended 1:5 in RNALater (Ambion; Life Technologies/Thermo Fisher Scientific, Waltham, MA, USA) and stored at -80 C until RNA extraction. Supernatant, containing the ELVs, was supplemented with a cocktail of protease inhibitors (Sigma-Aldrich, St Louis, MO, USA) and stored at -80 C until its use (Fig. 13).

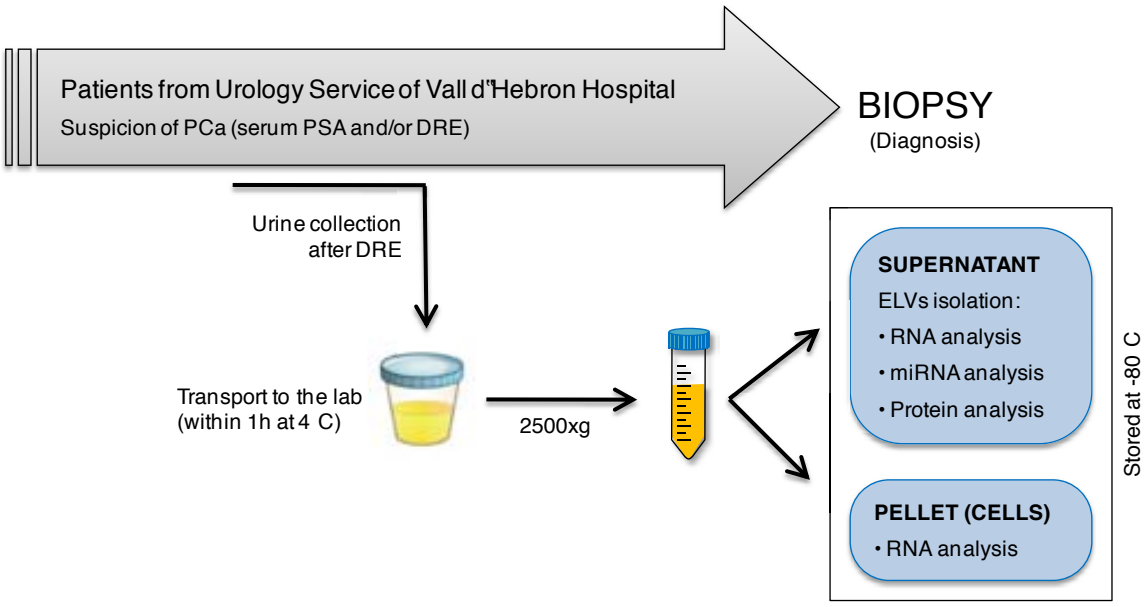

Figure 13. Urine samples collection and processing. After the initial centrifugation, supernatant (containing ELVs) and cellular pellet are processed and stored separately. ELVs and cells were used for different approaches.

1.1 Protein biomarkers in ELVs

1.1.1 Patients selection and inclusion criteria

Samples were obtained from men with suspicion of PCa due to abnormal DRE and/or serum PSA levels higher than 4ng/ml, referred for a first PB.

For this study we selected patients with a diagnosis of PCa and age matched controls, including those with benign pathologies of the prostate. Patients with other known tumors and/or previous PCa therapies were excluded from the study. The definitive diagnosis of the patients was achieved after PB. Samples were excluded in punctual cases, such as a clinical history of other cancers or the presence of an unrelated chronic or acute severe illness.

1.1.2 Samples used for the establishment of the ELVs isolation method

During this part of the project, random pooled samples obtained after DRE, regardless of the presence or absence of PCa. In addition, samples without previous DRE were obtained from healthy donors.

1.1.3 Clinico-pathological conditions of samples used in the characterization phase

For the characterization of the ELVs present in the urine samples after DRE, we used two pools of urines, one of them containing only benign samples and the other only PCa samples (Table 7).

Table 7. Summary of samples selected for the characterization phase.

	Sample	Age	Diagnosis / Gleason score	mL used
Benign	1	62	BPH	16
	2	85	BPH	20
	3	72	PIA	20
	4	74	PIA	20
	5	70	PIA	23
PCa	1	55	6 (3+3)	20
	2	78	7 (3+4)	25
	3	67	7 (4+3)	20
	4	82	7 (4+3)	20
	5	65	8 (4+4)	22

1.1.4 Clinico-pathological conditions of samples used in the discovery phase

For the proteomics discovery phase we used a total of 24 urine samples obtained after DRE from men undergoing PB. The samples were distributed in 3 groups (Table 8). In the benign group, patients presented BPH as only pathological condition.

Table 8. Summary of samples selected for the discovery phase.

Group	Number of samples	Age	Gleason score
Benign	8	63,8 (58 - 68)	-
Low risk PCa	8	69,4 (58 - 78)	7 (3+4)
High risk PCa	8	73,1 (60 - 85)	>7

1.1.5 Clinico-pathological conditions of samples used in the validation phase

For the validation phase, we used an independent and larger cohort of samples (n=107) (Table 9). As explained above, all urine samples were obtained after DRE from men undergoing PB.

Table 9. Summary of samples selected for the validation phase.

Group	Number of samples	Age	Diagnosis / Gleason score	No. cases
Benign	54	65,6 (53 - 78)	BPH	15
			PIA	16
			HGPIN	23
PCa	53	67,7 (51 - 87)	6 (3+3)	14
			7 (3+4)	8
			7 (4+3)	12
			8 (4+4)	12
			9 (4+5)	4
			9 (5+4)	2
			10 (5+5)	1

1.2 RNA biomarkers for HGPIN patients

1.2.1 Patients selection and inclusion criteria

All urine samples were obtained from the Department of Urology of the Vall d'Hebron Hospital in Barcelona between 2008 and 2013 and were taken from patients subjected to a repeat PB because of a previous biopsy result of HGPIN. Samples were collected in all cases within days before the second biopsy. Their first biopsy was recommended due to increased serum PSA levels (>4ng/mL) and/or an abnormal diagnostic DRE. Patients with other known tumors and/or previous PCa therapies were excluded from the study.

The diagnosis of all patients was achieved by transrectal ultrasound (TRUS)-guided PB. Biopsies were performed using an end-fire ultrasound transducer Falcon 2101 (BK Medical, Herlev, Denmark) and an automatic 18-gauge needle (Bard, Covington, GA, USA). The minimum number of cores removed in every procedure was 10, and between 1 and 8 additional cores were removed, according to the Vienna nomogram (27).

The study population consisted of 114 men, with a first PB result of HGPIN, who underwent at least two repeat PB. In 24 cases the second or subsequent biopsies revealed the presence of PCa, whereas in the rest of cases the patients were diagnosed with a benign pathology (Table 10).

Table 10. Clinico-pathological conditions of patients included in the study.

	Benign conditions		**Prostate cancer**	
	Total cases	90	Total cases	24
Clinical data		Average (min-max)		Average (min-max)
	Age	65.5 (49.2-82.7)	Age	68.5 (54.7-80.6)
	PSA level	7.3 (2.4-27.1)	PSA level	6.6 (4.4-14.0)
	free PSA	1.4 (0.2-6.3)	free PSA	1.1 (0.4-2.6)
	PSA ratio	18.6 (3.0-38.9)	PSA ratio	16.7 (6.7-34.1)
1st biopsy		Average (min-max)		Average (min-max)
	No. cores HGPIN	3 (1-8)	No. cores HGPIN	4.1 (1-8)
2nd biopsy		No. cases		No. cases
	HBP	21	G < 7	11
	PIA	17	G 7	10
	HGPIN	52	G > 7	3

G, Gleason score

2 ELVs isolation from urine

ELVs were purified following a differential ultracentrifugation method. Cell-free urine samples stored at -80ºC were thawed and first centrifuged at 16,500xg, 20min, to pellet the fraction of larger EVs and any possible remaining cell debris (P1). The supernatant (S1) was ultracentrifuged at 100,000xg for 120min (Sorvall ultracentrifuge, with AH-629 rotor). The resulting pellet was washed with PBS and centrifuged again at 100,000xg, 60min.

The final pellet was collected by re-suspension in the adequate buffer/solution, according to the desired use:

- To observe the exosomes by TEM, these were directly resuspended in fixing solution with paraformaldehyde 4% and samples were processed as described below.
- For protein studies, the final pellet was resuspended in 50μL PBS, of which 5μL were stored for NTA analysis, and the rest was mixed with 50μL RIPA 2X buffer.
- In the case of RNA and miRNA, the exosomes-enriched pellet was resuspended in the lysis buffer of the selected kit. RNeasy and miRNAeasy kits (Qiagen, Hilden, Germany) were used for RNA and miRNA extractions, respectively.

In an effort to improve this basic method, we assayed several modifications, as described below.

2.1 DTT treatment

In order to break the THP fibers and release the ELVs that could remain trapped in their net, P1 was treated with DTT (37ºC, 10min), and centrifuged again at 16,500xg, 20min. The supernatant (S2) was mixed with S1 before proceeding with the ultracentrifugations.

2.2 Sucrose cushion

Exosomes are known to “float” at a density of 1.13–1.15g/mL. Thanks to this distinctive feature they can be further purified from other contaminants by means of ultracentrifugation on continuous or discontinuous density gradients.

After the first ultracentrifugation, the pellet (enriched in ELVs) was resuspended in PBS 1X and layered on top of a density cushion composed of 20mM Tris/30% sucrose/deuterium oxide (D_2O)/HCl pH 7.35 (3.5mL). This was centrifuged at 100,000xg for 1h, and the floating vesicles were collected from the cushion layer by needle puncture. Finally, this fraction was centrifuged again at 100,000xg for 1h to eliminate the sucrose and the pellet was recovered by re-suspension in PBS 1X.

2.3 0.2µM filter

Since exosomes have a maximum size of ~150nm, the addition of a filtering step (0.2μM pore filter) might help purifying them from larger vesicles or other contaminants. In our case, this step was performed before the first 100,000xg ultracentrifugation.

2.4 RNAse treatment

In the case of the samples used for RNA or miRNA studies, the pellet resulting from the first ultracentrifugation was treated with RNAse A (Sigma-Aldrich) to degrade any possible non-exosomal (and therefore unprotected) RNA in co-precipitation. The RNase A was removed during the second ultracentrifugation step.

2.5 Trypsin treatment

To test whether or not specific proteins are inside or outside (attached to the membrane) of the ELVs, it is possible to treat these with trypsin during the isolation process. Specifically, the pellet resulting from the first ultracentrifugation was incubated for 20min at 37ºC with 0.1mg/mL of trypsin, as suggested in (235). This enzyme digests the proteins that are not protected by the lipid membrane, and consequently these are lost during the next ultracentrifugation step.

3 ELVs visualization and measurement

3.1 Transmission electron microscopy

TEM imaging of ELVs was conducted in collaboration with the Electron Microscopy Unit in the Centre Científic i Tecnològic from the University of Barcelona, Hospital Clinic. TEM imaging of ELVs was performed by two different methods: resin embedding of the samples and negative staining.

For the resin embedding, pellets recovered from the ultracentrifugation, containing the exosomes, where in the first place fixed with 2% glutaraldehyde for 2h at RT. Later, the samples were washed with PBS 1X by centrifugation, and resuspended in PBS 1X. A similar volume of 2% OsO_4 was added, and samples were incubated o/n at 4ºC. Finally, samples were centrifuged again, pellets were dehydrated in ethanol-acetone and embedded in resin. Resin blocks were cut using an ultramicrotome.

For the negative staining, exosomal preparations fixed with 4% paraformaldehyde were deposited on Formvar/Carbon-coated grids, which were negatively stained with uranyl acetate.

All preparations were examined using a transmission electron microscope JEOL JEM 1010 (Japan Electron Optics Laboratory Co., Tokyo, Japan).

3.2 Nanoparticle tracking analysis

The nanoparticle tracking analysis (NTA) was conducted in collaboration with the Grup d'Enginyeria de Materials (GEMAT) in Ramon Llull University, Institut Químic de Sarrià. Vesicles present in purified samples were analyzed by NTA using the NanoSight LM14 system (NanoSight Ltd., Amesbury, UK), configured with a high sensitivity digital camera system (Hamamatsu C11440 ORCA-Flash2.8, Hamamatsu City, Japan). Videos were analyzed using the NTA-software (version 2.3), with the minimal expected particle size, minimum track length, and blur set to automatic. Camera shutter speed and camera gain were set to maximum. Camera sensitivity and detection threshold were set close to maximum (15 or 16) and minimum (2 to 5), respectively, to reveal small particles. Ambient temperature was ranging from 23 to 25ºC. Samples were diluted in miliQ particles-free water.

During the discovery phase, one video of 60 seconds duration was recorded for each sample. For the samples of the validation phase, 3 videos were recorded and average measurements and standard deviations were calculated.

4 Cell culture and *in vitro* experiments

4.1 Cell lines

In our experiments we used the commercially available PCa cell lines PC-3, LNCaP and DU145, all of them obtained from American Type Culture Collection (Manassas, VA, USA).

4.2 Culture conditions

All cell lines were cultured in RPMI medium (PAA) supplemented with 10% fetal bovine serum (FBS; PAA Laboratories, Pasching, Austria), penicillin/streptomycin (1:100; Gibco; Life Techonologies/Thermo Fisher Scientific, Waltham, MA, USA) and L-glutamine (Gibco).

Plates were kept at 37ºC in a humidified atmosphere of 5% CO_2. For general maintenance of cells, they were replated two times per week. Only cells under passage number 30 were used in experiments.

4.3 Transfections

The plasmid containing the Integrin β3 sequence was purchased from Addgene (Plasmid 27289) (236).

Transfection was performed using Lipofectamine 2000 (Life Technologies), following manufacturer"s instructions. Cells were incubated with the reagents for 2-3h, and then the medium was replaced with fresh antibiotics-free medium. Protein expression was tested 24 or 48h after transfection.

4.4 Immunofluorescence

Cells used for immunofluorescence (IF) were always previously transfected with the plasmid containing Integrin β3. Transfections were carried out on 6-well plates, and cells were allowed to recover for 24h before seeding on coverslips.

Coverslips were coated with poly L-lysine 0,1mg/mL (Sigma-Aldrich) for 5min, and allowed to dry for at least 45min. Cells were then seeded at a density of 50,000 cells/well.

After 24h, cells were fixed with 4% paraformaldehyde for 20min at RT. Permeabilization was performed using 0,1% Triton X-100 for 10min at 4°C. Finally, a blocking step was performed with 10% FBS for 30min at RT.

Coverslips were incubated with primary antibody (appropriate dilution in 0.1% BSA) for 30min at RT, washed, and incubated with secondary antibody (appropriate dilution in 0.1% BSA) for 30min at RT. In experiments aimed to detect only one protein, nuclei were stained with TO-PRO-3 (Life Technologies).

Finally, coverslips were mounted with Vectashield and sealed with nail polish. Analysis of the cells was carried out with a confocal laser scanning microscopy Leica DMRB (Leica, Cambridge, UK).

4.4.1 Antibodies

Late endosomes marker: Anti-CD63 (NKI-C3) was produced in the laboratory of Dr Jacques Neefjes (NKI, Amsterdam) (dilution 1:100).

Studied PCa biomarker: Anti-αVβ3 (dilution 1:50; Merck Millipore, Darmstadt, Germany).

Secondary antibodies: Rabbit anti-Mouse Immunoglobulins/FITC (dilition 1:50; Dako Cytomation, Glostrup, Denmark) and Alexa Fluor® 594 Goat Anti-Rabbit IgG (H+L) Antibody (dilution 1:400; Life Technologies/Thermo Fisher Scietific).

5 Protein techniques

5.1 Protein extraction

5.1.1 From cells

Cells were scrapped from the culture plates and centrifuged at 500xg 5min, washed with PBS and centrifuged again at 500xg 5min. RIPA 1X lysis buffer was then added to the cell pellet and it was kept in a shaker at 4ºC for at least 30min, to facilitate the rupture of the cells. After this incubation, the mix was passed through a 20 gauge syringe needle to improve cell lysis. Finally, cell lysis product was centrifuged at max speed for 15min and the supernatant was stored at -20ºC.

5.1.2 From ELVs

Pellets recovered from the ultracentrifugation and resuspended in RIPA 1X lysis buffer were frozen at -20ºC. After thawing, samples were disrupted by sonication (LABSONIC M, Sartorius Stedim Biotech, Goettingen, Germany) at 100% amplitude for 4 pulses of 5 seconds each separated by 5 seconds pauses on ice. The extracted proteins were stored at -20ºC.

5.2 Protein quantification

An aliquot of each urine ELVs sample preparation was used for protein quantity estimation using the DC Protein Assay (Bio-Rad, Bio-Rad Laboratories, Hercules, CA, USA), following the manufacturer"s instructions.

Cell culture derived protein samples were quantified using the Coomassie (Bradford) Protein Assay Kit (Pierce/Thermo Fisher Scientific).

Samples, usually diluted 1 in 10, were compared in triplicates against serially diluted BSA as standard.

5.3 Western blotting

Exosome proteins were separated by 10% SDS-PAGE under reducing or non-reducing conditions and transferred to PVDF membranes. For blocking, membranes were soaked in 5% non-fat dried milk in TBS-Tween20 (0.01%). Proteins were immunodetected using antibodies against the protein of interest, always overnight at 4°C. Then the membranes were washed and incubated with a secondary HRP-coupled antibody 1h at room temperature. Finally, HRP signal was revealed using the Immobilon Western HRP Substrate (Merck Millipore), or ECL Western Blotting System (GE Healthcare, Little Chalfont, Buckinghamhsire, UK). If necessary, the intensity of the bands was densitometrically quantified using the ImageJ software (v. 1.45s).

5.3.1 Antibodies

Exosome markers: anti-TSG101 (dilution 1:500; Abcam, Cambridge, MA, USA), anti-CD81 (dilution 1:100; Santa Cruz Biotechnology, Santa Cruz, CA, USA), anti-Flotillin-1 (BD Biosciences, San Jose, CA, USA) and anti-Rab5 (dilution 1:2000; Abcam).

Prostate specific proteins: anti-PSA (dilution 1:100; Dako Cytomation)

Studied PCa biomarkers: anti-ITGB3 (dilution 1:2500; BD Biosciences).

Secondary antibodies: Rabbit anti-Mouse Immunoglobulins/HRP (dilution 1:2000; Dako Cytomation) and Goat anti-Rabbit Immunoglobulins/HRP (dilution 1:2000; Dako Cytomation).

5.4 Protein digestion

Filter-Aided Sample Preparation (FASP) was performed using a 10kDa molecular weight cutoff filter (Millipore), essentially according to the procedure described by Manza *et al*. (237). 20μg of sample in RIPA 1X buffer were loaded in the filter unit and washed twice with 8M urea, by centrifuging at 14000xg 15min. Proteins were reduced with 10mM DTT for 1h at RT, and alquilated with 30mM IAA 30min in the dark. The reaction was stopped with 37.5mM NAC (15min), and the solutions were removed by centrifugation at 14000xg 15min. The samples were then washed once with 1M urea. The resulting concentrate was diluted with 40μL of 1M urea, containing 20μg of trypsin, and it was incubated overnight 37ºC for the digestion of the proteins. Finally, tryptic peptides were collected in

a clean tube, by centrifugation at 14000xg 10min, and this filtrate was acidified with 0.3-0.5µL of concentrated formic acid. Samples were stored at -20ºC until further analysis.

5.5 LC-MS/MS

5.5.1 Experiments

Proteomic analysis by LC-MS was conducted in collaboration with the Proteomics Platform in the Parc Científic de Barcelona. LC-MS analysis was carried out using a label-free approach. After digestion, the samples were diluted in formic acid 1% and 500ng of protein were injected into a C18 precolumn (75µm Oi, 25cm, nano Acquity, 1.7µm BEH column, Waters Corporation, Milford, MA, USA). The peptides were separated with a flow of 250 nL/min, using a 180min gradient from 2 to 35% followed by a 10min gradient from 35 to 60%, both of acetonitrile containing 0.1% of formic acid. The eluted peptides were ionized using a fused-silica tip (PicoTipTM, New Objective, Woburn, MA, USA), applying an approximate voltage of 2000V.

Peptides masses (m/z 350-1700) were measured in Full Scan MS with a resolution of 60,000 FWHM at 400 m/z in an Orbitrap Velos mass spectrometer (Thermo Fisher Scientific). CID MS/MS acquisition was performed following a data-dependent strategy, selecting up until 10 of the most abundant peptides (with at least 500 counts) for fragmentation, using helium as collision gas with a normalized collision energy of 38%.

5.5.2 Data analysis

Analysis of the resulting data was carried out measuring the ion peak intensities and applying four different workflows (described below), in order to increase the reliability of the results.

For representation of the results, Venn diagrams were created using the VENNY web application (238).

Workflow 1: Progenesis LC-MS

First, data were analyzed with the software Progenesis LC-MS (Nonlinear Dynamics, Newcastle upon Tyne, UK). This is a commercial software that has been specifically designed to quantify relative amount of proteins in label-free proteomics approaches. This platform has all the necessary tools to carry out the complete analysis process in an

integrated manner. Raw data were acquired with Thermo Xcalibur (v.2.1.0.1140; Thermo Fisher Scientific) and .raw files were converted into Mascot generic files (MGF) with Proteome Discoverer software (v.1.3.0.339, Thermo Fisher Scientific). The conversion of the raw data (binary files) to the standard MGF peak list format is necessary before it can be used for input in proteomic search engines.

The basic steps performed with the Progenesis LC-MS software were as follows.

1. Map alignment to warp the 2D maps of different replicate runs to remove effects derived from peptides eluting at different times from the LC stage in different runs, ensuring that same-peptide signals are compared.
2. Feature detection, comprising the identification of the isotope pattern of the peptide, including the separation of overlapping peptides, and quantification using an area-under-the-curve method.
3. Peptide identification using an external search engine. Identification was performed using the Sequest browser (Thermo Fisher Scientific), against the SwissProt database (v. Oct. 2012). Protein identifications with at least two identical peptides were considered significant. This generated list of proteins was the one used for comparison purposes with previously published exosomal protein lists.
4. Statistical analysis using the abundance signals for the features matched to an identified peptide.

Workflow 2: MSstats

Protein relative quantification was achieved by extracting the peptide areas with the Proteome Discoverer software suite (v1.3.0.339, Thermo Fisher Scientific) followed by median normalization. Only unique peptides per protein were used for the differential protein quantification analysis with the linear mixed-effects model implemented in the R package MSstats v1.0 (239). When a peptide was missing completely in a condition, the nointeraction (default) option was used, which indicates that the quantified interferences are random artifacts that should be considered as noise.

Workflows 3 and 4: OpenMS + different R packages

Raw data files were converted to mzML (an open data format for storage and exchange of MS data, proprietary file formats such as the Thermo Fisher Scientific .raw have to be

converted to an open data format before they can be used in open source software pipelines) and MGF using the ProteoWizard msconvert program (240).

MS/MS data was searched against Uniprot SwissProt Homo sapiens database 2012-10-30 using Mascot software v2.4 (Matrix Science, London, UK). Search tolerances were 200ppm for the precursor and 0.5m/z units for fragment ions. Two missed cleavages were permitted for semitryptic peptides. Carbamidomethylation of cysteines was set as a fixed modification, while methionine oxidation, acetylation of protein N-terminal and pyro-glu from E and Q peptide N-terminal were set as a variable modification. Searched peptide-spectrum matches (PSMs) were then subjected to PeptideProphet (v4.6) validation using accurate mass model and semisupervised approach (241). Finally, ProteinProphet (v4.6) was used for protein inference using Occam"s razor option.

Quantitative data processing was carried out with OpenMS software (242). Briefly, high-resolution MS1 profile peaks were centroided to their corresponding monoisotopic peaks using PeakPeakerHiRes algorithm with signal-to-noise set to 0. The centroided data was then used for feature detection (FeatureFinderCentroided algorithm). Mass trace m/z tolerance was set to 0.025m/z units, peaks were required to present a symmetric shape, and minimum and maximal feature charge state were 2 and 5, respectively. Confident PSMs (minimum PeptideProphet probability = 0.90) were used to annotate features; in addition, feature-PSM was only matched if their experimental m/z was at most 5 ppm apart, the elution time of the PSM was at most 5 seconds from the feature elution time range, and the charge state of both feature and PSM also matched. Annotated LC-MS feature maps were then aligned using MapAlignerPoseClustering algorithm (based on a non-linear model) to correct peptide elution time fluctuations using high confidence annotated features in common across replicates as landmarks for algorithm correction reference. Finally, aligned LC-MS feature maps were linked (FeatureLinkerUnlabeledQT algorithm) across all samples, generating a consensus feature map used for all downstream statistical analyses.

All the statistical analyses were performed using R programming packages. First, consensus feature map was imported into R and intensity values transformed (logarithm base 2). To correct for systematic errors, data normalization was performed using EigenMS algorithm from DanteR package (243). Following normalization, differential protein abundance was determined using 2 statistical test approaches. First (workflow 3), peptide-level CensorANOVA algorithm (DanteR package) was applied to the data as described in (244). Note that the CensorANOVA algorithm imputes missing values prior to statistical analysis. In the second approach (workflow 4), log-transformed, normalized

data was converted back to absolute intensity and all feature intensities of a protein were summed up (peptide-to-protein roll-up). Then protein-level ANOVA test was carried out with DanteR package. Finally, statistical test p-values were corrected using Benjamini-Hochberg method (245).

5.6 SRM

Selected reaction monitoring (SRM) analysis was performed in collaboration with the Proteomics Unit in the Centre for Genomic Regulation (CRG), Barcelona. A total of 64 proteins were selected for the targeted experiment by SRM based either on the results from the label free experiment using the different strategies or on the information retrieved from the literature.

5.6.1 Monitored peptides selection

Skyline MS1 filtering (246) was used to extract and process ion intensity chromatograms from MS1 scans of all the identified peptide precursors from the 64 selected proteins across the 24 experiments. Al the ions were manually inspected and the integration of the area of the precursor ions was reviewed.

The extracted area of the peptides was used as input for a new analysis with MSStats v1.0 in which the number of missed values was significantly decreased thanks to the manual validation. New ratios between groups were calculated and, for those proteins that were significantly changing according to this analysis, another MSStats analysis was performed considering each peptide as an independent protein. Then, peptides for the SRM experiment were selected according the following criteria: the difference between the fold change ratio of the individual peptide compared with the fold change of the protein when considering all the peptides (the lower the better); the significance of the change when it was calculated from data from a single peptide and the intensity of the peptide (the more intense the better). In the case of proteins that were not significantly changing, peptides selection was based on their intensity.

5.6.2 Experiments

SRM measurements were performed with unfractionated samples on a hybrid triple quadrupole / ion trap mass spectrometer (5500 Q-Trap, AB Sciex Instruments, Foster, CA, USA) equipped a reversed-phase chromatography 25-cm column with an inner diameter of

75 μM, packed with 1.9 μM C18 particles (NikkyoTechnos Co., Ltd. Japan) and a 2-cm pre-column (Acclaim PepMap 100, C18, 15 μM, 100-A).Loading buffer: H_2O, 0.1% formic acid, eluting buffer: ACN, 0.1% formic acid Flow rate: 250nL/min. Gradient: From 7 to 40% eluting buffer in 60min. Blank runs were performed between the SRM measurements of biological samples to avoid sample carryover. Measurements were done in scheduled SRM mode, using a MRM detection window of 300 seconds and a total cycle time of 2.5 seconds. For each heavy/light pair 5 transitions were monitored.

5.6.3 Data analysis

Transition groups corresponding to the targeted peptides were evaluated with Skyline v2.5 based on co-elution of the transition traces associated with a targeted peptide, both in its light and heavy form; and the correlation between the light SRM relative intensities and the heavy counterpart. Areas of all transitions of either the light or the heavy peptides were summed and the corresponding ratio was calculated. Protein ratios between the two groups were calculated with the linear mixed-effects model implemented in the R package MSstats v2.0 (247).

6 Nucleic acid techniques

6.1 RNA extraction and expression analysis

6.1.1 From cell culture

Total RNA was extracted from cells using the TRIzol reagent (Invitrogen; LifeTechnologies/Thermo Fisher Scientific), according to the manufacturer"s instructions, and stored at -80ºC until retrotranscription step.

RNA extracted from cells was reverse-transcribed to obtain cDNA prior to RT-qPCR reactions. These were performed on a LightCycler machine (Roche Applied Science, Indianapolis, IN, USA), always in duplicate. Data analysis was carried out using the LightCycler 480 software (v. 1.5). For the relative expression analysis, the 2^(-ΔΔCt) method was applied.

6.1.2 From ELVs

For total RNA extraction, we used the RNeasy kit (Qiagen), following the manufacturer"s instructions and stored at -80ºC until retrotranscription step. RNA quality was assessed 2100 Bioanalyzer instrument (Agilent Technologies, Palo Alto, CA, USA).

Since we expected to obtain a very low RNA yield from the ELVs present in urine, cDNA obtained from the reverse transcription reactions was pre-amplified before using it for RT-qPCR with TaqMan PreAmp Master Mix (Applied Biosystems, Foster City, CA, USA).

RT-qPCR reactions were carried out in triplicate on an ABI Prism 7900HT qPCR machine (Applied Biosystems). Data analysis was carried out using the ABI Prism 7900 SDS Software v2.4.1 (Applied Biosystems).

Normalization of data was carried out using the number of ELVs per sample, as determined by NTA, according to the equation Ct+log2(vesicles/mL).

6.1.3 From urine sediment

Total RNA of the urine cellular fraction was extracted using the QIAmp Viral Kit (Qiagen), following the manufacturer"s instructions and stored at -80ºC until retrotranscription step.

Reverse-transcriptase polymerase chain reaction of extracted RNA was conducted to determine expression of and 6 endogenous genes (see Table 15 in the Results section) and 17 target genes (see Table 16 in the Results section). cDNA obtained from the reverse transcription was pre-amplified using RealTime ready cDNA Pre-Amp Master, in combination with RealTime ready Pre-Amp Primer Pools (Roche).

All RT-qPCR reactions were carried out in triplicate on RealTime ready custom qPCR plates (Roche) and fluorescent signals were measured in a LightCycler 480 II (Roche). Data analysis was carried out using the LightCycler 480 software (v. 1.5).

From the initial set of 114 samples, samples with *PSA* Ct values ≥29 were and/or geometric mean of all Ct values ≥27 were excluded due to a low amount of cDNA. To this final cohort, outlier detection by boxplots was applied. Outlier detection was performed by computing the Kolmogorov-Smirnov statistic Ka between each sample"s distribution and the distribution of the pooled data.

Relative gene expression was calculated by the ΔΔCt method as previously described (248). The endogenous reference gene for the data normalization was selected from a

list of 6 commonly used housekeeping genes: Hypoxanthine Phosphoribosyltransferase 1 (*HPRT*), Glyceraldehyde-3-Phosphate Dehydrogenase (*GAPDH*), Delta-Aminolevulinate Synthase 1 (*ALAS1*), TATA Box Binding Protein (*TBP*), Beta-2-microglobulin (*B2M*), Kallikrein-3 / Prostate Specific Antigen (*KLK3*). The selection criteria was the lowest coefficient of variation, lowest Ct geometric mean, without differences between groups (calculated by Mann-Whitney-Wilcoxon test) and with an area between the receiver-operating characteristic (ROC) curve and the no-discrimination line (area under the curve; AUC) close to 0.5, guided by Kılıç *et al*., 2014 (249).

Statistical analysis

Univariate tests and univariate and multivariate logistic regressions were used to examine associations between PCa diagnostic status and testing genes. For this purpose, we used test (250) and Random Forest method for variable importance measurement (251). Both methodologies were evaluated by Leave-one-out cross-validation (LOOCV) to correct the bias estimated from them. Conjointly, we used the ROC analysis to assess genes performance (with 95% confidence interval).

We created all possible models using combinations of the most significant genes obtained in the univariate analysis and applied multivariate logistic regression to them. The Akaike information criterion (AIC) (252) based backward selections were used to drop insignificant terms in all the resulting models via stepwise generalized linear models (GLM) (253) and to obtain better models.

The number of PBs potentially avoided by the use of the proposed biomarkers was calculated by adding up the number of true negatives and the number of false negatives, and divided by the total studied population to turn it into a percentage.

All analyses were performed in R (254).

6.2 miRNA extraction and expression analysis

For extraction of miRNA, miRNeasy (Qiagen) was used, following the manufacturer‟s instructions and stored at -80ºC until retrotranscription step.

The cDNA obtained from the reverse transcription reactions was pre-amplified before using it for RT-qPCR with TaqMan PreAmp Master Mix (Applied Biosystems).

For the miRNA expression profile study in ELVs we used TaqMan Array Human MicroRNA Cards. Reactions were performed on an ABI Prism 7900HT machine (Applied Biosystems). The data analysis was carried out using the ExpressionSuite Software v1.0.2 (Applied Biosystems). Those miRNAs with Ct values >33 or an amplification score ≥1 were regarded as undetected.

Normalization of data was carried out using the number of ELVs per sample, as determined by NTA, according to the equation Ct+log2(vesicles/mL).

6.2.1 miRNA targets analysis

After the miRNA expression analysis, the top deregulated miRNAs were selected for a brief study of their targets. To extract this information, we used miRTarBase (release 4.5, November 2013), a database of experimentally validated miRNA-target interactions (255).

For the study of interactions between the target genes and their enrichment in KEGG pathways, the STRING v9.1 web application was used (256).

RESULTS

RESULTS OF THE OBJECTIVE 1

Identification of new protein biomarkers for PCa in urinary exosome-like vesicles

1 Establishment of the ELVs isolation method from urine samples

1.1 Type of urine sample and DTT treatment

As a first task, we aimed to determine whether or not the collection of the urine directly after the DRE procedure would increase the presence of ELVs in the sample, as it has been described before for other prostate-derived products (135). For this purpose, we collected a total of 5 urine samples directly after DRE and we mixed them (pool post-DRE urine). Moreover, 3 urine samples from healthy donors from the lab were collected and mixed (pool normal urine). Indeed, as shown in Fig. 14, the performance of a DRE right before the sample collection helps enriching the ELVs population in the urine samples.

At the same time, we aimed to improve the ELVs recovery yield, with the addition of a DTT treatment that is meant to break the THP fibers that trap these vesicles in the first steps of the centrifugation protocols. In order to do that, we used the same sample pools explained above. As shown in Fig. 14, DTT treatment produced an increase in the amount of exosomal markers, as well as prostate-derived proteins (such as PSA), detected by Western blot (WB).

1.2 Filtering out the larger components

Once we established the usefulness of the DTT treatment, we sought to further improve the technique by the addition of a filtering step, which would eliminate from the sample all components larger than 200nm (microvesicles, apoptotic bodies, other non-exosome vesicle contaminants, etc.).

In order to have enough starting material, and therefore, be able to compare different methodologies, we pooled different urine samples obtained directly after DRE. The filtering method was then compared with the defined gold standard method (DTT) in 1.1. Purification of ELVs was done in triplicate.

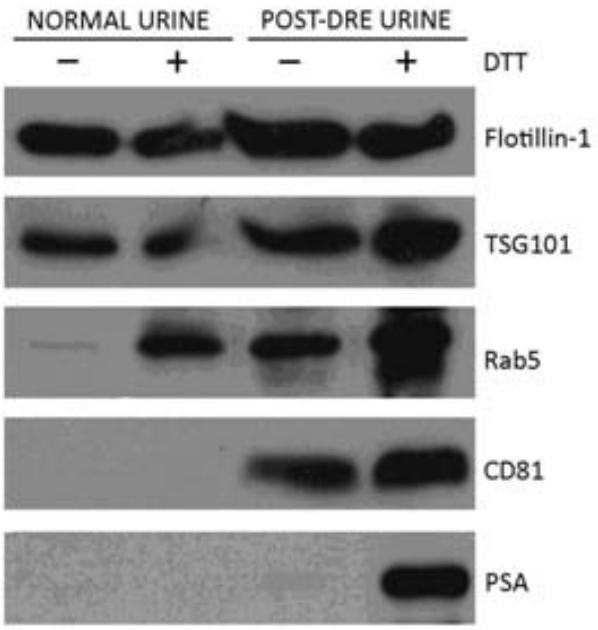

Figure 14. Western blot of isolated ELVs. The exosomal markers FLOT1, TSG101, Rab5 and CD81 were tested, in addition to the prostate-specific protein PSA. Best protein yield and resolution were obtained in post-DRE urine samples, and with DTT denaturing treatment.

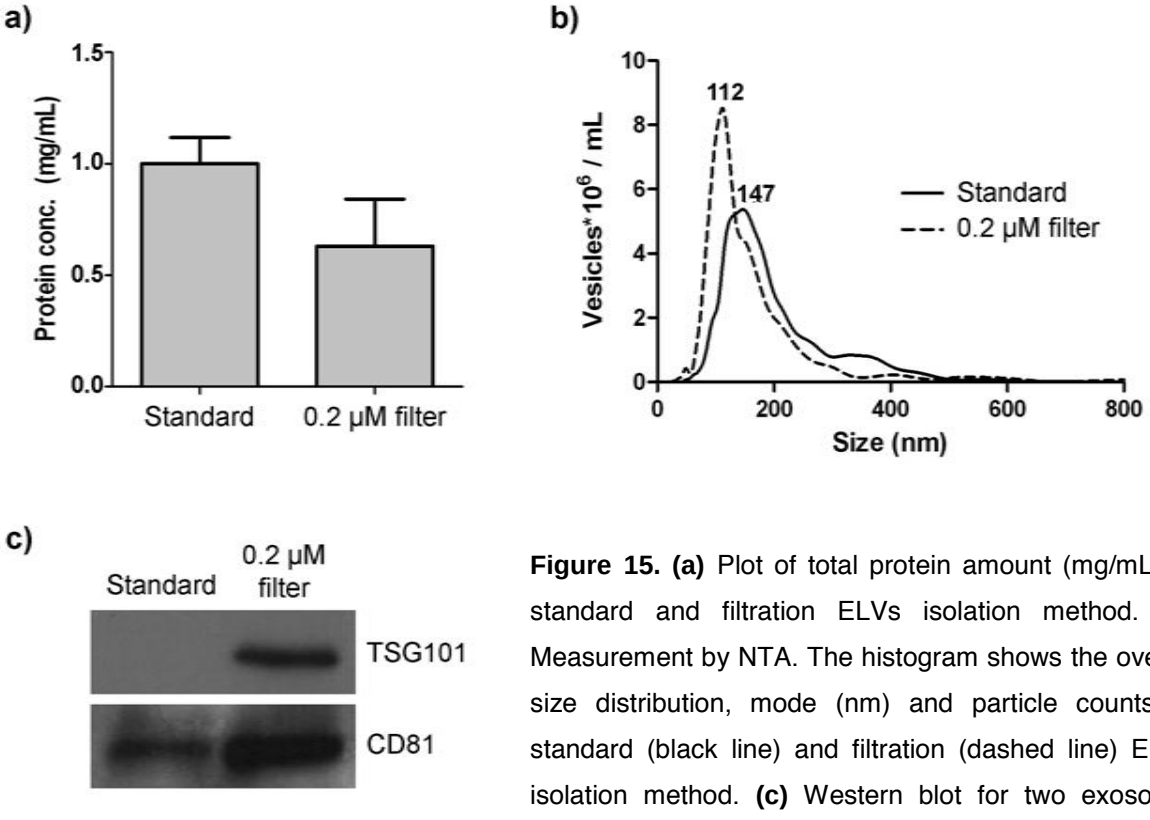

Figure 15. (a) Plot of total protein amount (mg/mL) of standard and filtration ELVs isolation method. **(b)** Measurement by NTA. The histogram shows the overall size distribution, mode (nm) and particle counts of standard (black line) and filtration (dashed line) ELVs isolation method. **(c)** Western blot for two exosomal markers, TSG101 and CD81. These results seem to indicate that the addition of a filtering step causes a loss of material, which most probably corresponds to non-exosomal contaminants.

As expected, with the filtration of the samples, a smaller amount of total protein was recovered (Fig. 15a). Nevertheless, when analyzed by NTA, better results were obtained if the samples were filtered, compared to the method without that step. The general particle size was smaller, which correlates better with the expected size for exosomes, and the distribution peak was narrower, with very few particles above 200 nm (Fig. 15b). These results seem to indicate that the fraction of protein that is lost probably corresponds to larger particles or other non-exosome vesicle contaminants, and therefore that the modified protocol indeed helps improving the purity of the exosomes.

Finally, we verified this observation by WB. Both TSG101 and CD81 (known exosomal markers) were detected with a higher intensity in the filtered samples by WB (Fig. 15c).

1.3 Flotation on sucrose cushion

In any ultracentrifugation protocol, exosomes are co-precipitated with other types of vesicles of the same size, and potentially with big protein complexes or aggregates. To overcome this intrinsic technique limitation, it is possible to take advantage of the characteristic flotation of exosomes in a 30% sucrose cushion (density 1.210g/cm3).

In order to test whether the sucrose gradient can improve ELVs purification we pooled different urine samples obtained directly after DRE, in order to have enough starting material to compare different methodologies. Two pools were created; PCa urine samples and benign (including age-matched controls). The sucrose gradient method was compared with the defined gold standard method (filtering) in 1.2. Purification of ELVs was done in duplicate for each condition.

When we assayed the sucrose method, the first thing noticeable was its poor reproducibility, resulting in a high variability between samples, or even between technical replicates of the same sample.

In Fig. 16, we can observe the vesicles isolation outcome from two pools of samples (Benign and PCa). Compared to the filtering technique, with the sucrose method only equal or less protein was recovered at the end of the process, pointing to a loss of material. However, this loss does not seem to be the same or even similar among all the samples. By WB, we observed a decreased signal of the exosome marker CD81 (benign pool) or, even more remarkable, a high variability between replicates (PCa pool).

These results can be at least partially explained by the high complexity of the technique, which makes it difficult to replicate exactly the same conditions in different experiments.

All in all, we discarded the sucrose method for multiple sample comparison experiments, and decided to use the more reproducible filtering method. As a conclusion we selected filtering method as a gold standard method allowing ELVs purification in a high-throughput fashion.

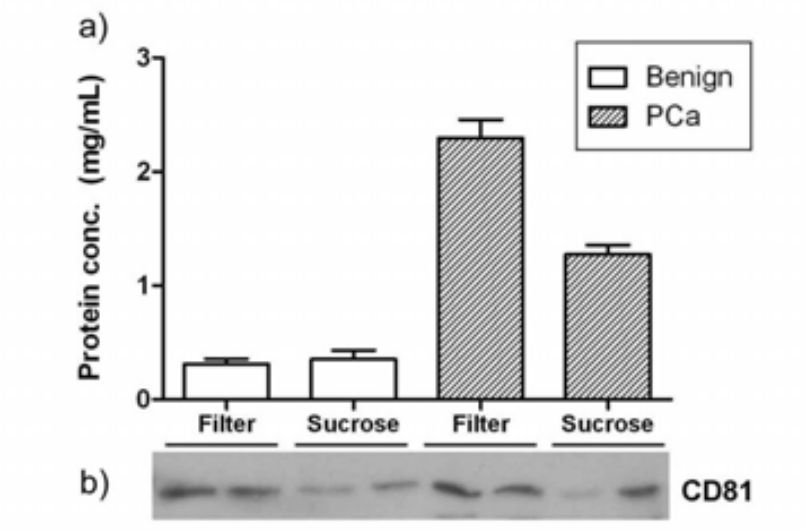

Figure 16. (a) Plot representing the total amount of protein obtained in the different ELVs isolation methods and pools of urine samples. **(b)** Intensity of the CD81 exosome marker in the same samples, detected by WB. Note the high variability of the sucrose method final outcome, between different samples (it causes loss of protein in the PCa pool, but not in the benign pool) as well as between technical replicates (CD81 shows different intensity).

1.4 RNase A treatment

All the modifications commented so far aim to achieve the best possible exosomal protein purification and recovery, as that is the main interest of this thesis. However, in some cases it can be necessary or more convenient to study the mRNA and miRNA contained within the exosomes. Therefore, in this specific task we aimed to standardize RNA and miRNA extraction from urinary ELVs.

As commented in the case of proteins, it is possible that big aggregates containing RNA, as well as free RNA present in the urine, precipitate together with the vesicles during the

ultracentrifugation protocol. We assayed whether or not RNase treatment would degrade the external free RNA, not protected by a lipid membrane.

To do that, we pooled different urine samples obtained directly after DRE, which allowed us to have enough starting material for comparing different methodologies. By using the gold standard ELV purification method described above (filtering method – 1.2), RNAse A (Invitrogen) treatment was tested. The performance of resultant mRNA was assessed by Bioanalyzer (Agilent Technologies).

The Bioanalyzer profile is different depending on RNAse A treatment. Without the treatment we can observe two peaks corresponding to the ribosomal RNA 18S and 28S, which is supposed to exist as free RNA within the urine. When the RNase treatment is applied, the Bioanalyzer profile is similar to that obtained by others (188,257) (Fig. 17). With these results, our decision was to apply the RNAse A treatment in all the studies conducted with RNA from isolated ELVs.

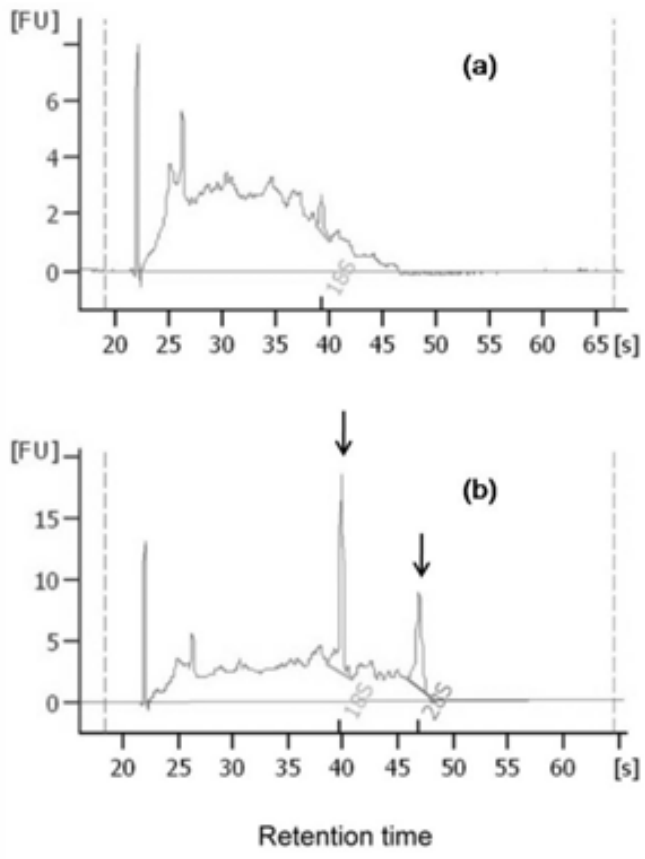

Figure 17. Two examples of exosomal RNA profiling. (a) with and **(b)** without RNase A treatment. In the second case we can see two peaks corresponding to the 18S and 28S ribosomal RNA (arrows), not expected in exosomes, whereas with the RNase A treatment these peaks appear to be degraded. FU, arbitrary fluorescent units.

2 Urinary ELVs characterization

In parallel to the isolation method establishment, we performed a brief characterization of the ELVs recovered from urine samples, measuring their size and number, and assessing their protein, RNA and miRNA cargo.

2.1 Electron microscopy

Due to their small size, the only possible way to visualize the individual particles is by electron microscopy. In our case, we chose to study the morphology of the vesicles both by resin embedding of the pellet and by negative staining. In order to have enough starting material for testing different methodologies, we pooled different urine samples obtained directly after DRE.

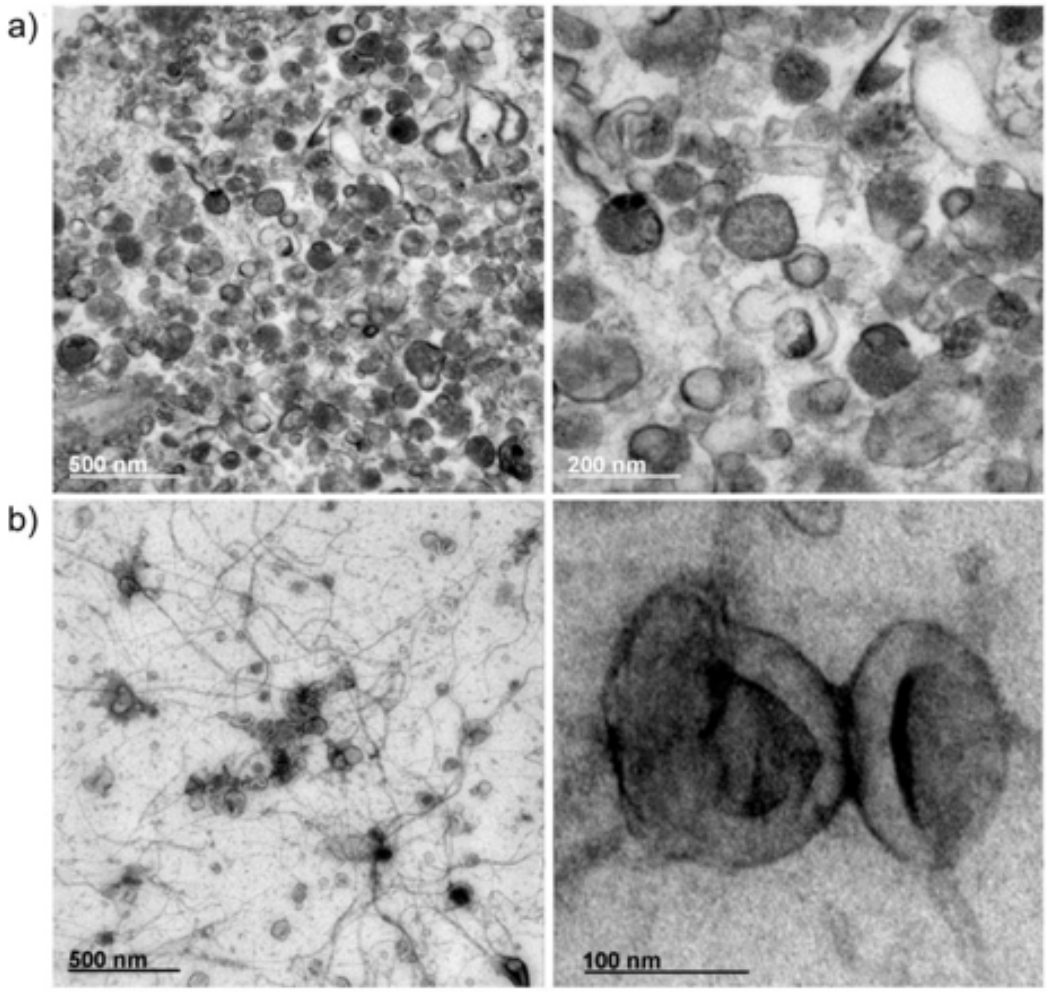

Figure 18. TEM photograph s of ELVs isolated from urine. (a) Pictures taken using the resin embedding technique. We can see that the vesicles contain material of different electron-densities. **(b)** Pictures taken using the negative staining technique. In the left the THP fibers are clearly visible. The vesicles present the typical cup-shaped morphology.

In the resin embedding technique, samples are contained in a resin block that is cut in slices prior to observation, allowing us to see the inside of the vesicles. We could observe the presence of ELVs of the expected size (~100nm) and, moreover, it is possible to appreciate the existence of material of different electron-densities inside the vesicles (Fig. 18a). In the negative staining photographs we could observe rounded vesicles of approximately the same size as before, which show the cup-shaped morphology characteristic of the technique. In the pooled samples used for electron microscopy the THP fibers were not removed during the isolation protocol and, for this reason, we could observe a net of fibers in some of the photographs (Fig. 18b).

2.2 Nanoparticle Tracking Analysis

By NTA it is possible to count and measure at the same time a heterogeneous population of vesicles. In order to estimate the urinary ELVs population characteristics and to assess if they are influenced by changes in the prostatic conditions, we used two pools of samples: one including only benign samples and one including only PCa samples.

From the comparison of the pooled benign and tumoral samples by NTA, we found that the number of ELVs per mL was larger in the case of the PCa samples (Fig. 19). This observation is also supported by the protein and RNA quantification data for these pools

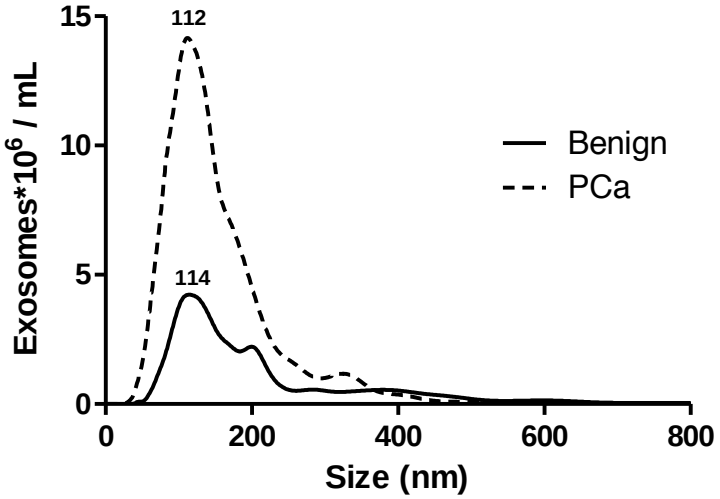

Figure 19. ELVs size and concentration, measured by NTA, for two pools of samples. Each of the pools included only either benign (black line) or PCa (dashed line) samples.

(data not shown), indicating that indeed we obtained a higher amount of vesicles from the PCa pool. Besides, we could observe that the average size of the particles was similar between the two types of sample, a sign of the similar nature of both recovered populations.

2.3 Proof of concept: Qualitative molecular characterization

With the same pools of sample used in the NTA analysis (2.2), we started a molecular characterization phase of the ELVs content. This characterization was carried out at three levels: protein, mRNA and miRNA.

2.3.1 Protein cargo

Several exosomal protein markers were assayed by WB, getting a positive result for all of them, thus indicating that ELVs are a representative part of the total protein in the sample. At the same time, the presence of the prostate-specific protein PSA was also confirmed in the ELVs fraction (Fig. 20).

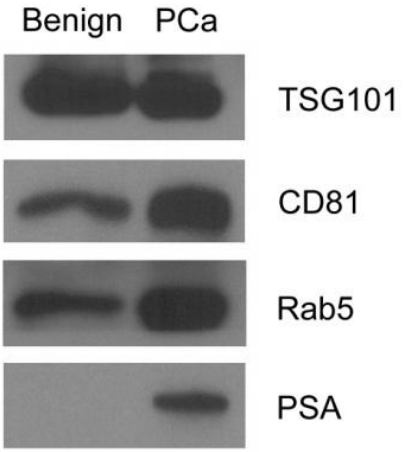

Figure 20. Western blot analysis of ELVs isolated from benign and PCa pools of samples. Several proteins described in the literature as exosomal markers were found. Additionally, the protein PSA was detectable in the PCa pool of samples.

Since PSA is a soluble protein, secreted by cells to the extracellular media where it performs its function, it seemed relevant to further investigate its presence in the vesicles fraction. To elucidate the location of this protein (i.e. inside the vesicles and protected by the lipid membrane or, by the contrary, on the outside), we treated the ELVs with trypsin during the isolation process. The resulting trypsinized vesicles were studied by WB, showing that PSA is completely degraded by trypsin (Fig. 21a). This result leaves us with two possibilities: a) PSA is attached to the surface of exosomes or, b) PSA is part of protein complexes and these are co-isolated with the vesicles.

To test these two possibilities, we isolated ELVs from a new pool of samples (obtained after DRE) utilizing the sucrose isolation method, which helps removing virtually all protein complexes and/or aggregates, thanks to their different flotation density. Surprisingly, in the recovered fraction of exosomes-like floating vesicles we still found PSA (Fig. 21b). However, the PSA/CD81 ratio was lower in the case of the sucrose method. Accordingly, it is possible that a fraction of PSA travels attached to vesicles, while the rest is part of protein aggregates.

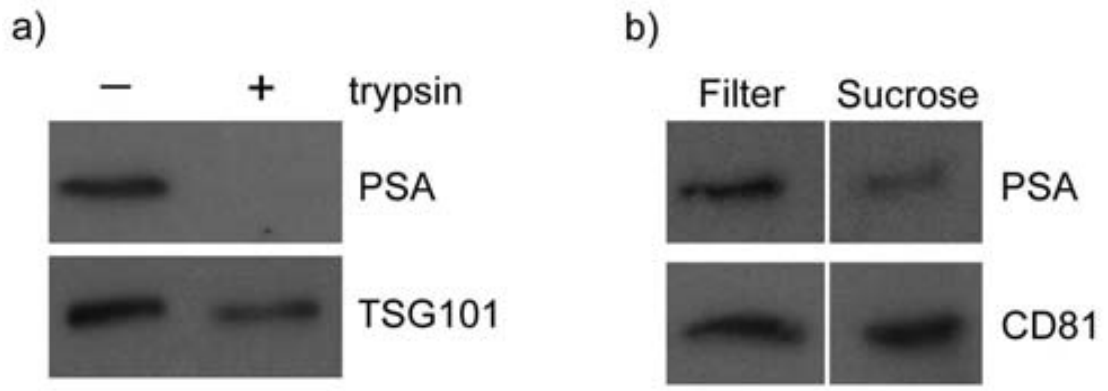

Figure 21. (a) When a trypsin treatment is applied to ELVs during the isolation protocol, PSA is degraded, which clearly indicates its location on the outside of the vesicles. On the contrary, TSG101 is protected from trypsinization, and therefore still detectable. **(b)** Western blot showing the presence of PSA in both the ELVs fraction recovered from the filtering protocol and in the more purified exosomes with the sucrose flotation protocol. CD81 was used as exosomes loading control. The white separation indicates a space between non-contiguous lanes in the same blot.

2.3.2 mRNA cargo

The expression of the prostate-related mRNAs *PSGR*, *PCA3*, *PSMA* and *KLK3* (Kallikrein-3, gene coding the PSA protein) was analyzed by RT-qPCR, together with the expression of the commonly used endogenous gene *GAPDH*. All of them were detectable in our ELV-derived RNA material, with one exception: *PCA3* was undetectable in the benign pool of samples.

At present, there is no standard method of normalization for exosomal mRNA data, since reliable endogenous reference genes have not been described so far. For this reason, the total number of vesicles per mL in the sample was used for expression data normalization.

Our data indicate an overexpression of all the assayed genes in the PCa pool (Fig. 22).

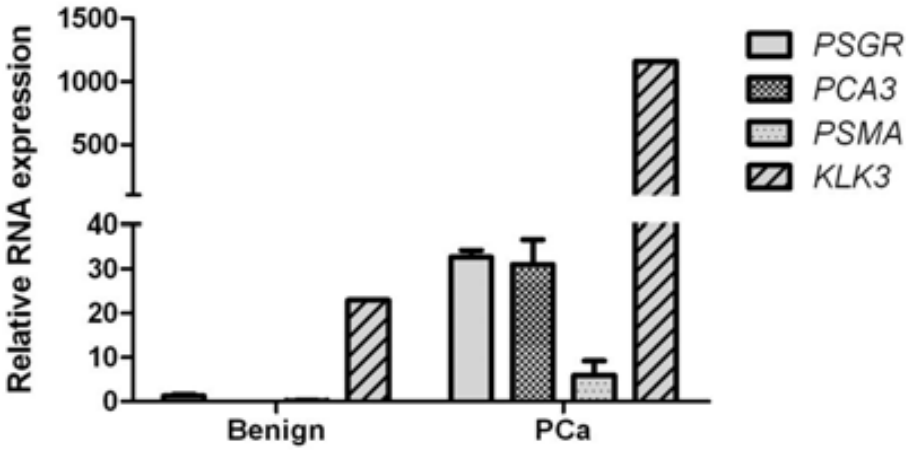

Figure 22. Levels of expression of prostate-derived genes *PSGR*, *PCA3*, *PSMA* and *KLK3* in urinary ELVs, studied by RT-qPCR. Data were normalized by number of ELVs per mL. Results point towards an overexpression of these molecules in ELVs derived from PCa samples.

2.3.3 miRNA cargo

Finally, the pools of samples were used for the expression analysis of a total of 758 miRNAs. In the case of the benign samples, we obtained a quantifiable amount in 307 (40.5%) of miRNAs tested, whereas in the PCa samples we could quantify 343 (45.3%) of them. From these miRNAs, 276 were common to both samples, whereas 31 were specific of the benign group of samples, and 67 were only detected in the PCa pool. Hence, a total of 374 miRNAs (54.6%) were detected in urinary ELVs, independently form the sample origin (Fig. 23).

In order to make an estimation of the relative expression levels of these 374 miRNAs between the two pooled samples, data was normalized by the number of ELVs in each sample. All miRNAs with an increase or decrease higher than 2 fold were considered differentially expressed between the two samples (Fig. 22b). The top 6 miRNAs with a highest fold change between samples, both over and underexpressed, are shown on Table 11.

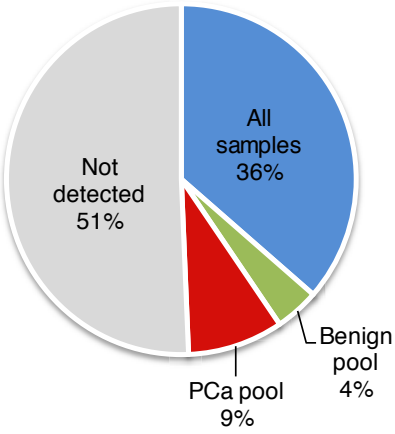

Figure 23. Percentage of miRNAs, from the total of 758 studied, detected in the different types of pooled samples.

Table 11. Top 6 differentially expressed miRNAs between the benign and PCa pools of samples.

Overexpressed in PCa	Underexpressed in PCa
hsa-miR-339-5p	hsa-miR-9-3p
hsa-miR-1300	hsa-miR-223-3p
hsa-miR-590-3p	hsa-miR-142-3p
hsa-miR-196b-5p	hsa-miR-450b-5p
hsa-miR-484	hsa-miR-23b-3p
hsa-miR-886-5p	hsa-miR-450a-5p

Since the main function miRNAs is to act as gene suppressors, the most common scenario in cancer tissues is the down-regulation of those linked to RNA targets involved in cancer development and progression, which are suppressed in normal conditions. To test the implication of the top 6 down-regulated miRNAs found in urinary ELVs in the context of PCa, their targets (only those experimentally validated) were determined and their enrichment in KEGG pathways was studied. The results show that the most represented pathways were *Pathways in cancer* and *Prostate cancer*, while the list included also other pathways related to cells adhesion and hormonal signaling (Table 12 and Fig. 24).

Table 12. KEGG pathways analysis of the top 6 underexpressed miRNAs targets. Cancer and prostate-related networks were found significant.

Pathway	p-value
Pathways in cancer	<0,001
Prostate cancer	0,001
Gap junction	0,009
Small cell lung cancer	0,009
Chronic myeloid leukemia	0,009
Focal adhesion	0,022
Pancreatic cancer	0,022
Oocyte meiosis	0,024
GnRH signaling pathway	0,043

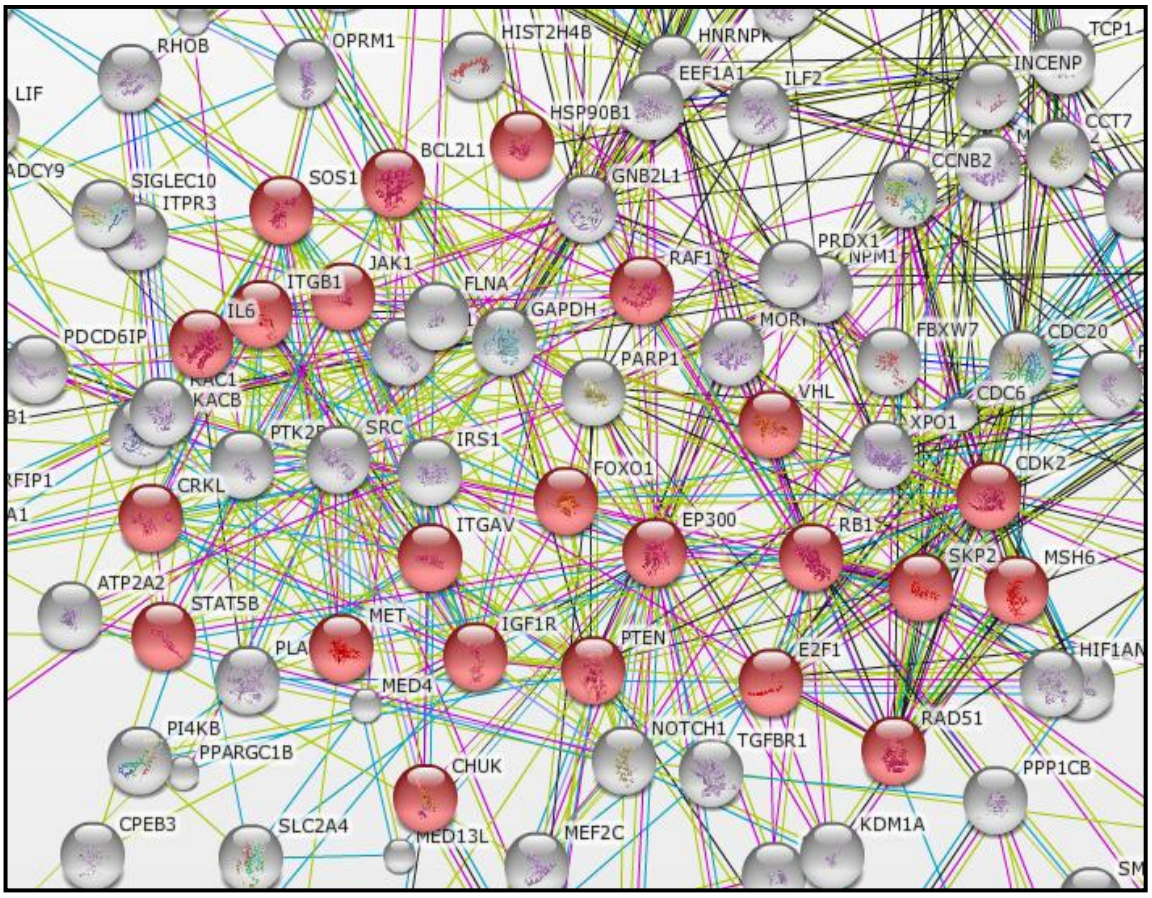

Figure 24. Snapshot of part of the interaction network formed by the targets of the top 6 underexpressed miRNAs. The red color indicates molecules implicated in the *Pathways in cancer* network.

3 Proteomic profiling of urinary ELVs

3.1 Discovery phase

To identify candidate biomarkers for PCa, we compared the ELVs purified from urine supernatants obtained after DRE from 16 PCa patients (8 with Gleason score = 7(3+4), considered low risk; and 8 with Gleason score > 7, considered high risk patients) and 8 from age-matched controls, using LC-MS/MS label-free proteomics technology.

3.1.1 Identified proteins

In the complete set of 24 analyzed samples, a total of 1673 different proteins have been identified. Of them, 983 appeared in at least one sample of each of the 3 studied groups. The average number of proteins identified in each individual sample was 594 (ranging from 143 to 932). The number of proteins identified per sample did not seem to correlate with the study group to which that particular sample belongs.

Among the 1673 proteins detected, we find classical exosome markers (such as CD63, CD9, CD81, TSG101 or Alix), as well as proteins related to the prostate (PSA, PSMA, PAP).

Our results were compared with two urine ELV-derived protein lists previously published by other authors, in order to determine their level of similarity. In the first study used for this purpose, Gonzales *et al*. analyzed a pool of normal urine samples, following a differential ultracentrifugation isolation protocol for the isolation of the ELVs (258). The results were also compared with a more recently published article, where Principe *et al*. studied a pool of post-DRE urine samples from PCa patients, isolating the vesicles by flotation in a sucrose cushion (234). A total of 433 proteins were common to the three lists, among which we find exosomal markers and some prostate-derived proteins. Other prostate-specific proteins were common only between our list and the study using post-DRE PCa samples (Fig. 25).

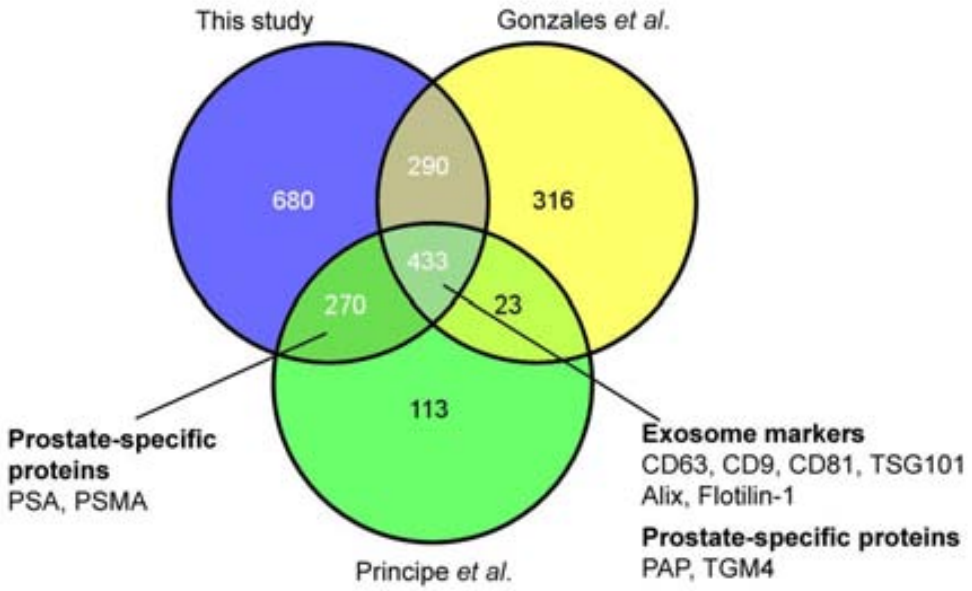

Figure 25. Comparison of proteins identified in our study with other lists published in the literature (234, 258). Note that the exosome markers are common to all the lists, as well as some prostate-related proteins. Interestingly, other prostate-related proteins are only common to our study and Principe et al., who also used post-DRE PCa samples.

3.1.2 Quantification methods comparison

Since the best strategy for label-free proteomic data analysis is still far from being established, we decided to use different data analysis workflows, in order to increase the reliability of the results.

Each one of the four workflows applied yielded a different list of proteins with a differential expression between the groups. The workflow 1 (W1) identified 171 significant proteins, the workflow 2 (W2) 71, the workflow 3 (W3) 278 and the workflow 4 (W4) 288. Only 3 of these proteins were repeated in all the methods, showing the high variability of the analysis, while many others were common to two or three of them (Fig. 26).

Figure 26. Comparison of the number of proteins identified as differentially expressed according to the four different workflows applied.

3.1.3 Candidate biomarkers

To select our candidate biomarkers to be further validated, results from the four workflows were merged. This yielded a list of 157 proteins repeated in at least two methods. However, it is not possible to monitor so many peptides by targeted proteomics at the same time, and this result needed to be revised.

Due to the high similarity between W3 and W4, proteins identified only by these workflows were overrepresented. Consequently, it was decided to narrow down these lists. For this purpose, only the candidates with a p-value<0.01 and fold change >2 or <-2 were taken into account.

After this process, the four final lists were put together again, obtaining a list of 45 proteins repeated in at least two of the methods. To this list, we added 19 proteins (significant in only one of the methods) based on their biological relevance and/or significance level (Table 13).

Table 13. List of proteins identified as deregulated in PCa. These 64 candidate proteins were further validated in a large cohort of patients using SRM.

Gene symbol	Protein	Uniprot accession	Workflow	Peptide selected for SRM
ACPP	**Prostatic acid phosphatase**	P15309	1, 2, 3, 4	SPIDTFPTDPIK
APOA4	**Apolipoprotein A-IV**	P06727	3, 4	LEPYADQLR
ATP6V1B1	**V-type proton ATPase subunit B, kidney isoform**	P15313	1, 2, 3	TVC[CAM]SVNGPLVVLDR
C2orf18	**Solute carrier family 35 member F6 / Transmembrane protein C2orf18**	Q8N357	1, 3, 4	WADNFMAEGC[CAM]GGSK
CA4	**Carbonic anhydrase 4**	P22748	1, 2, 3	FFFSGYDK
CD63	**CD63 antigen**	P08962	2, 4	VMSEFNNNFR
CD82	**CD82 antigen**	P27701	1, 2	GEEDNSLSVR
CIB1	**Calcium and integrin-binding protein 1**	Q99828	1, 2, 4	DGTINLSEFQHVISR
CRYZ	**Quinone oxidoreductase**	Q08257	1, 2	VFEFGGPEVLK
DBNL	**Drebrin-like protein**	Q9UJU6	1, 2	FQDVGPQAPVGSVYQK
DPP3	**Dipeptidyl peptidase 3**	Q9NY33	1, 3, 4	LFVQDEK
DPYS	**Dihydropyrimidinase**	Q14117	1, 4	TC[CAM]TPTPVER
FAM108C1	**Abhydrolase domain-containing protein FAM108C1**	Q6PCB6	1, 2, 4	ELDAVEVFFSR
FAM177A1	**Protein FAM177A1**	Q8N128	1, 2, 4	IASVLGISTPK
GLIPR2	**Golgi-associated plant pathogenesis-related protein 1**	Q9H4G4	1, 3, 4	ASASDGSSFVVAR
GNG4	**Guanine nucleotide-binding protein G(I)/G(S)/G(O) subunit gamma-4**	P50150	1, 3, 4	EDPLIIPVPASENPFR
GNS	**N-acetylglucosamine-6-sulfatase**	P15586	3, 4	SDVLVEYQGEGR
GSS	**Glutathione synthetase**	P48637	1, 2	C[CAM]PDIATQLAGTK
ITGB3	**Integrin beta-3**	P05106	3, 4	EATSTFTNITYR
KLK3	**Prostate-specific antigen**	P07288	1, 4	SVILLGR
NAPRT1	**Nicotinate phosphoribosyltransferase**	Q6XQN6	1, 2	LDSGDLLQQAQEIR
PCYT2	**Ethanolamine-phosphate cytidylyltransferase**	Q99447	3, 4	GPPVFTQEER
PDCD6IP	**Programmed cell death 6-interacting protein**	Q8WUM4	1, 2	ELPELLQR
PGM1	**Phosphoglucomutase-1**	P36871	1, 2, 3	ADNFEYSDPVDGSISR
PPAP2A	**Lipid phosphate phosphohydrolase 1**	O14494	1, 2, 4	GVFC[CAM]NDESIK
PRSS8	**Prostasin**	Q16651	1, 2	LGAHQLDSYSEDAK
PTPN13	**Tyrosine-protein phosphatase non-receptor type 13**	Q12923	1, 4	NFFGPEFVK
RPSA	**40S ribosomal protein SA**	P08865	3, 4	YVDIAIPC[CAM]NNK
RRAS	**Ras-related protein R-Ras**	P10301	1, 4	IC[CAM]SVDGIPAR

SCIN	**Adseverin**	Q9Y6U3	3, 4	SLGGQAVQIR
SLC26A2	**Sulfate transporter**	P50443	1, 2	FVAPLYYINK
SLC26A4	**Pendrin**	O43511	1, 2, 4	SVLAAVVIANLK
SLC4A4	**Choline transporter-like protein 4**	Q53GD3	1, 2, 3, 4	NEFSQTVGEVFYTK
STEAP2	**Metalloreductase STEAP2**	Q8NFT2	1, 2	EIENLPLR
STEAP4	**Metalloreductase STEAP4**	Q687X5	1, 2, 4	ILVDISNNLK
TGM4	**Protein-glutamine gamma-glutamyltransferase 4**	P49221	1, 4	GFIIAEIVESK
TMBIM1	**Protein lifeguard 3**	Q969X1	1, 2, 3, 4	AVSDSFGPGEWDDR
TMPRSS2	**Transmembrane protease serine 2**	O15393	1, 3, 4	VLLIETQR
TOLLIP	**Toll-interacting protein**	Q9H0E2	1, 2, 4	LNITVVQAK
TSG101	**Tumor susceptibility gene 101 protein**	Q99816	1, 2	DGTISEDTIR
TSPAN9	**Tetraspanin-9**	O75954	1, 3	NAWNIIQAEMR
UBC	**Polyubiquitin-C**	P0CG48	1, 2	TLSDYNIQK
VPS26A	**Vacuolar protein sorting-associated protein 26A**	O75436	3, 4	ELALPGELTQSR
VPS28	**Vacuolar protein sorting-associated protein 28 homolog**	Q9UK41	1, 2	DC[CAM]VSPSEYTAAC[CAM]SR
VTN	**Vitronectin**	P04004	2, 3	VDTVDPPYPR
AMY2B	**Alpha-amylase 2B**	P19961	2	LVGLLDLALEK
ATP11B	**Probable phospholipid-transporting ATPase IF**	Q9Y2G3	1	EHDLFFK
ATP6V0D1	**V-type proton ATPase subunit d 1**	P61421	1	LLFEGAGSNPGDK
ATP8B1	**Probable phospholipid-transporting ATPase IC**	O43520	1	VYEEIEK
DNASE1	**Deoxyribonuclease-1**	P24855	2	YDIALVQEVR
FAM49B	**Protein FAM49B**	Q9NUQ9	1	AWGAVVPLVGK
GALK1	**Galactokinase**	P51570	1	HSLASSEYPVR
GK5	**Putative glycerol kinase 5**	Q6ZS86	1	AILESIAFR
ITGAV	**Integrin alpha-V**	P06756	3	IYIGDDNPLTLIVK
LPAR3	**Lysophosphatidic acid receptor 3**	Q9UBY5	1	TNVLSPHTSGSISR
MPI	**Mannose-6-phosphate isomerase**	P34949	1	TEVPGSVTEYK
NUDT2	**Bis(5'-nucleosyl)-tetraphosphatase [asymmetrical]**	P50583	1	DYDVEIR
PCYOX1	**Prenylcysteine oxidase 1**	Q9UHG3	1	IFSQETLTK
PYGL	**Glycogen phosphorylase, liver form**	P06737	1	YEYGIFNQK
SDCBP2	**Syntenin-2**	Q9H190	2	VDQAIQAQVR
SERPINB13	**Serpin B13**	Q9UIV8	1	FLTEISK
SGSH	**N-sulphoglucosamine sulphohydrolase**	P51688	2	ADLAAQYTTVGR
TOM1L2	**TOM1-like protein 2**	Q6ZVM7	1	IVELISR
VPS35	**Vacuolar protein sorting-associated protein 35**	Q96QK1	1	VLETTVEIFNK

3.2 Validation phase

3.2.1 Samples characteristics

After the validation phase sample preparation (n=107), and together with the information from samples included in the discovery (n=24), NTA and protein quantification data were available for large group of samples (total n=131). A regression analysis performed on these data showed that there is a good correlation between the number of ELVs counted by NTA and the total amount of protein in the sample, indicating that most of the obtained protein does indeed belong to the vesicles (Fig. 27).

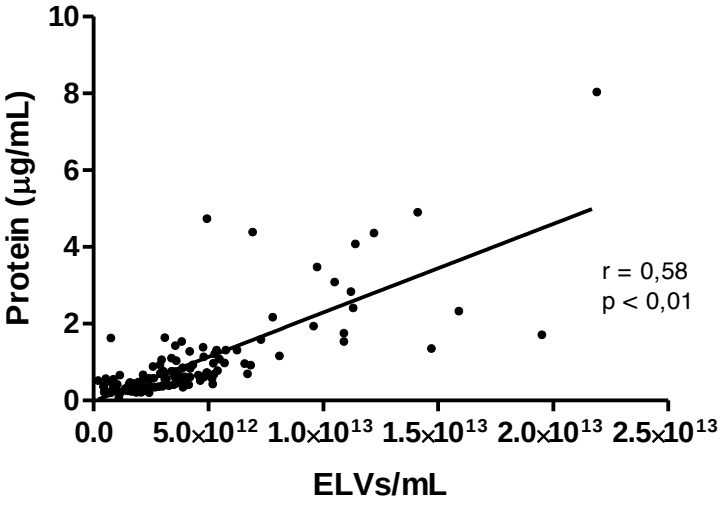

Figure 27. Regression analysis showing a good correlation between the number of ELVs counted by NTA and the total amount of protein recovered from the same sample.

Moreover, the amount of ELVs and total protein recovered from the samples in the different groups was studied. By NTA, we observed a tendency towards a lower number of vesicles in the PCa samples when the average values of the curves (for all the samples in each group) were represented. Concordantly, the amount of protein obtained in the PCa samples was significantly lower than in the samples from the benign group (Fig. 28).

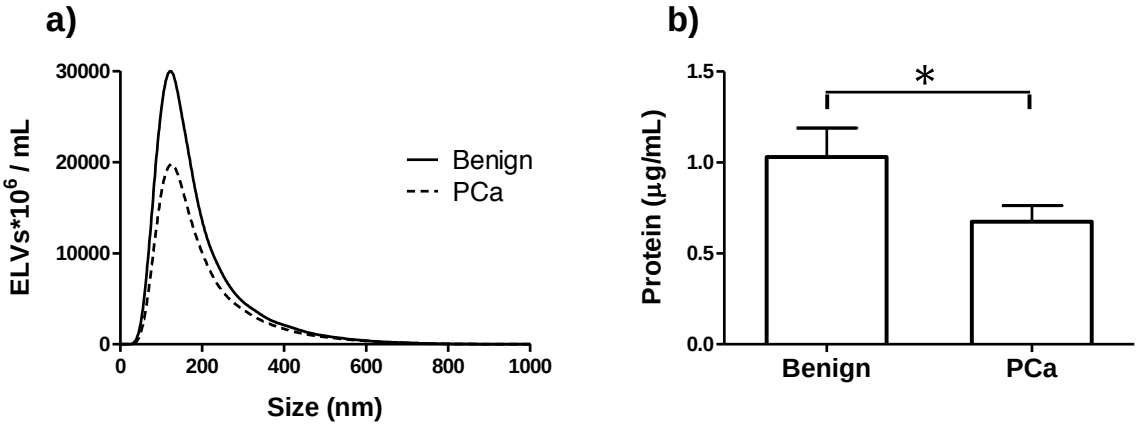

Figure 28. (a) Representation of the average values of the NTA measurements for the different groups of samples: benign (black line) or PCa (dashed line). **(b)** Total amount of protein obtained in the benign *vs.* PCa group. Both results indicate a lower amount of urinary ELVs in the PCa group.

3.2.2 Validated biomarkers

Targeted proteomics analysis (SRM) was used to validate the 64 candidate biomarkers identified in the discovery phase.

An independent cohort of 107 urine samples collected after DRE was recruited for this validation study. The samples were distributed into two groups: tumor samples (n=53), which include 19 high-grade tumors (Gleason score ≤ 7) and 34 low-grade tumors (Gleason score >7); and benign samples (n=54). ELVs were isolated following the same optimized protocol described above.

One proteotypic peptide (a peptide sequence that is found in only a single known protein and therefore can be used to identify that protein) was selected for each protein (see Table 13), allowing the monitoring of all 64 proteins in one run per sample.

As a result, 15 out of the 64 initial protein candidates were confirmed to follow the same trend observed in the discovery phase, and therefore proven to be good prospective biomarkers (Table 14).

Table 14. List of the 15 proteins that were successfully validated by SRM, from the initial 64 candidates, in a cohort of 107 samples.

Gene symbol	Protein	Uniprot accession	p-value	Fold change
SCIN	**Adseverin**	Q9Y6U3	<0.01	1.34
GNS	**N-acetylglucosamine-6-sulfatase**	P15586	<0.01	1.40
TGM4	**Transglutaminase-4**	P49221	<0.01	0.60
CA4	**Carbonic anhydrase 4**	P22748	<0.01	1.40
SDCBP2	**Syntenin-2**	Q9H190	<0.01	1.20
PRSS8	**Prostasin**	Q16651	<0.01	0.83
SLC26A4	**Pendrin**	O43511	<0.01	1.21
ITGB3	**Integrin beta-3**	P05106	<0.01	1.22
ACPP	**Prostatic acid phosphatase**	P15309	0.01	0.75
ITGAV	**Integrin alpha-V**	P06756	0.01	1.20
NUDT2	**Bis(5'-nucleosyl)-tetraphosphatase [asymmetrical]**	P50583	0.01	0.77
GALK1	**Galactokinase 1**	P51570	0.02	0.86
ATP6V1B1	**V-type proton ATPase subunit B, kidney isoform**	P15313	0.02	1.15
PTPN13	**Tyrosine-protein phosphatase non-receptor type 13**	Q12923	0.03	1.16
PCYOX1	**Prenylcysteine oxidase 1**	Q9UHG3	0.03	1.18

4 *In vitro* studies; Integrin αVβ3

In our list of 15 validated proteins, the two subunits that form the Integrin αVβ3 were found: Integrin β3 (ITGB3) and Integrin αV (ITGAV). Due to the interesting coincidence of both in the list and, moreover, showing similar deregulation patterns in PCa, it was decided to study their expression in PCa cell lines and whether they are located in vesicles (endosomes) inside the cells.

By RTqPCR, it was found that ITGB3 is overexpressed in the more aggressive PCa cell lines PC3 and Du145, while lower expression was observed in LNCaP cells. However, ITGAV has a more stable expression pattern in the different cell lines. Results for ITGB3 were validated by WB in the same cell lines, confirming a direct relation between RNA

and protein expression levels. Human Umbilical Vein Endothelial Cells (HUVEC) were used as positive control in all cases (Fig. 29).

Since the level of expression of ITGB3 is quite low in all the PCa cell lines, it was impossible to detect by immunofluorescence (IF). For this reason, PC3 cells were transfected with a plasmid containing this protein. We would expect this exogenous ITGB3 to bind to the endogenous ITGAV, forming the Integrin αVβ3. To test this premise, IF was carried out with an antibody that recognizes specifically the Integrin complex, only when both subunits are together. Indeed, the Integrin αVβ3 was detectable, only in transfected cells, and localized in vesicles (Fig. 30).

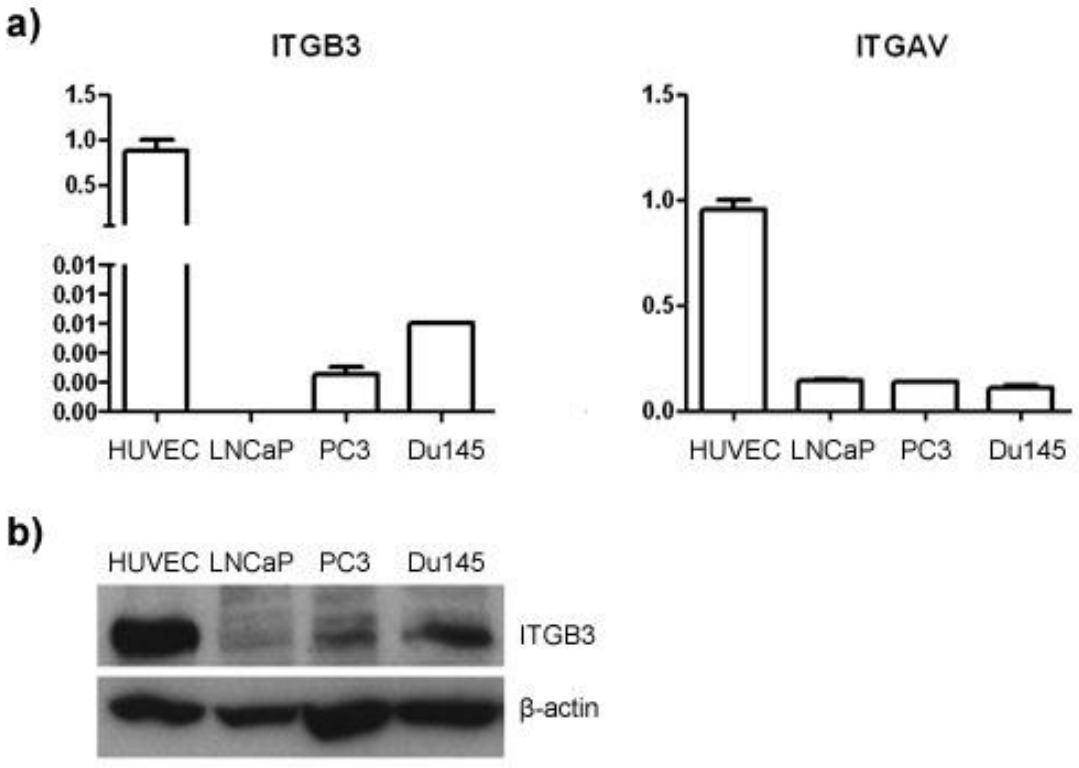

Figure 29. (a) RNA expression levels of ITGB3 and ITGAV in different PCa cell lines, as well as in HUVEC cell line used as a positive control. The aggressive cell lines (PC3 and Du145) express more ITGB3, while the levels of ITGAV remain constant between the cell lines. Note that both graphics have a different scale, being the levels of ITGAV higher than those of ITGB3. **(b)** The expression levels of ITGB3 where validated by WB.

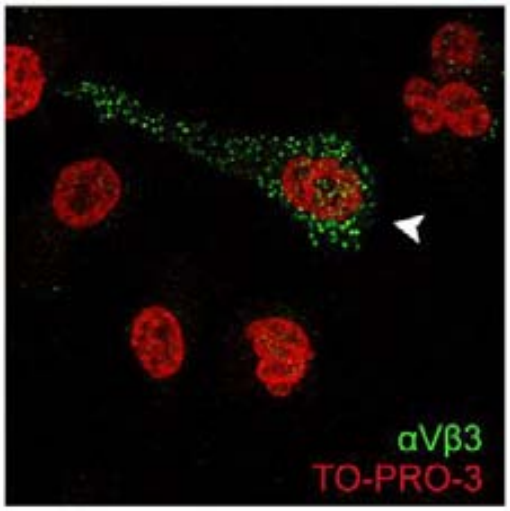

Figure 30. IF picture of PC3 cells, using an antibody against Integrin αVβ3. The positive cell (arrowhead) has been successfully transfected with the ITGB3 plasmid, while the cells around it remain negative. We can observe as well that this integrin appears to be distributed in vesicles inside the cell. Nuclei are stained in red with the TO-PRO-3 reagent.

At this point, the remaining question was whether the Integrin αVβ3 is localized in late endosomes (a part of which will be secreted as exosomes) or in other type of structures. To give an answer to this question, we assayed the co-localization of this protein complex with CD63, a known marker of late endosomes. As a result we saw that almost all the vesicles containing Integrin αVβ3 contain also CD63 (Fig. 31).

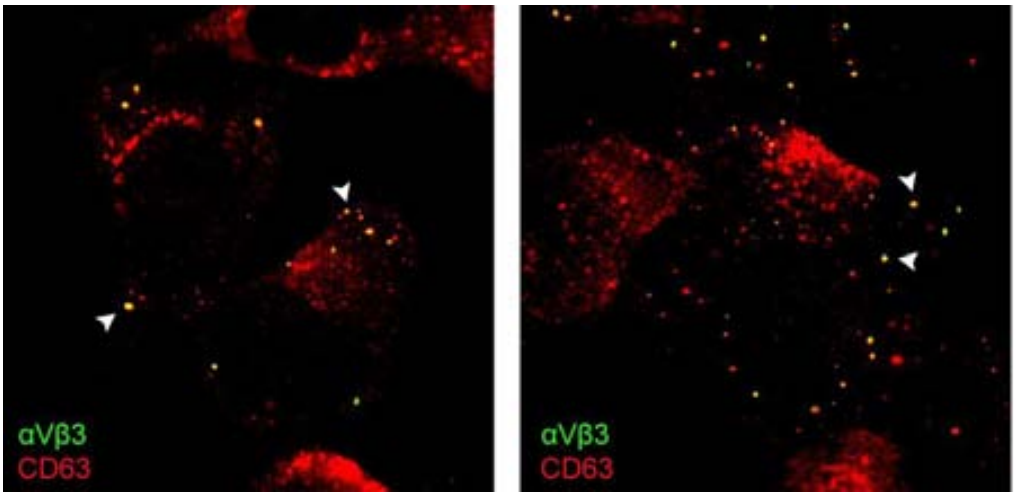

Figure 31. Immunofluorescence of PC3 cells using two antibodies. Green, anti-αVβ3; red, anti-CD63. The great majority of vesicles containing the Integrin present also CD63 (yellow vesicles), a marker of late endosomes. Arrowheads point to some good examples of vesicles presenting where αVβ3 co-localizes with CD63.

RESULTS OF THE OBJECTIVE 2

Evaluation of the performance of RNA-based PCa biomarkers in HGPIN patients referred for repeat biopsy

1 Samples performance

All patients enrolled in the study were men undergoing repeat PB to rule out PCa when HGPIN was previously identified. Urine was obtained directly after DRE, and urinary cells werepelleted and processed for further analysis. For the initial sample cohort studied, 90 out of the 114 specimens yielded sufficient prostate derived cells (high PSA Ct value) or overall amount of RNA (high geometric mean of all Ct values) for analysis, corresponding to an informative specimen rate of 78.9% (benign 78.9% and PCa 21.1%).

Analysis of these samples by boxplots showed that none of them should be considered as an outlier (Annex I, Suppl. Fig. 1).

2 Data normalization

Statistical analysis of the gene expression results showed that the mRNA that best fit the established criteria was *TBP*, hence it was the one used for the standardization of the target genes expression (Table 15). By the contrary, we could observe that the commonly used normalizing gene *PSA* behaves as a biomarker itself, being its levels increased in the PCa samples, and for this reason it is also included in the group of target genes (Table 15).

Table 15. Selection of the endogenous reference gene. *TBP*, which shows the best values in most of the considered variables, was the gene selected for data normalization in our experiments.

Gene	AUC	Coefficient of variation	Ct geometric mean	p-value*
ALAS1	0.51	15.0%	22.9	0.88
B2M	0.51	14.5%	23.6	0.87
GAPDH	0.49	17.4%	16.1	0.92
HPRT	0.55	22.7%	16.7	0.52
TBP	0.49	13.0%	23.3	0.92
KLK3	0.33	13.5%	25.9	0.03

* The p-value corresponds to the Mann-Whitney-Wilcoxon test results.

3 Target genes expression analysis

Using a univariate analysis, differences in the mean expression of genes between groups were studied. Among all the studied RNA levels, 7 of them showed significant differences ($p<0.05$) between PCa and benign conditions (Table 16). In the case of *PSMA* four different primer pairs were used, to detect specific combinations of isoforms.

Before proceeding with the next steps of the study, all significant markers were cross-validated using the LOOCV method. The genes *CDH1*, *PSMA*, *GOLM1*, *KLK3*, *PSGR* and *PCA3* were selected for further characterization (Fig. 32), under the criterion of all individual outcomes being significant.

Then, a multivariate regression analysis was applied, to test whether the variables could have a better performance when combined in a multiplex model. This analysis resulted several models that can distinguish between benign conditions and PCa better than the individual targets RNA levels. The best 3 models out of 36 are shown in Fig. 32 (for information about all the 36 models see Annex I, Suppl. Table 1). Fixing the sensitivity at 95%, we obtained specificities ranging from 41% to 58%. The positive predictive value (PPV) and negative predictive value (NPV) ranged from 30% to 38%, and from 97% to 98%, respectively. Applying these models, it would be possible to save from 33% and up to 47% of the repeat biopsies practiced. The multiplex models presented surpass *PCA3* performance in all cases (Fig. 33).

Table 16. Target genes for the detection of PCa in patients with a previous diagnosis of HGPIN. A total of 7 genes show significant p-values: *CDH1*, *PSMA*, *GOLM1*, *KLK3*, *PSGR*, *PCA3* and *SPINK1*.

Symbol	Name	p-value*
ABCA5	ATP-binding cassette, sub-family A (ABC1), member 5	0.335
AGR2	Anterior gradient 2	0.464
AURKA	Aurora kinase A	0.748
CDH1	Cadherin 1, type 1, E-cadherin (epithelial)	<0.001
CHKA	Choline kinase alpha	0.858
EN2	Engrailed homeobox 2	0.726
GOLM1	Golgi membrane protein 1	0.004
KLK3	Kallikrein-related peptidase 3 / Prostate specific antigen (PSA)	0.032
PCA3	Prostate cancer associated 3	0.008
PSGR	Olfactory Receptor, Family 51, Subfamily E, Member 2 / Prostate specific G-coupled receptor	<0.001
PSMA	Folate Hydrolase 1 / Prostate-Specific Membrane Antigen (Isoforms 1, 2, 3, 4, 5)	0.011
PSMA	Folate Hydrolase 1 / Prostate-Specific Membrane Antigen (Isoforms 1, 2, 3, 4)	0.005
PSMA	Folate Hydrolase 1 / Prostate-Specific Membrane Antigen (Isoforms 1, 3, 5)	0.032
PSMA	Folate Hydrolase 1 / Prostate-Specific Membrane Antigen (Isoforms 3, 4)	0.012
PTPRC	Protein tyrosine phosphatase, receptor type, C	0.097
S100A9	S100 calcium binding protein A9	0.960
SLC12A1	Solute carrier family 12 (sodium/potassium/chloride transporters), member 1	0.632
SPINK1	Serine peptidase inhibitor, Kazal type 1	0.042
TIMP4	TIMP metallopeptidase inhibitor 4	0.113
UPK2	Uroplakin 2	0.069

* The p-value corresponds to the Mann-Whitney-Wilcoxon test results.

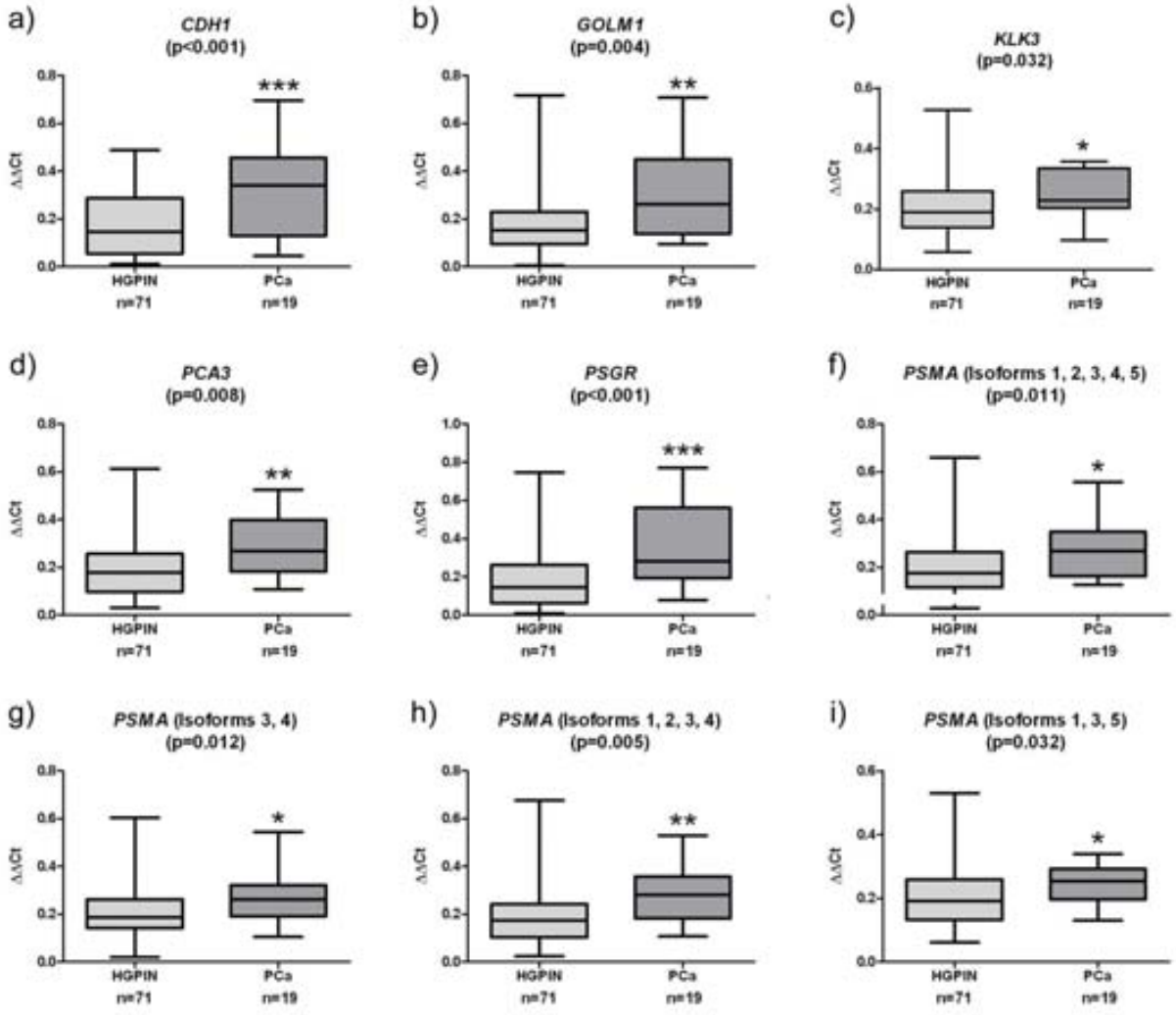

j)

Variables	AUC	AUC LOOCV	PPV	NPV	Specificity (Sensitivity 95%)	Estimated TRUS-PB avoided
CDH1	0.77	0.73	29%	96%	37%	30%
GOLM1	0.72	0.68	25%	95%	25%	21%
KLK3	0.66	0.61	25%	95%	24%	20%
PCA3	0.70	0.66	27%	96%	30%	24%
PSGR	0.75	0.73	27%	96%	32%	27%
PSMA (Isoforms 1, 2, 3, 4, 5)	0.69	0.65	27%	96%	32%	27%
PSMA (Isoforms 1, 2, 3, 4)	0.71	0.67	26%	95%	27%	22%
PSMA (Isoforms 1, 3, 5)	0.66	0.61	25%	95%	25%	21%
PSMA (Isoforms 3, 4)	0.69	0.65	25%	95%	24%	20%

k)

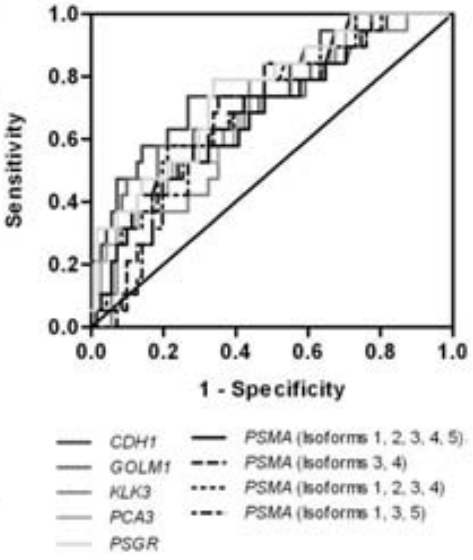

Figure 32. Characterization of candidate urine-derived RNA biomarkers for PCa. (a) to **(i)**, RT-qPCR was performed on urinary sediment cDNA obtained from patients referred for a repeat TRUS-PB after a previous diagnosis of HGPIN. Expression in patients with negative Bx result (light gray) or patients with PCa (dark gray) is shown, only for the biomarkers that were significant predictors (see Table 16). Normalization was performed using the ΔΔCt method with *TBP*. P-values from the univariate analysis for the discrimination between benign and PCa groups are indicated. **(j)** For each one of the biomarkers AUC value, PPV, NPV, specificity and estimated percentage of saved PB were calculated. **(k)** ROC curves for the individual PCa biomarkers.

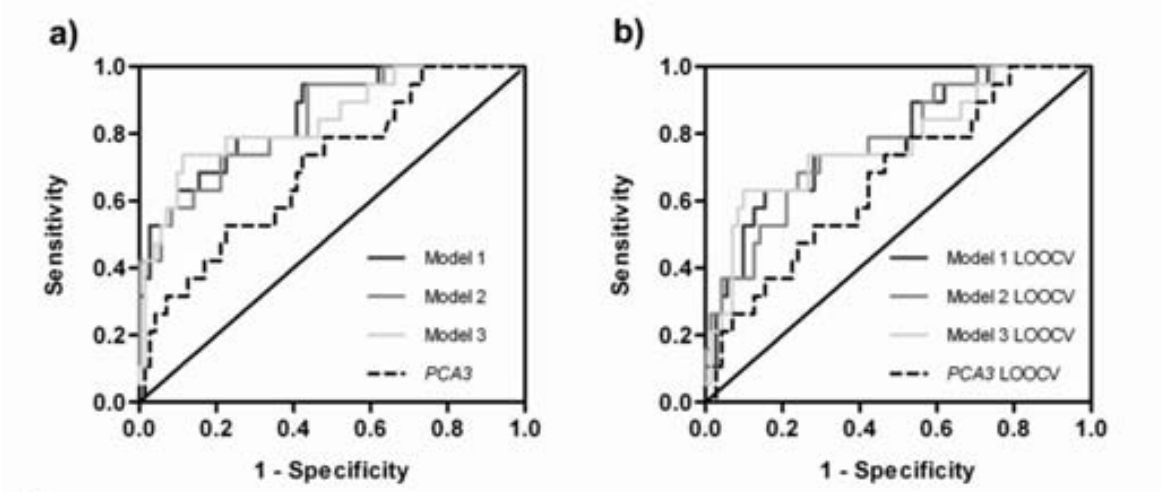

c)

Model	Variables	AUC	PPV	NPV	Specificity (Sensitivity 95%)	Estimated TRUS-PB avoided
1	*KLK3* + *PSMA* (Isoforms 3, 4) + *PSMA* (Isoforms 1, 3, 5) + *PSGR* + *CDH1*	0.86	38%	98%	58%	47%
2	*KLK3* + *PSMA* (Isoforms 3, 4) + *PSMA* (Isoforms 1, 3, 5) + *PSGR* + *GOLM1*	0.84	37%	98%	56%	46%
3	*KLK3* + *PSMA* (Isoforms 3, 4) + *PSGR* + *CDH1*	0.81	30%	97%	41%	33%
-	*PCA3*	0.70	27%	96%	30%	24%

d)

Model (LOOCV)	Variables	AUC	PPV	NPV	Specificity (Sensitivity 95%)	Estimated TRUS-PB avoided
1	*KLK3* + *PSMA* (Isoforms 3, 4) + *PSMA* (Isoforms 1, 3, 5) + *PSGR* + *CDH1*	0.78	29%	97%	38%	31%
2	*KLK3* + *PSMA* (Isoforms 3, 4) + *PSMA* (Isoforms 1, 3, 5) + *PSGR* + *GOLM1*	0.77	30%	97%	41%	33%
3	*KLK3* + *PSMA* (Isoforms 3, 4) + *PSGR* + *CDH1*	0.77	29%	96%	37%	30%
-	*PCA3*	0.66	25%	95%	25%	21%

Figure 33. Several multiplex models of urine biomarkers outperform *PCA3* for the detection of PCa in HGPIN patients referred for repeat PB. (a-c) Multivariate regression analysis resulted in a number of multiplex models, of which the best three were selected. These models include combinations of *KLK3*, *PSMA*, *PSGR*, *CDH1* and *GOLM1* as predictors of PCa. ROC curves were generated according to the predicted probabilities derived from each one of the models. All the multiplexed models (gray lines) present a higher AUC, PPV, NPV and specificity than *PCA3* alone (black dotted line). The multiplex models would also help avoiding a higher number of unnecessary PB than *PCA3* alone. **(b-d)** As in (a-c), but LOOCV results were used to generate the curves. The AUC, PPV, NPV, specificity and percentage of saved PB of the LOOVC models are greater than for LOOCV *PCA3*.

DISCUSSION

PCa is the second most frequently diagnosed cancer worldwide (74). Nevertheless, the PCa screening methods used today present considerable limitations. There is no doubt that early detection of aggressive cancers is beneficial, and there is randomized data showing that PSA screening results in earlier stages at diagnosis, improved oncologic outcomes after treatment, and lower PCa mortality rates. However, neither PSA nor the DRE are highly accurate, leading to a significant rate of unnecessary biopsies mostly due to high PSA levels, which can be elevated not only because of PCa but also because of other prostatic pathologies (259).

While it is clear that over-diagnosis and over-treatment are quite significant in the current practices of PCa screening, the disease remains a lethal condition in about 30,000 men every year (75). For this reason, the complete abandonment of screening methods would be detrimental for these patients. This situation is known as the diagnostic dilemma of PCa. At the moment, screening for PCa by PSA levels measurement is highly prevalent in developed countries. However, in order to improve the utility and benefit of PSA screening, it has been suggested that the practice should be decreased for low-risk individuals or those unlikely to benefit from screening, halting further screening when appropriate, and utilizing observational strategies in patients unlikely to suffer clinically significant effects of prostate cancer over their anticipated life expectancy (260).

Moreover, in many PBs that do not show malignancy, a non-cancerous pathology of the prostate is found (261). A particularly clinically relevant benign condition is HGPIN, widely regarded as a likely precursor to PCa. Some recent studies have suggested that molecular findings associated with HGPIN might be able to predict which men are more likely to have cancer on re-biopsy (262). For this reason, its encounter in a first PB guarantees an intensive surveillance over the years. One study has reported that 77% of urologists consider the presence of HGPIN in absence of cancer in PB indication for a re-biopsy (263). Consequently, men with a first PB positive for HGPIN usually undergo a close clinical follow-up over several years, including multiple repeat biopsies (73). However, only in a part of these patients an aggressive form of PCa will be eventually found.

In summary, a great number of the PBs practiced nowadays are unnecessary, causing pointless discomfort to the patient and extra expenses to the health care system. In the last years, a lot of effort has been put into the identification of new biomarkers for PCa that would improve the current situation. However, so far only *PCA3*, a non-coding RNA found in the urine sediments obtained after DRE, has been translated into the clinics. This RNA is currently utilized in a commercially available test under the name

PROGENSA® *PCA3*, approved by the US Food and Drug Administration (FDA) in 2012 (140,264). In this assay, *PCA3* and *KLK3* mRNAs are quantified, and the PCA3 Score is calculated as the ratio of *PCA3* and *KLK3* (*PCA3* mRNA/*KLK3* mRNA x 1000). PROGENSA® *PCA3* assay has been demonstrated to be useful when combined with other patient information to aid in the decision of whether to recommend a repeat PB in men 50 years or older who have had at least one previous negative PB (141), but its utility for PCa early diagnosis is still under investigation.

Because of the location of the prostate in the body, in direct contact with the urethra, desquamated cells and secreted products, such as soluble proteins and exosomes, can be detected in urine**. The main aim of this thesis was the identification of new biomarkers for PCa in urine, in order to develop a non-invasive method for the early and accurate detection of PCa, both in a first PB setting (Objective 1) and in patients already diagnosed with HGPIN (Objective 2).**

As commented above, urine has been intensively studied as a source of biomarkers for PCa, since it represents a non-invasive and easy-to-obtain fluid in direct contact with the prostate (136). However, the low protein concentration, the presence of salts and the dynamic range of protein expression in urine turn it into a fluid quite difficult to study at the protein level (265). Urinary exosomes contain proteins, lipids and RNAs which conform only ~3% of the excreted urinary protein content. Therefore, when ELVs are purified, their protein content is enriched >30-fold while at the same time high-abundance soluble proteins are removed, enhancing the detectability of low-abundant proteins (222,266). Accordingly, the specific enrichment of exosomes and ELVs present in the urine might represent a good alternative to total soluble protein as a potential source for new biomarkers.

In the first place, here we present a characterization and a comprehensive proteomic study of ELVs present in urine of men that undergo prostatic massage by DRE previously to the collection of the samples, due to a suspicion of PCa (Objective 1).

DRE is a standard procedure complimentary to the PSA test for the detection of PCa, fully implemented in the clinical routine in Spain, as well as in the rest of Europe (although not in the US). This practice involves applying pressure to the prostate gland, what induces the release of its contents. If a urine sample is collected shortly after DRE, the prostatic secretions will be washed with the voided urine and, therefore, this will be enriched in prostate-derived products. This enrichment phenomenon has been widely demonstrated before, both for protein content derived from prostatic secretions (267) and for cells exfoliated from the prostate (268,269). In this study, it appears clear that the

performance of a DRE prior collection of the sample also helps increasing the amount of ELVs present in the urine, presumably from a prostatic origin. These results are in agreement with a recently published article on RNA biomarkers in ELVs (270).

One of the most significant challenges involving the use of exosomes or ELVs for the discovery of new biomarkers is the lack of standard and reliable isolation methods. The isolation of exosomes from biological fluids is rather complex, since these also contain protein complexes and, certainly, other kinds of vesicles (not derived from MVBs, such as microvesicles and apoptotic bodies), which are frequently co-isolated with the population of interest. Accordingly, the best method of isolation is still a discussion topic in the field.

As a way to acknowledge the possibility of having not only exosomes in our samples, but also other extracellular vesicles or contaminants, the vesicles used in this study have been named ELVs. In any case, the presence of exosomes as a significant part of the obtained material has been verified by the detection of several exosome-specific markers both by WB and by mass spectrometry.

Due to the current limitations of the isolation of vesicles, our first aim was to establish a reliable and reproducible protocol, maintaining a compromise with the highest purity possible. Consequently, we propose a protocol based on differential ultracentrifugation, with two additional steps: (i) a treatment with DTT to break the THP fibers that trap the vesicles during the initial centrifugation cycles, and (ii) a filtering step to remove any vesicles or particles larger than 200 nm (Fig. 34).

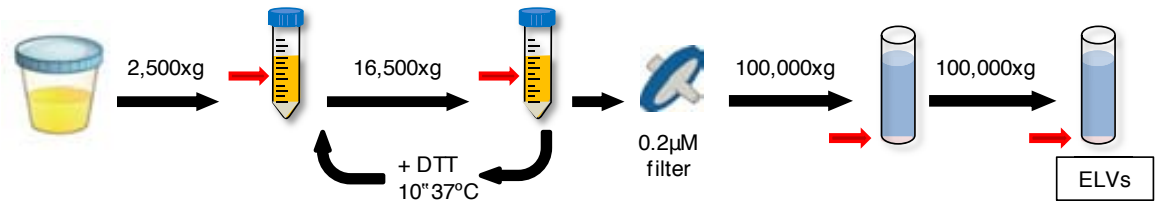

Figure 34. Protocol used for the isolation of EVLs from urine samples. This method involves two high-speed centrifugations and a 0.2 M filtering steps to remove larger contaminants. A DTT steps is also included, in order to maximize the recovery of ELVs that might be trapped in the THP networks during the centrifugations. Finally, the samples are ultracentrifuged to precipitate the ELVs. Red arrows indicate the fraction recovered after each step (i.e., supernatant or pellet).

Many alternatives to our method have been described by other authors (210,211). One of the most widely used and probably the best current approach to obtain pure exosomes is by centrifugation on a 30% sucrose cushion and recovery of the floating vesicles. Unfortunately, this method is rather complex and involves several steps that

might be difficult to reproduce between experiments, yielding highly variable results in our hands. Moreover, this protocol often causes a significant loss of material. Sometimes this problem can be overcome by the addition of more starting material but, when working with individual human samples (such as urine samples) this loss might make it impossible to move forward towards the “omics” experiments, such as MS, since a certain minimum amount of protein is required for trypsin digestion. Our recommendation would be to use the sucrose flotation method for studies requiring an extreme purity of the exosomes, such as descriptive or functional studies, but to opt for a simpler technique if the analysis and comparison of a large number of samples in a high-throughput fashion is preferred. Thus, here we decided to use a non-sucrose method for analyzing the protein content of ELVs obtained from a large number of urine samples. To our knowledge, no high-throughput proteomic study has been done before on individual urine samples aiming for the discovery of PCa ELVs-derived biomarkers.

Currently, there is extensive information about the composition of exosomes freely available in online databases such as ExoCarta (http://www.exocarta.org), which has been compiled from diverse studies. However, due to the lack of standardization of the methods commented above, the material isolated and used for analysis in each of those studies might differ considerably. For this reason, it is not uncommon to find conflicts between data from different sources.

Within the data presented in this study, PSA is a good example of this fact. PSA is typically secreted via the classical rough endoplasmic reticulum and Golgi apparatus secretory pathway. Previously, the absence of PSA in ELVs from PCa cell lines has been reported (229,232). However, presence of this protein in ELVs is still a matter of discussion, since other studies have found it in ELVs isolated from urine and blood from both PCa patients and healthy donors (233,234,271). Our results agree with the latter, finding PSA in urinary ELVs even after sucrose cushion purification. In view of these data, we can speculate that the incorporation of PSA into ELVs cargo, probably attached to their surface (as suggested by the removal of PSA by the trypsin incubation of ELVs), might take place after the independent secretion of this protein. The interaction of PSA and other soluble molecules with ELVs after these have been released might be an interesting point to address in future studies.

Beyond the protein content of ELVs, many authors have also been interested in the nucleic acids present in these vesicles. In the context of PCa, it has been shown that urinary ELVs contain *PCA3*, *TMPRSS:ERG*, two RNAs associated with the prostatic gland (230). In PCa cell lines-derived ELVs, the presence of *KLK3* has also been

demonstrated (229). The presence of these genes in the urinary vesicles opens a possibility for further research, in order to elucidate whether they follow the same patterns of expression that in the prostate tissue and, in this case, if their use as biomarkers might improve the already existing diagnostic tools. Indeed, more recently, both *PCA3* and *TMPRSS*:*ERG* have been pointed as potential PCa biomarkers in urinary ELVs (270).

Using pooled urine samples, we have tested the expression of *KLK3*, *PSMA* and *PSGR*, in addition to the previously described *PCA3*. The combination of *PSMA*, *PSGR* and *PCA3* for improving PCa early diagnosis was previously described in our lab. Their combination in a 3-marker model showed 95% sensitivity and 50% specificity in men presenting PSA levels between 4-10ng/mL and no previous PB (147). Here, we aimed to prove the existence of these RNA makers within urinary ELVs. As a result, it has been confirmed that all of these RNAs are detectable in urinary ELVs. Moreover, our data indicate a possible overexpression of these molecules in PCa samples. Without a doubt, these results need to be taken cautiously, since they originate from the comparison of only two pools of samples. However, they highlight the relevance of RNA-based PCa biomarkers in urinary ELVs and their potential to improve PCa early diagnosis, laying the foundations for future research on this area.

Next to the RNA study described above, the miRNAs present in the ELVs from the same samples have also been identified and analyzed. In the results derived from these experiments we can observe that the vesicles contain a wide range of different miRNAs, many of which show relatively stable levels of expression between the two pools of samples, whereas others seem to be specifically enriched in benign or PCa conditions. It is known that, globally, there is a trend towards the down-regulation of miRNAs in cancer, suggesting that many of them may act suppressing proliferation and promoting differentiation (272). Taking this into consideration, the targets of the most down-regulated in PCa miRNAs from our study were analyzed, showing a striking representation of networks related to cancerous processes. Again, these results are unquestionably preliminary and should be interpreted cautiously, but they might represent evidence of the functional importance of miRNA in ELVs.

The core of the project presented in this first objective of the thesis was to analyze the differences in protein content between urinary ELVs derived from PCa *versus* benign samples. This comparison was achieved by protein expression measurement applying an LC-MS/MS approach.

During the first part of the project, a set comprised of 24 patient samples was analyzed using a label-free shotgun proteomics approach for relative quantification. Samples were divided in 3 groups: benign (no PCa), low risk and high risk PCa. In the low risk PCa group only samples with a Gleason score of 7(3+4) were included, since cancer cases presenting this grade are the most commonly found and usually do not represent an immediate life threat for patients. In the high risk group only samples with a Gleason score ≥7 were included; these advanced tumors are less often encountered due to the high sensibility of the screening methods, but their presence implies a poorer prognosis for these patients.

Due to the high complexity of the data generated by label-free proteomics, its analysis is a very challenging task. The data processing workflow for a label-free quantitative proteomics experiment begins with matching spectra to peptides by database searching for protein identification, followed by protein quantification, which may also involve a data normalization strategy and statistical assessment. These stages in data processing usually require software scripts and algorithms for efficient automation (273). Consequently, numerous commercial and open-source software tools have been developed for this purpose in the last years. Frequently, selection of the most appropriate tool for data processing is a difficult decision due to the lack of evidence about their compared performance and reliability.

In view if the above, our choice was to apply four different quantification workflows in parallel and finally compare and merge the obtained results. This decision has proven valuable, since all four of the methods have contributed proteins successfully validated in the next phase of the project.

In quantitative proteomics experiments with clinical samples, mostly small (in our case, n=24) and well-characterized cohorts are investigated to discover protein alteration related to a particular disease. In following validation experiments, biomarker candidates need to be further validated by investigating a large patient cohort (in our case, n=107) that is independent from the sample set used in the discovery phase.

All the samples used in the project were measured by NTA, in parallel to the proteomic analysis. A general increased secretion of ELVs in cancer-derived cell lines and, more particularly, in blood samples of cancer patients, has been described before (274,275). While we also expected to see an increase in the number of ELVs present in urine samples derived from PCa patients, it was striking to see the opposite effect. Indeed, the samples collected from PCa patients present less ELVs than the samples collected from benign counterparts. However, the decline in the levels of certain prostate-related

molecules such as PSA in the urine of PCa patients has also been described before (135,276). These results might be related to the loss of polarity and glandular structure that the prostate undergoes during the cancer development, forcing the release of part of its secretions towards the blood vessels instead of the usual secretion towards the gland ducts that end in the urethra.

Whereas immunological methods like tissue micro arrays or ELISA represent the traditional way of validation, targeted MS-based approaches like SRM are emerging as additional alternatives (277). In our project, a SRM methodology was applied, in order to facilitate the simultaneous quantification of a large number of candidate proteins. After this phase, we obtained as a result a list of 15 protein biomarkers that show a differential expression between benign and PCa urinary ELV samples.

Among the 15 validated biomarkers, we found several that can be of special interest due to their functional significance. All these molecules seem to be very good candidates for further research, in order to individually characterize them and establish their possible roles in PCa development and progression.

A good example of relevant biological significance is SCIN. It has been implicated in the local disassembly of cortical filamentous actin, which constitutes a barrier to the movement of vesicles to release sites, to allow translocation of secretory vesicles in preparation for exocytosis (278,279). Moreover, SCIN is highly expressed in human PCa specimens, and plays an important role in the proliferation of PCa cells (280).

TGM4 is a protein almost uniquely expressed in the prostate gland (281), that has been proved down-regulated in the prostate carcinoma glands compared to the corresponding normal glands (282).

More loosely related to our main concern, PCa, but still interesting, is NUDT2. This protein promotes proliferation of breast carcinoma cells and is a potent prognostic factor in human breast carcinomas (283).

Maybe the most exciting result, from our point of view, was the finding of the integrin subunits ITGB3 and ITGAV, showing the same grade of deregulation in PCa urinary ELVs. Due to this striking coincidence, it was decided to initiate further research on these proteins, being the first steps of the *in vitro* experiments included in this thesis.

Integrins are heterodimeric trans-membrane receptors composed of an α-subunit and a β-subunit. ITGB3 and ITGAV associate to form the integrin αVβ3. Integrins are widely known to mediate cell-matrix interaction, and the integrin αVβ3 has the ability of binding

to a variety in extracellular matrix proteins, including vitronectin, osteopontin, and bone sialoprotein (284). Integrins also play a role in cell signaling by activation of phosphorilation cascades, activating cell proliferation and migration (285). Integrin αVβ3 has been associated with the process of angiogenesis in solid tumors (286). In the particular case of PCa, it has been described as involved in the development and progression of tumors, promoting adhesion and migration of cells (287) and facilitating metastasis to the bone (288).

We have conducted an expression analysis of both integrin subunits in PCa cell lines. These experiments revealed that the expression of ITGAV remained constant among all the cell lines, while ITGB3 presented higher expression levels in the more aggressive cell lines PC3 and Du145, compared to LNCaP.

Nevertheless, the endogenous expression level of ITGB3 is not sufficient for detection by IF, forcing us to work with transfected cells. Following this type of experiments, we have proven that the exogenously expressed ITGB3 in PCa cells binds endogenous ITGAV to form the integrin αVβ3.

Finally, to determine the subcellular localization of αVβ3 in the transfected cells, we performed double fluorescent confocal analysis using an established marker, CD63, to identify the subcellular compartment of interest: late endosomes or MVBs. From early endosomes, proteins either recycle to the cell surface or become incorporated into ILVs into the endosomal lumen. In late endosomes, also called MVBs. CD63 is enriched on the intraluminal vesicles, which can either fuse with lysosomes or be secreted as exosomes through fusion with the plasma membrane (289). We have shown that αVβ3 co-localizes in late endosomes with the protein CD63 inside the cells. This might confirm that a possible fate for the αVβ3 contained in intracellular vesicles, if not destined for degradation, is to be secret in exosomes.

In summary, our results provide a strong basis for future biomarker research for PCa in ELVs. The next steps might include a further validation of the newly discovered biomarkers by immunoassay techniques such as WB or enzyme-linked immunosorbent assay (ELISA). Furthermore, it would be of interest to perform a functional characterization of the integrins, assessing their role in the development and progression of PCa, or their possible involvement in the metastatic process. Other of the new protein biomarkers described in this study might as well be interesting candidates for validation of their localization in endosomes, and further functional analysis. Moreover, it would be of great interest to perform more statistic tests in the validation phase cohort, to elucidate

whether the validated biomarkers could also differentiate aggressive from low risk forms of PCa.

The future of PCa detection might benefit from research of biomarkers in ELVs, such as the results presented in this study. This new approach may help identifying more specific biomarkers than the currently known and utilized for diagnosis of PCa, distinguishing aggressive from clinically insignificant PCa and other benign conditions and, therefore, avoiding PCa related over-diagnosis and over-treatment.

In any case, the field of biomarkers from extracellular vesicles is still in its infancy, and important challenges need to be addressed before these can be translated into a clinical setting. These challenges include the development and standardization of high-throughput isolation methods and criteria for data normalization between samples. Also, the development of a high-throughput platform to analyze urinary EVs, such as an enzyme-linked immunosorbent assay, is desirable (290).

In contrast with the extracellular vesicles research, the use of RNA-based biomarkers in the urinary cell fraction for the detection of PCa has been largely explored (291). However, in the context of men referred for a re-biopsy due to a first diagnosis of HGPIN, much remains to be done. Currently, these cases still represent a complicated dilemma for clinicians, having to decide whether the patient would benefit from an aggressive surveillance including multiple PBs or, by the contrary, a less intensive type of follow-up is needed.

In order to develop an RTqPCR-based test that would help in the clinical practice to differentiate those HGPIN cases that present with a hidden PCa from those that are benign conditions and therefore to save unnecessary PBs, we analyzed the expression of 17 genes in a cohort of 90 patients (Objective 2). Most of the markers used in this study where previously reported as PCa urinary biomarkers (148,150,151,264,292), while others were selected because of their known relation with PCa tissue (293–297).

First of all, we sought to find the best gene to be used as endogenous reference gene. Urine contains a highly variable mixture of cells of different origins and, to date, there is no consensus about the best way to normalize gene expression data retrieved from this source. The general trend is to use the *KLK3* mRNA expression for this purpose. However, this is not an ideal solution, since those patients who present with negative biopsy usually tend to have fewer cells of prostatic origin in their post-DRE urine than their malignant counterparts. One possible explanation to the could be the loss of cell-cell contacts in cancer, that would facilitate the desquamation of cells (298). For this

reason, levels of *KLK3* in urine vary in relation to the presence or absence of PCa, being itself a biomarker able to distinguish between the two groups, as we have proven in this study. The increased levels of *KLK3* in PCa patients may lead researchers to overlook other biomarkers that follow the same pattern of expression. There are other widely used reference genes, constitutively expressed by all cells, which might be useful in the case of urine samples as well. We have assayed 5 of these universal housekeeping genes RNAs, concluding that they are an alternative to the use of *KLK3* for normalization. *TBP* was the most stable RNA among all samples and. For that reason, we propose *TBP* as a candidate control gene for urinary cell samples.

Besides the endogenous genes characterization and selection, the main aim of this study was to establish a profile of biomarkers useful to rule out PCa in repeat PB in a cohort of patients previously diagnosed with HGPIN.

Using a univariate analysis approach, we have demonstrated the differential expression of the genes *PCA3*, *PSMA*, *PSGR*, *KLK3*, *GOLM1* and *CDH1*. All of them appear overexpressed in PCa urine samples with compared to urine from patients presenting isolated HGPIN. The AUCs for these markers ranged from 0.66 to 0.77. Fixing the sensitivity at 95%, the obtained specificities for the individual markers ranged between 24% and 37%.

In the context of PCa detection, the feasibility of a *PCA3* gene-based molecular assay in urine has been extensively demonstrated, and it is currently utilized in a commercially available test under the name PROGENSA® *PCA3*, as commented above. In a recent study including 177 patients undergoing repeat PB, the reported sensitivity, specificity, PPV and NPV of *PCA3* (score cut-off of 20) in PCa diagnosis were 91.7%, 25.6%, 31.5% and 89.5%, respectively; the use of *PCA3* measurements would have avoided 21% of biopsies (299). In our hands, using a cohort of 90 patients, the specificity, PPV and NPV values at a fixed sensitivity of 91.7% were of 30%, 26% and 93%, respectively, while 25.1% of PB could had been avoided. Therefore, our results are comparable to previously published data.

Interestingly, several of the genes assayed in this study outperformed *PCA3* for the detection of PCa in repeat PB. Specially, *CDH1* and *PSGR* show notably higher AUC values compared to *PCA3* (0.77 and 0.75 *vs*. 0.70).

As a single marker may not necessarily reflect the multifactorial, multifocal and heterogeneous nature of PCa, a combination of various biomarkers would clearly improve performance over a single biomarker (300). The use of multiple markers, in

combination with clinical and demographic data, will aid in predicting patients who are at risk for developing PCa and for assessing their prognoses.

Through multivariate analysis we have established three multiplex models comprising different combinations of *KLK3*, *PSMA*, *PSGR*, *GOLM1* and *CDH1*. Each one of these models greatly outperforms *PCA3* score (multiplex models AUC=0.81-0.86 *vs. PCA3* AUC=0.70), as well as all the other assayed target genes when used alone, for the detection of PCa. With a fixed sensitivity of 95%, the specificity of the three panels was of 41-58%, compared to the 30% of *PCA3*.

It is worth noting that our multiplex models would allow saving up to 47% of the repeat PBs practiced. For this calculation, we used the formula of: % biopsies saved = true negatives (test negative and biopsy negative) + false negatives (test negative and biopsy positive) / all patients. Although this would imply that one could save a biopsy by incorrectly classifying (test negative and biopsy positive) a patient as not having PCa, the number of false negatives to obtain a sensitivity of 95% is negligible (in this study one patient; NPV ≥ 97%).

In the last years, a variety of techniques have appeared for the optimization of PB, in an attempt to minimize the percentage of false-negative PB results. TRUS-guided biopsy is still the standard approach; however, this technique has multiple limitations owing to the operator's inability in most cases to directly visualize and target prostate lesions. Magnetic resonance imaging (MRI) of the prostate can overcome many of these limitations by directly depicting areas of abnormality and allowing targeted biopsies (301).

Biomarkers-based tests are also been developed and investigated, with the aim of providing a more accurate means of PCa detection in repeat PBs cohorts. A promising new test based on serum PSA is called the Prostate Health Index (PHI), which has recently been approved in the United States, Europe and Australia. PHI is a mathematical formula that combines total PSA, free PSA and the [-2] form of proPSA (the inactive precursor of PSA), into a single score that can be used to aid in clinical decision-making (302). Several reports have documented the performance of PHI in large groups of patients, reporting AUC values ranging from 0.68 to 0.74 (303–308).

Porpiglia *et al*. performed a study comparing the predictive value of *PCA3*, MRI-guided PB and PHI in the repeat biopsy setting. They found that the most significant contribution for PCa detection was provided by MRI-guided PB, with an AUC of 0.94. In fact, the inclusion of PCA3 and/or PHI to models containing MRI-guided PB did not substantially

improve the net benefit. At a high sensitivity (95%) the association of the biomarkers with MRI-guided PB displayed results comparable to those of MRI-guided PB alone, showing a specificity of 57% (309). These results indicate that MRI-guided PB has a high diagnostic accuracy in identifying patients with PCa in the repeat PB setting; however, its combination with *PCA3* or PHI does not improve the overall performance. In future studies, it might be interesting to address the value of combining with MRI-guided PB more accurate models such as the ones resulting from our data, in order to further increase its specificity.

A possible limitation of our study is that the second biopsy outcome was used as the definitive diagnosis of the patient. However, there is still a small chance of missing a PCa in this second biopsy. In some cases, PCa is finally diagnosed after a third or even subsequent PBs. For this reason, we cannot discard the possibility of having misclassified a small number of patients in our study.

In summary, we have shown that a multiplexed RTqPCR assay on urine sediments from patients presenting for a repeat PB due to a diagnosis of HGPIN can significantly improve the predictive ability when compared to *PCA3* or any other assayed gene when used alone. Further evaluation and validation of these biomarkers in larger and independent cohorts is highly desirable, in order to confirm these results. In the future, a multiplexed urine-based diagnostic test for PCa with a higher specificity but the same sensitivity as the serum PSA test, could be used for an easier management of patients with HGPIN, helping clinicians to determine which patients could benefit from a repetition of the PB.

In conclusion and taking all together, the data presented in this thesis represent a significant advance in the standard formula for PCa diagnosis. Both of the two approaches followed in this study (protein in ELVs and RNA-based in urinary sediments, for a first and second PB setting, respectively) have yielded promising results. However, validation studies on larger, multi-centric cohorts are needed for establishment of a valid PCa biomarker. Implementation of more specific tools for the detection of PCa in the clinical practice will contribute to improve the quality of health care and reduce the costs at the same time.

CONCLUSIONS

1. The isolation of ELVs from urine samples can be achieved by differential ultracentrifugation, incorporating a DTT treatment and a filtering step, in a reliable and reproducible manner.

2. Characterization of urinary ELVs at the mRNA level revealed the presence of the prostate-related genes *KLK3*, *PCA3*, *PSGR* and *PSMA*. When analyzed in pooled samples, these genes followed the same pattern of expression described for prostate tissue and urinary sediments, being overexpressed in PCa.

3. Characterization of urinary ELVs at the miRNA level in pooled samples revealed that the most down-regulated miRNAs in PCa specifically target genes implicated in cancer development pathways.

4. The number of ELVs present in urine samples from PCa patients was lower than the number of ELVs present in urine samples from benign counterparts.

5. ELVs isolated from urine of PCa patients present a different proteomic profile when compared with ELVs isolated from urine of benign counterparts. A final list of 15 proteins have been validated using a targeted proteomic approach.

6. Among the proteins differentially expressed in urinary ELVs derived from PCa, ITGB3 and ITGAV, two integrin subunits that together form the heterodimeric integrin αVβ3, were found. Integrin αVβ3 can be detected in vesicles inside PCa cells, co-localizing with the late endosomes marker CD63, thus confirming its probable release in exosomes.

7. The integrin αVβ3 or other of the novel biomarkers found in urinary ELVs in this study could be a useful new approach for the detection of PCa in body fluids.

8. The normalization of gene expression data in urinary sediments, by using the universal endogenous gene *TBP* might be an alternative to the commonly used *KLK3*, since the expression levels of the former are not influenced by the presence of a PCa.

9. In the context of repeat PBs, due to a previous diagnosis of HGPIN, the urinary sediment expression levels of the genes *PCA3*, *PSMA*, *PSGR*, *KLK3*, *GOLM1* and *CDH1* can predict the presence of an undetected PCa.

10. Multiplex models, including several PCa mRNA biomarkers (*KLK3*, *PSMA*, *PSGR*, *GOLM1* and *CDH1*) in urinary sediments, outperforms all the genes when used individually for the detection of PCa.

11. The use of these panels of biomarkers in clinical practice could help the clinicians to rule out PCa, potentially saving unnecessary repeat PBs and constituting a step towards the improvement of the HGPIN cases management.

12. The next step will be to move on towards the validation of these urinary ELVs protein-based and urinary sediment mRNA-based biomarkers using a much larger cohort of samples. Then it should be possible to translate these findings to a much easier format for incorporation into diagnostic kits or tests that will be more accessible and applicable in clinical practice.

13. All together, proteomic and transcriptomic analyses constitute an important step towards the accurate diagnosis of PCa, which currently represents a setback in our ability to treat patients appropriately. Thus, protein- and mRNA-based biomarkers should have a rapid application in the clinics and, together with serum PSA and DRE, potentially influence decisions that could improve the health system, while reducing the number of unnecessary biopsies.

BIBLIOGRAPHY

1. Lee CH, Akin-Olugbade O, Kirschenbaum A. Overview of prostate anatomy, histology, and pathology. Endocrinol Metab Clin North Am. 2011;40:565–575, viii–ix.

2. Timms BG. Prostate development: a historical perspective. Differ Res Biol Divers. 2008;76:565–77.

3. Selman SH. The McNeal prostate: a review. Urology. 2011;78:1224–8.

4. McNeal JE. Regional morphology and pathology of the prostate. Am J Clin Pathol. 1968;49:347–57.

5. McNeal JE. Origin and evolution of benign prostatic enlargement. Invest Urol. 1978;15:340–5.

6. McNeal JE. The zonal anatomy of the prostate. The Prostate. 1981;2:35–49.

7. Greer EV. New Developments in Stem Cell Research. Nova Publishers; 2007.

8. Tewari A. Prostate Cancer: A Comprehensive Perspective. Springer; 2013.

9. Gillenwater JY. Adult and Pediatric Urology. Lippincott Williams & Wilkins; 2002.

10. Abate-Shen C, Shen MM. Molecular genetics of prostate cancer. Genes Dev. 2000;14:2410–34.

11. Myers RP, Cheville JC, Pawlina W. Making anatomic terminology of the prostate and contiguous structures clinically useful: historical review and suggestions for revision in the 21st century. Clin Anat N Y N. 2010;23:18–29.

12. Hammerich KH, Ayala GE, Wheeler TM. Anatomy of the prostate gland and surgical pathology of prostate cancer. Prostate Cancer. Cambridge University Press; 2008.

13. Hudson DL, Guy AT, Fry P, O'Hare MJ, Watt FM, Masters JR. Epithelial cell differentiation pathways in the human prostate: identification of intermediate phenotypes by keratin expression. J Histochem Cytochem Off J Histochem Soc. 2001;49:271–8.

14. Bonkhoff H, Stein U, Remberger K. The proliferative function of basal cells in the normal and hyperplastic human prostate. The Prostate. 1994;24:114–8.

15. Maitland NJ, Frame FM, Polson ES, Lewis JL, Collins AT. Prostate cancer stem cells: do they have a basal or luminal phenotype? Horm Cancer. 2011;2:47–61.

16. Yuan T-C, Veeramani S, Lin M-F. Neuroendocrine-like prostate cancer cells: neuroendocrine transdifferentiation of prostate adenocarcinoma cells. Endocr Relat Cancer. 2007;14:531–47.

17. Kumar VL, Majumder PK. Prostate gland: Structure, functions and regulation. Int Urol Nephrol. 1995;27:231–43.

18. Kirby RS. An Atlas of Prostatic Diseases (Third Edition). Taylor & Francis; 2003.

19. Strittmatter F, Gratzke C, Stief CG, Hedlund P. Current pharmacological treatment options for male lower urinary tract symptoms. Expert Opin Pharmacother. 2013;14:1043–54.

20. Untergasser G, Madersbacher S, Berger P. Benign prostatic hyperplasia: age-related tissue-remodeling. Exp Gerontol. 2005;40:121–8.

21. Siiteri PK, Wilson JD. Dihydrotestosterone in prostatic hypertrophy. J Clin Invest. 1970;49:1737–45.

22. Izumi K, Mizokami A, Lin W-J, Lai K-P, Chang C. Androgen receptor roles in the development of benign prostate hyperplasia. Am J Pathol. 2013;182:1942–9.

23. Gandaglia G, Briganti A, Gontero P, Mondaini N, Novara G, Salonia A, et al. The role of chronic prostatic inflammation in the pathogenesis and progression of benign prostatic hyperplasia (BPH). BJU Int. 2013;112:432–41.

24. Kumar R, Malla P, Kumar M. Advances in the design and discovery of drugs for the treatment of prostatic hyperplasia. Expert Opin Drug Discov. 2013;8:1013–27.

25. Pinheiro LC, Martins Pisco J. Treatment of benign prostatic hyperplasia. Tech Vasc Interv Radiol. 2012;15:256–60.

26. Rieken M, Bachmann A. Laser treatment of benign prostate enlargement-which laser for which prostate? Nat Rev Urol. 2014;11:142–52.

27. Bechis SK, Otsetov AG, Ge R, Olumi AF. Personalized Medicine for Management of Benign Prostatic Hyperplasia. J Urol. 2014;192:16–23.

28. Krieger JN, Nyberg L Jr, Nickel JC. NIH consensus definition and classification of prostatitis. JAMA J Am Med Assoc. 1999;282:236–7.

29. Kirby RS, Lowe D, Bultitude MI, Shuttleworth KE. Intra-prostatic urinary reflux: an aetiological factor in abacterial prostatitis. Br J Urol. 1982;54:729–31.

30. De Marzo AM, Platz EA, Sutcliffe S, Xu J, Grönberg H, Drake CG, et al. Inflammation in prostate carcinogenesis. Nat Rev Cancer. 2007;7:256–69.

31. Krieger JN, Egan KJ, Ross SO, Jacobs R, Berger RE. Chronic pelvic pains represent the most prominent urogenital symptoms of “chronic prostatitis.”Urology. 1996;48:715–721; discussion 721–722.

32. Duclos AJ, Lee C-T, Shoskes DA. Current treatment options in the management of chronic prostatitis. Ther Clin Risk Manag. 2007;3:507–12.

33. Sugar LM. Inflammation and prostate cancer. Can J Urol. 2006;13 Suppl 1:46–7.

34. De Marzo AM, Marchi VL, Epstein JI, Nelson WG. Proliferative inflammatory atrophy of the prostate: implications for prostatic carcinogenesis. Am J Pathol. 1999;155:1985–92.

35. Elkahwaji JE. The role of inflammatory mediators in the development of prostatic hyperplasia and prostate cancer. Res Rep Urol. 2012;5:1–10.

36. Woenckhaus J, Fenic I. Proliferative inflammatory atrophy: a background lesion of prostate cancer? Andrologia. 2008;40:134–7.

37. Putzi MJ, De Marzo AM. Morphologic transitions between proliferative inflammatory atrophy and high-grade prostatic intraepithelial neoplasia. Urology. 2000;56:828–32.

38. Wang W, Bergh A, Damber J-E. Morphological transition of proliferative inflammatory atrophy to high-grade intraepithelial neoplasia and cancer in human prostate. The Prostate. 2009;69:1378–86.

39. Nelson WG, De Marzo AM, Deweese TL, Lin X, Brooks JD, Putzi MJ, et al. Preneoplastic prostate lesions: an opportunity for prostate cancer prevention. Ann N Y Acad Sci. 2001;952:135–44.

40. Wagenlehner FME, Elkahwaji JE, Algaba F, Bjerklund-Johansen T, Naber KG, Hartung R, et al. The role of inflammation and infection in the pathogenesis of prostate carcinoma. BJU Int. 2007;100:733–7.

41. Häggman MJ, Macoska JA, Wojno KJ, Oesterling JE. The relationship between prostatic intraepithelial neoplasia and prostate cancer: critical issues. J Urol. 1997;158:12–22.

42. Joshua AM, Evans A, Van der Kwast T, Zielenska M, Meeker AK, Chinnaiyan A, et al. Prostatic preneoplasia and beyond. Biochim Biophys Acta. 2008;1785:156–81.

43. Bostwick DG, Shan A, Qian J, Darson M, Maihle NJ, Jenkins RB, et al. Independent origin of multiple foci of prostatic intraepithelial neoplasia: comparison with matched foci of prostate carcinoma. Cancer. 1998;83:1995–2002.

44. Montironi R, Mazzucchelli R, Lopez-Beltran A, Cheng L, Scarpelli M. Mechanisms of disease: high-grade prostatic intraepithelial neoplasia and other proposed preneoplastic lesions in the prostate. Nat Clin Pract Urol. 2007;4:321–32.

45. Drago J. Introductory remarks and workshop summary. Urology. 1992;39 (Suppl.):S2–S8.

46. Bostwick DG, Liu L, Brawer MK, Qian J. High-Grade Prostatic Intraepithelial Neoplasia. Rev Urol. 2004;6:171–9.

47. Montironi R, Mazzucchelli R, Algaba F, Lopez-Beltran A. Morphological identification of the patterns of prostatic intraepithelial neoplasia and their importance. J Clin Pathol. 2000;53:655–65.

48. Herawi M, Kahane H, Cavallo C, Epstein JI. Risk of prostate cancer on first re-biopsy within 1 year following a diagnosis of high grade prostatic intraepithelial neoplasia is related to the number of cores sampled. J Urol. 2006;175:121–4.

49. Curado M, Edwards B, Shin H, Store H, Ferlay J, Heanue M. Cancer incidence in five continents [Internet]. Lyon: IARC Scientific Publications; 2007. Available from: http://www-dep.iarc.fr

50. Qian J, Wollan P, Bostwick DG. The extent and multicentricity of high-grade prostatic intraepithelial neoplasia in clinically localized prostatic adenocarcinoma. Hum Pathol. 1997;28:143–8.

51. Sinha AA, Quast BJ, Reddy PK, Lall V, Wilson MJ, Qian J, et al. Microvessel density as a molecular marker for identifying high-grade prostatic intraepithelial neoplasia precursors to prostate cancer. Exp Mol Pathol. 2004;77:153–9.

52. Epstein JI, Netto GJ. Biopsy Interpretation of the Prostate. Lippincott Williams & Wilkins; 2008.

53. Gallardo-Arrieta F, Doll A, Rigau M, Mogas T, Juanpere N, García F, et al. A transcriptional signature associated with the onset of benign prostate hyperplasia in a canine model. The Prostate. 2010;70:1402–12.

54. Tomlins SA, Mehra R, Rhodes DR, Cao X, Wang L, Dhanasekaran SM, et al. Integrative molecular concept modeling of prostate cancer progression. Nat Genet. 2007;39:41–51.

55. Bostwick DG, Brawer MK. Prostatic intra-epithelial neoplasia and early invasion in prostate cancer. Cancer. 1987;59:788–94.

56. Jones JS. Prostate Cancer Diagnosis: PSA, Biopsy and Beyond. Springer; 2012.

57. Morote J, Raventós CX, Encabo G, López M, de Torres IM. Effect of high-grade prostatic intraepithelial neoplasia on total and percent free serum prostatic-specific antigen. Eur Urol. 2000;37:456–9.

58. Bishara T, Ramnani DM, Epstein JI. High-grade prostatic intraepithelial neoplasia on needle biopsy: risk of cancer on repeat biopsy related to number of involved cores and morphologic pattern. Am J Surg Pathol. 2004;28:629–33.

59. Gokden N, Roehl KA, Catalona WJ, Humphrey PA. High-grade prostatic intraepithelial neoplasia in needle biopsy as risk factor for detection of adenocarcinoma: current level of risk in screening population. Urology. 2005;65:538–42.

60. Kronz JD, Allan CH, Shaikh AA, Epstein JI. Predicting cancer following a diagnosis of high-grade prostatic intraepithelial neoplasia on needle biopsy: data on men with more than one follow-up biopsy. Am J Surg Pathol. 2001;25:1079–85.

61. Zlotta AR, Raviv G, Schulman CC. Clinical prognostic criteria for later diagnosis of prostate carcinoma in patients with initial isolated prostatic intraepithelial neoplasia. Eur Urol. 1996;30:249–55.

62. Moore CK, Karikehalli S, Nazeer T, Fisher HAG, Kaufman RP, Mian BM. Prognostic significance of high grade prostatic intraepithelial neoplasia and atypical small acinar proliferation in the contemporary era. J Urol. 2005;173:70–2.

63. Loeb S, Roehl KA, Yu X, Han M, Catalona WJ. Use of prostate-specific antigen velocity to follow up patients with isolated high-grade prostatic intraepithelial neoplasia on prostate biopsy. Urology. 2007;69:108–12.

64. Akhavan A, Keith JD, Bastacky SI, Cai C, Wang Y, Nelson JB. The proportion of cores with high-grade prostatic intraepithelial neoplasia on extended-pattern needle biopsy is significantly associated with prostate cancer on site-directed repeat biopsy. BJU Int. 2007;99:765–9.

65. Hou H, Li X, Chen X, Wang C, Zhang G, Wang H, et al. Prediction value of high-grade prostatic intraepithelial neoplasia for prostate cancer on repeat biopsies. Chin-Ger J Clin Oncol. 2011;10:410–4.

66. Park K, Dalton JT, Narayanan R, Barbieri CE, Hancock ML, Bostwick DG, et al. TMPRSS2:ERG Gene Fusion Predicts Subsequent Detection of Prostate Cancer in Patients With High-Grade Prostatic Intraepithelial Neoplasia. J Clin Oncol Off J Am Soc Clin Oncol. 2014;32:206–11.

67. Helpap B. The significance of the P504S expression pattern of high-grade prostatic intraepithelial neoplasia (HGPIN) with and without adenocarcinoma of the prostate in biopsy and radical prostatectomy specimens. Virchows Arch Int J Pathol. 2006;448:480–4.

68. Montironi R, Mazzucchelli R, Stramazzotti D, Pomante R, Thompson D, Bartels PH. Expression of pi-class glutathione S-transferase: two populations of high grade prostatic intraepithelial neoplasia with different relations to carcinoma. Mol Pathol MP. 2000;53:122–8.

69. Morote J, Fernández S, Alaña L, Iglesias C, Planas J, Reventós J, et al. PTOV1 expression predicts prostate cancer in men with isolated high-grade prostatic intraepithelial neoplasia in needle biopsy. Clin Cancer Res Off J Am Assoc Cancer Res. 2008;14:2617–22.

70. Zhao Z, Zeng G. Increased serum level of early prostate cancer antigen is associated with subsequent cancer risk in men with high-grade prostatic intraepithelial neoplasia. Endocr Relat Cancer. 2010;17:505–12.

71. Auprich M, Augustin H, Budäus L, Kluth L, Mannweiler S, Shariat SF, et al. A comparative performance analysis of total prostate-specific antigen, percentage free prostate-specific antigen, prostate-specific antigen velocity and urinary prostate cancer gene 3 in the first, second and third repeat prostate biopsy. BJU Int. 2012;109:1627–35.

72. Morote J, Rigau M, Garcia M, Mir C, Ballesteros C, Planas J, et al. Behavior of the PCA3 gene in the urine of men with high grade prostatic intraepithelial neoplasia. World J Urol. 2010;28:677–80.

73. Chin AI, Dave DS, Rajfer J. Is Repeat Biopsy for Isolated High-Grade Prostatic Intraepithelial Neoplasia Necessary? Rev Urol. 2007;9:124–31.

74. Jemal A, Bray F, Center MM, Ferlay J, Ward E, Forman D. Global cancer statistics. CA Cancer J Clin. 2011;61:69–90.

75. Siegel R, Ma J, Zou Z, Jemal A. Cancer statistics, 2014. CA Cancer J Clin. 2014;64:9–29.

76. Potosky AL, Miller BA, Albertsen PC, Kramer BS. The role of increasing detection in the rising incidence of prostate cancer. JAMA J Am Med Assoc. 1995;273:548–52.

77. Siegel R, Naishadham D, Jemal A. Cancer statistics, 2013. CA Cancer J Clin. 2013;63:11–30.

78. Ito K. Prostate cancer in Asian men. Nat Rev Urol. 2014;11(4):197–212.

79. Howlader N, Noone A, Krapcho M, Garshell J, Neyman N, Altekruse S, et al. SEER Cancer Statistics Review, 1975-2010. Bethesda: National Cancer Institute; 2013.

80. Damaschke NA, Yang B, Bhusari S, Svaren JP, Jarrard DF. Epigenetic susceptibility factors for prostate cancer with aging. The Prostate. 2013;73:1721–30.

81. Mordukhovich I, Reiter PL, Backes DM, Family L, McCullough LE, O'Brien KM, et al. A review of African American-white differences in risk factors for cancer: prostate cancer. Cancer Causes Control CCC. 2011;22:341–57.

82. Powell IJ. The Precise Role of Ethnicity and Family History on Aggressive Prostate Cancer: A Review Analysis. Arch Esp Urol. 2011;64:711–9.

83. Chen L-S, Fann JC-Y, Chiu SY-H, Yen AM-F, Wahlfors T, Tammela TL, et al. Assessing Interactions of Two Loci (rs4242382 and rs10486567) in Familial Prostate Cancer: Statistical Evaluation of Epistasis. PLoS ONE. 2014;9:e89508.

84. Ewing CM, Ray AM, Lange EM, Zuhlke KA, Robbins CM, Tembe WD, et al. Germline mutations in HOXB13 and prostate-cancer risk. N Engl J Med. 2012;366:141–9.

85. Shang Z, Zhu S, Zhang H, Li L, Niu Y. Germline homeobox B13 (HOXB13) G84E mutation and prostate cancer risk in European descendants: a meta-analysis of 24,213 cases and 73, 631 controls. Eur Urol. 2013;64:173–6.

86. Dean M, Lou H. Genetics and genomics of prostate cancer. Asian J Androl. 2013;15:309–13.

87. Castro E, Eeles R. The role of BRCA1 and BRCA2 in prostate cancer. Asian J Androl. 2012;14:409–14.

88. Sfanos KS, De Marzo AM. Prostate cancer and inflammation: the evidence. Histopathology. 2012;60:199–215.

89. Blair A, Malker H, Cantor KP, Burmeister L, Wiklund K. Cancer among farmers. A review. Scand J Work Environ Health. 1985;11:397–407.

90. Van der Gulden JW, Kolk JJ, Verbeek AL. Prostate cancer and work environment. J Occup Med Off Publ Ind Med Assoc. 1992;34:402–9.

91. Doolan G, Benke G, Giles G. An Update on Occupation and Prostate Cancer. Asian Pac J Cancer Prev APJCP. 2014;15:501–16.

92. Parent M-E, Désy M, Siemiatycki J. Does exposure to agricultural chemicals increase the risk of prostate cancer among farmers? McGill J Med MJM Int Forum Adv Med Sci Stud. 2009;12:70–7.

93. Nelson WG, Demarzo AM, Yegnasubramanian S. The diet as a cause of human prostate cancer. Cancer Treat Res. 2014;159:51–68.

94. De Pergola G, Silvestris F. Obesity as a major risk factor for cancer. J Obes. 2013;2013:291546.

95. Mahmoud AM, Yang W, Bosland MC. Soy isoflavones and prostate cancer: a review of molecular mechanisms. J Steroid Biochem Mol Biol. 2014;140:116–32.

96. Madu CO, Lu Y. Novel diagnostic biomarkers for prostate cancer. J Cancer. 2010;1:150.

97. Humphrey PA. Histological variants of prostatic carcinoma and their significance: Prostatic carcinoma variants. Histopathology. 2012;60:59–74.

98. Liu A, Wei L, Gardner WA, Deng C-X, Man Y-G. Correlated alterations in prostate basal cell layer and basement membrane. Int J Biol Sci. 2009;5:276–85.

99. Gleason DF, Mellinger GT. Prediction of prognosis for prostatic adenocarcinoma by combined histological grading and clinical staging. J Urol. 1974;111:58–64.

100. Humphrey PA. Gleason grading and prognostic factors in carcinoma of the prostate. Mod Pathol Off J U S Can Acad Pathol Inc. 2004;17:292–306.

101. Berg KD, Toft BG, Røder MA, Brasso K, Vainer B, Iversen P. Prostate needle biopsies: interobserver variation and clinical consequences of histopathological re-evaluation. APMIS Acta Pathol Microbiol Immunol Scand. 2011;119:239–46.

102. Melia J, Moseley R, Ball RY, Griffiths DFR, Grigor K, Harnden P, et al. A UK-based investigation of inter- and intra-observer reproducibility of Gleason grading of prostatic biopsies. Histopathology. 2006;48:644–54.

103. Edge SB, Compton CC. The American Joint Committee on Cancer: the 7th edition of the AJCC cancer staging manual and the future of TNM. Ann Surg Oncol. 2010;17:1471–4.

104. Lotan TL, Epstein JI. Clinical implications of changing definitions within the Gleason grading system. Nat Rev Urol. 2010;7:136–42.

105. Guidelines EAoU. European Association of Urology; 2010.

106. Cheng L, Montironi R, Bostwick DG, Lopez-Beltran A, Berney DM. Staging of prostate cancer. Histopathology. 2012;60:87–117.

107. Datta K, Muders M, Zhang H, Tindall DJ. Mechanism of lymph node metastasis in prostate cancer. Future Oncol Lond Engl. 2010;6:823–36.

108. Jin J-K, Dayyani F, Gallick GE. Steps in Prostate Cancer Progression that lead to Bone Metastasis. Int J Cancer J Int Cancer. 2011;128:2545–61.

109. Roodman GD. Mechanisms of bone metastasis. N Engl J Med. 2004;350:1655–64.

110. Mackiewicz-Wysocka M, Pankowska M, Wysocki PJ. Progress in the treatment of bone metastases in cancer patients. Expert Opin Investig Drugs. 2012;21:785–95.

111. Coleman RE. Metastatic bone disease: clinical features, pathophysiology and treatment strategies. Cancer Treat Rev. 2001;27:165–76.

112. Pienta KJ. Critical appraisal of prostate-specific antigen in prostate cancer screening: 20 years later. Urology. 2009;73:S11–20.

113. Obort AS, Ajadi MB, Akinloye O. Prostate-Specific Antigen: Any Successor in Sight? Rev Urol. 2013;15:97–107.

114. Catalona WJ, Hudson MA, Scardino PT, Richie JP, Ahmann FR, Flanigan RC, et al. Selection of optimal prostate specific antigen cutoffs for early detection of prostate cancer: receiver operating characteristic curves. J Urol. 1994;152:2037–42.

115. Carter HB, Partin AW, Walsh PC, Trock BJ, Veltri RW, Nelson WG, et al. Gleason score 6 adenocarcinoma: should it be labeled as cancer? J Clin Oncol Off J Am Soc Clin Oncol. 2012;30:4294–6.

116. Roobol MJ, Kerkhof M, Schröder FH, Cuzick J, Sasieni P, Hakama M, et al. Prostate cancer mortality reduction by prostate-specific antigen-based screening adjusted for nonattendance and contamination in the European Randomised Study of Screening for Prostate Cancer (ERSPC). Eur Urol. 2009;56:584–91.

117. Stattin P, Carlsson S, Holmström B, Vickers A, Hugosson J, Lilja H, et al. Prostate Cancer Mortality in Areas With High and Low Prostate Cancer Incidence. J Natl Cancer Inst. 2014;106(3):dju007.

118. Heidenreich A, Abrahamsson P-A, Artibani W, Catto J, Montorsi F, Van Poppel H, et al. Early detection of prostate cancer: European Association of Urology recommendation. Eur Urol. 2013;64:347–54.

119. Artibani W. Landmarks in prostate cancer diagnosis: the biomarkers. BJU Int. 2012;110:8–13.

120. Basler J. The Digital Rectal Examination in Prostate Cancer Screening. In: MD IMT, MD MIR, MD EAK, editors. Prostate Cancer Screen. Humana Press; 2001. page 91–6.

121. Sutton MA, Gibbons RP, Correa RJ. Is deleting the digital rectal examination a good idea? West J Med. 1991;155:43–6.

122. Flanigan RC, Catalona WJ, Richie JP, Ahmann FR, Hudson MA, Scardino PT, et al. Accuracy of digital rectal examination and transrectal ultrasonography in localizing prostate cancer. J Urol. 1994;152:1506–9.

123. Gosselaar C, Kranse R, Roobol MJ, Roemeling S, Schröder FH. The interobserver variability of digital rectal examination in a large randomized trial for the screening of prostate cancer. The Prostate. 2008;68:985–93.

124. Smith DS, Catalona WJ. Interexaminer variability of digital rectal examination in detecting prostate cancer. Urology. 1995;45:70–4.

125. Ismail MT, Gomella LG. Transrectal prostate biopsy. Urol Clin North Am. 2013;40:457–72.

126. Scattoni V, Maccagnano C, Zanni G, Angiolilli D, Raber M, Roscigno M, et al. Is extended and saturation biopsy necessary? Int J Urol Off J Jpn Urol Assoc. 2010;17:432–47.

127. Ukimura O, Coleman JA, de la Taille A, Emberton M, Epstein JI, Freedland SJ, et al. Contemporary role of systematic prostate biopsies: indications, techniques, and implications for patient care. Eur Urol. 2013;63:214–30.

128. Scattoni V, Zlotta A, Montironi R, Schulman C, Rigatti P, Montorsi F. Extended and saturation prostatic biopsy in the diagnosis and characterisation of prostate cancer: a critical analysis of the literature. Eur Urol. 2007;52:1309–22.

129. Heidenreich A, Bastian PJ, Bellmunt J, Bolla M, Joniau S, van der Kwast T, et al. EAU guidelines on prostate cancer. part 1: screening, diagnosis, and local treatment with curative intent-update 2013. Eur Urol. 2014;65:124–37.

130. Joniau S, Tosco L, Briganti A, Vanden Broeck T, Gontero P, Karnes RJ, et al. Results of surgery for high-risk prostate cancer. Curr Opin Urol. 2013;23:342–8.

131. Siegel R, DeSantis C, Virgo K, Stein K, Mariotto A, Smith T, et al. Cancer treatment and survivorship statistics, 2012. CA Cancer J Clin. 2012;62:220–41.

132. Singh J, Trabulsi EJ, Gomella LG. Is there an optimal management for localized prostate cancer? Clin Interv Aging. 2010;5:187–97.

133. Mitin T, Blute M, Lee R, Efstathiou J. Management of lymph node-positive prostate cancer: the role of surgery and radiation therapy. Oncol Williston Park N. 2013;27:647–55.

134. Hong JH, Kim IY. Nonmetastatic Castration-Resistant Prostate Cancer. Korean J Urol. 2014;55:153–60.

135. Drake RR, White KY, Fuller TW, Igwe E, Clements MA, Nyalwidhe JO, et al. Clinical collection and protein properties of expressed prostatic secretions as a source for biomarkers of prostatic disease. J Proteomics. 2009;72:907–17.

136. Rigau M, Olivan M, Garcia M, Sequeiros T, Montes M, Colas E, et al. The Present and Future of Prostate Cancer Urine Biomarkers. Int J Mol Sci. 2013;14:12620–49.

137. Bussemakers MJ, van Bokhoven A, Verhaegh GW, Smit FP, Karthaus HF, Schalken JA, et al. DD3: a new prostate-specific gene, highly overexpressed in prostate cancer. Cancer Res. 1999;59:5975–9.

138. Ferreira LB, Palumbo A, Mello KD de, Sternberg C, Caetano MS, Oliveira FL de, et al. PCA3 noncoding RNA is involved in the control of prostate-cancer cell survival and modulates androgen receptor signaling. BMC Cancer. 2012;12:507.

139. Durand X, Moutereau S, Xylinas E, de la Taille A. Progensa™ PCA3 test for prostate cancer. Expert Rev Mol Diagn. 2011;11:137–44.

140. Rittenhouse H, Blase A, Shamel B, Schalken J, Groskopf J. The long and winding road to FDA approval of a novel prostate cancer test: our story. Clin Chem. 2013;59:32–4.

141. Gittelman MC, Hertzman B, Bailen J, Williams T, Koziol I, Henderson RJ, et al. PCA3 molecular urine test as a predictor of repeat prostate biopsy outcome in men with previous negative biopsies: a prospective multicenter clinical study. J Urol. 2013;190:64–9.

142. Haese A, de la Taille A, van Poppel H, Marberger M, Stenzl A, Mulders PFA, et al. Clinical utility of the PCA3 urine assay in European men scheduled for repeat biopsy. Eur Urol. 2008;54:1081–8.

143. Kirby R, Fitzpatrick JM. Optimising repeat prostate biopsy decisions and procedures. BJU Int. 2012;109:1750–4.

144. Truong M, Yang B, Jarrard D. Towards the Detection of Prostate Cancer in Urine: A Critical Analysis. J Urol. 2013;189:422–9.

145. Leyten GHJM, Hessels D, Jannink SA, Smit FP, de Jong H, Cornel EB, et al. Prospective multicentre evaluation of PCA3 and TMPRSS2-ERG gene fusions as diagnostic and prognostic urinary biomarkers for prostate cancer. Eur Urol. 2014;65:534–42.

146. Nguyen P-N, Violette P, Chan S, Tanguay S, Kassouf W, Aprikian A, et al. A panel of TMPRSS2:ERG fusion transcript markers for urine-based prostate cancer detection with high specificity and sensitivity. Eur Urol. 2011;59:407–14.

147. Rigau M, Ortega I, Mir MC, Ballesteros C, Garcia M, Llauradó M, et al. A three-gene panel on urine increases PSA specificity in the detection of prostate cancer. The Prostate. 2011;71:1736–45.

148. Rigau M, Morote J, Mir MC, Ballesteros C, Ortega I, Sanchez A, et al. PSGR and PCA3 as biomarkers for the detection of prostate cancer in urine. The Prostate. 2010;70:1760–7.

149. Salami SS, Schmidt F, Laxman B, Regan MM, Rickman DS, Scherr D, et al. Combining urinary detection of TMPRSS2:ERG and PCA3 with serum PSA to predict diagnosis of prostate cancer. Urol Oncol. 2013;31:566–71.

150. Laxman B, Morris DS, Yu J, Siddiqui J, Cao J, Mehra R, et al. A first-generation multiplex biomarker analysis of urine for the early detection of prostate cancer. Cancer Res. 2008;68:645–9.

151. Jamaspishvili T, Kral M, Khomeriki I, Vyhnankova V, Mgebrishvili G, Student V, et al. Quadriplex model enhances urine-based detection of prostate cancer. Prostate Cancer Prostatic Dis. 2011;14:354–60.

152. Palanichamy JK, Rao DS. miRNA dysregulation in cancer: towards a mechanistic understanding. Front Genet. 2014;5:54.

153. Brase JC, Johannes M, Schlomm T, Fälth M, Haese A, Steuber T, et al. Circulating miRNAs are correlated with tumor progression in prostate cancer. Int J Cancer J Int Cancer. 2011;128:608–16.

154. Bryant RJ, Pawlowski T, Catto JWF, Marsden G, Vessella RL, Rhees B, et al. Changes in circulating microRNA levels associated with prostate cancer. Br J Cancer. 2012;106:768–74.

155. Nguyen HCN, Xie W, Yang M, Hsieh C-L, Drouin S, Lee G-SM, et al. Expression Differences of Circulating MicroRNAs in Metastastic Castration Resistant Prostate Cancer and Low-risk, Localized Prostate Cancer. The Prostate. 2013;73:346–54.

156. Haj-Ahmad TA, Abdalla MA, Haj-Ahmad Y. Potential Urinary miRNA Biomarker Candidates for the Accurate Detection of Prostate Cancer among Benign Prostatic Hyperplasia Patients. J Cancer. 2014;5:182–91.

157. Casanova-Salas I, Rubio-Briones J, Calatrava A, Mancarella C, Masiá E, Casanova J, et al. Identification of miR-187 and miR-182 as Biomarkers of Early Diagnosis and Prognosis in Patients with Prostate Cancer Treated with Radical Prostatectomy. J Urol. 2014;192(1):252–9.

158. Lewis H, Lance R, Troyer D, Beydoun H, Hadley M, Orians J, et al. miR-888 is an expressed prostatic secretions-derived microRNA that promotes prostate cell growth and migration. Cell Cycle Georget Tex. 2014;13:227–39.

159. Srivastava A, Goldberger H, Dimtchev A, Ramalinga M, Chijioke J, Marian C, et al. MicroRNA profiling in prostate cancer--the diagnostic potential of urinary miR-205 and miR-214. PloS One. 2013;8:e76994.

160. Kuner R, Brase JC, Sültmann H, Wuttig D. microRNA biomarkers in body fluids of prostate cancer patients. Methods San Diego Calif. 2013;59:132–7.

161. Roobol MJ, Haese A, Bjartell A. Tumour markers in prostate cancer III: biomarkers in urine. Acta Oncol Stockh Swed. 2011;50 Suppl 1:85–9.

162. Schostak M, Schwall GP, Poznanović S, Groebe K, Müller M, Messinger D, et al. Annexin A3 in urine: a highly specific noninvasive marker for prostate cancer early detection. J Urol. 2009;181:343–53.

163. Lu Q, Zhang J, Allison R, Gay H, Yang W-X, Bhowmick NA, et al. Identification of extracellular delta-catenin accumulation for prostate cancer detection. The Prostate. 2009;69:411–8.

164. Russo AL, Jedlicka K, Wernick M, McNally D, Kirk M, Sproull M, et al. Urine analysis and protein networking identify met as a marker of metastatic prostate cancer. Clin Cancer Res Off J Am Assoc Cancer Res. 2009;15:4292–8.

165. Hutchinson LM, Chang EL, Becker CM, Ushiyama N, Behonick D, Shih M-C, et al. Development of a sensitive and specific enzyme-linked immunosorbent assay for thymosin beta15, a urinary biomarker of human prostate cancer. Clin Biochem. 2005;38:558–71.

166. Katafigiotis I, Tyritzis SI, Stravodimos KG, Alamanis C, Pavlakis K, Vlahou A, et al. Zinc α2-glycoprotein as a potential novel urine biomarker for the early diagnosis of prostate cancer. BJU Int. 2012;

167. Hessels D, Schalken JA. Urinary biomarkers for prostate cancer: a review. Asian J Androl. 2013;15:333–9.

168. Cary KC, Cooperberg MR. Biomarkers in prostate cancer surveillance and screening: past, present, and future. Ther Adv Urol. 2013;5:318–29.

169. Raposo G, Stoorvogel W. Extracellular vesicles: Exosomes, microvesicles, and friends. J Cell Biol. 2013;200:373–83.

170. Rodríguez-Suárez E, Gonzalez E, Hughes C, Conde-Vancells J, Rudella A, Royo F, et al. Quantitative proteomic analysis of hepatocyte-secreted extracellular

vesicles reveals candidate markers for liver toxicity. J Proteomics. 2014;103:227–40.

171. Cocucci E, Racchetti G, Meldolesi J. Shedding microvesicles: artefacts no more. Trends Cell Biol. 2009;19:43–51.

172. Pan BT, Johnstone RM. Fate of the transferrin receptor during maturation of sheep reticulocytes in vitro: selective externalization of the receptor. Cell. 1983;33:967–78.

173. Harding C, Heuser J, Stahl P. Receptor-mediated endocytosis of transferrin and recycling of the transferrin receptor in rat reticulocytes. J Cell Biol. 1983;97:329–39.

174. Théry C. Exosomes: secreted vesicles and intercellular communications. F1000 Biol Rep. 2011;3:15.

175. Harding CV, Heuser JE, Stahl PD. Exosomes: Looking back three decades and into the future. J Cell Biol. 2013;200:367–71.

176. Gould SJ, Raposo G. As we wait: coping with an imperfect nomenclature for extracellular vesicles. J Extracell Vesicles. 2013;2:10.3402/jev.v2i0.20389.

177. Théry C, Ostrowski M, Segura E. Membrane vesicles as conveyors of immune responses. Nat Rev Immunol. 2009;9:581–93.

178. Coleman BM, Hanssen E, Lawson VA, Hill AF. Prion-infected cells regulate the release of exosomes with distinct ultrastructural features. FASEB J Off Publ Fed Am Soc Exp Biol. 2012;26:4160–73.

179. Fang Y, Wu N, Gan X, Yan W, Morrell JC, Gould SJ. Higher-order oligomerization targets plasma membrane proteins and HIV gag to exosomes. PLoS Biol. 2007;5:e158.

180. Soekmadji C, Russell PJ, Nelson CC. Exosomes in prostate cancer: putting together the pieces of a puzzle. Cancers. 2013;5:1522–44.

181. Dragovic RA, Gardiner C, Brooks AS, Tannetta DS, Ferguson DJP, Hole P, et al. Sizing and phenotyping of cellular vesicles using Nanoparticle Tracking Analysis. Nanomed. 2011;7:780–8.

182. Van der Pol E, Böing AN, Harrison P, Sturk A, Nieuwland R. Classification, functions, and clinical relevance of extracellular vesicles. Pharmacol Rev. 2012;64:676–705.

183. Gyorgy B, Szabo TG, Pasztoi M, Pal Z, Misjak P, Aradi B, et al. Membrane vesicles, current state-of-the-art: emerging role of extracellular vesicles. Cell Mol Life Sci. 2011;68:2667–88.

184. Choi D-S, Kim D-K, Kim Y-K, Gho YS. Proteomics, transcriptomics, and lipidomics of exosomes and ectosomes. PROTEOMICS. 2013;13(10-11):1554–71.

185. Michael A, Bajracharya SD, Yuen PST, Zhou H, Star RA, Illei GG, et al. Exosomes from Human Saliva as a Source of microRNA Biomarkers. Oral Dis. 2010;16:34–8.

186. Graner MW, Alzate O, Dechkovskaia AM, Keene JD, Sampson JH, Mitchell DA, et al. Proteomic and immunologic analyses of brain tumor exosomes. FASEB J Off Publ Fed Am Soc Exp Biol. 2009;23:1541–57.

187. Andre F, Schartz NEC, Movassagh M, Flament C, Pautier P, Morice P, et al. Malignant effusions and immunogenic tumour-derived exosomes. Lancet. 2002;360:295–305.

188. Valadi H, Ekström K, Bossios A, Sjöstrand M, Lee JJ, Lötvall JO. Exosome-mediated transfer of mRNAs and microRNAs is a novel mechanism of genetic exchange between cells. Nat Cell Biol. 2007;9:654–9.

189. Montecalvo A, Larregina AT, Shufesky WJ, Beer Stolz D, Sullivan MLG, Karlsson JM, et al. Mechanism of transfer of functional microRNAs between mouse dendritic cells via exosomes. Blood. 2012;119:756–66.

190. Hessvik NP, Sandvig K, Llorente A. Exosomal miRNAs as Biomarkers for Prostate Cancer. Front Genet. 2013;4:36.

191. Kharaziha P, Ceder S, Li Q, Panaretakis T. Tumor cell-derived exosomes: A message in a bottle. Biochim Biophys Acta. 2012;1826:103–11.

192. Pant S, Hilton H, Burczynski ME. The multifaceted exosome: biogenesis, role in normal and aberrant cellular function, and frontiers for pharmacological and biomarker opportunities. Biochem Pharmacol. 2012;83:1484–94.

193. Van Niel G, Porto-Carreiro I, Simoes S, Raposo G. Exosomes: a common pathway for a specialized function. J Biochem (Tokyo). 2006;140:13–21.

194. Edgar JR, Eden ER, Futter CE. Hrs- and CD63-dependent competing mechanisms make different sized endosomal intraluminal vesicles. Traffic Cph Den. 2014;15:197–211.

195. Henne WM, Buchkovich NJ, Emr SD. The ESCRT pathway. Dev Cell. 2011;21:77–91.

196. Stuffers S, Sem Wegner C, Stenmark H, Brech A. Multivesicular endosome biogenesis in the absence of ESCRTs. Traffic Cph Den. 2009;10:925–37.

197. Van Niel G, Charrin S, Simoes S, Romao M, Rochin L, Saftig P, et al. The tetraspanin CD63 regulates ESCRT-independent and -dependent endosomal sorting during melanogenesis. Dev Cell. 2011;21:708–21.

198. De Gassart A, Geminard C, Fevrier B, Raposo G, Vidal M. Lipid raft-associated protein sorting in exosomes. Blood. 2003;102:4336–44.

199. Trajkovic K, Hsu C, Chiantia S, Rajendran L, Wenzel D, Wieland F, et al. Ceramide triggers budding of exosome vesicles into multivesicular endosomes. Science. 2008;319:1244–7.

200. Villarroya-Beltri C, Baixauli F, Gutiérrez-Vázquez C, Sánchez-Madrid F, Mittelbrunn M. Sorting it out: Regulation of exosome loading. Semin Cancer Biol. 2014;doi: 10.1016/j.semcancer.2014.04.009. [Epub ahead of print].

201. Simons M, Raposo G. Exosomes--vesicular carriers for intercellular communication. Curr Opin Cell Biol. 2009;21:575–81.

202. Ostrowski M, Carmo NB, Krumeich S, Fanget I, Raposo G, Savina A, et al. Rab27a and Rab27b control different steps of the exosome secretion pathway. Nat Cell Biol. 2010;12:19–30; sup pp 1–13.

203. Corrado C, Raimondo S, Chiesi A, Ciccia F, De Leo G, Alessandro R. Exosomes as Intercellular Signaling Organelles Involved in Health and Disease: Basic Science and Clinical Applications. Int J Mol Sci. 2013;14:5338–66.

204. Vlassov AV, Magdaleno S, Setterquist R, Conrad R. Exosomes: current knowledge of their composition, biological functions, and diagnostic and therapeutic potentials. Biochim Biophys Acta. 2012;1820:940–8.

205. Lakkaraju A, Rodriguez-Boulan E. Itinerant exosomes: emerging roles in cell and tissue polarity. Trends Cell Biol. 2008;18:199–209.

206. Azmi AS, Bao B, Sarkar FH. Exosomes in cancer development, metastasis, and drug resistance: a comprehensive review. Cancer Metastasis Rev. 2013;32:623–42.

207. Qu J-L, Qu X-J, Zhao M-F, Teng Y-E, Zhang Y, Hou K-Z, et al. Gastric cancer exosomes promote tumour cell proliferation through PI3K/Akt and MAPK/ERK activation. Dig Liver Dis Off J Ital Soc Gastroenterol Ital Assoc Study Liver. 2009;41:875–80.

208. Peinado H, Lavotshkin S, Lyden D. The secreted factors responsible for pre-metastatic niche formation: old sayings and new thoughts. Semin Cancer Biol. 2011;21:139–46.

209. Cvjetkovic A, Lotvall J, Lasser C. The influence of rotor type and centrifugation time on the yield and purity of extracellular vesicles. J Extracell Vesicles. 2014;3:10.3402/jev.v3.23111.

210. Alvarez ML, Khosroheidari M, Ravi RK, DiStefano JK. Comparison of protein, microRNA, and mRNA yields using different methods of urinary exosome isolation for the discovery of kidney disease biomarkers. Kidney Int. 2012;82:1024–32.

211. Tauro BJ, Greening DW, Mathias RA, Ji H, Mathivanan S, Scott AM, et al. Comparison of ultracentrifugation, density gradient separation, and immunoaffinity capture methods for isolating human colon cancer cell line LIM1863-derived exosomes. Methods San Diego Calif. 2012;56:293–304.

212. Taylor DD, Zacharias W, Gercel-Taylor C. Exosome isolation for proteomic analyses and RNA profiling. Methods Mol Biol Clifton NJ. 2011;728:235–46.

213. Grant R, Ansa-Addo E, Stratton D, Antwi-Baffour S, Jorfi S, Kholia S, et al. A filtration-based protocol to isolate human plasma membrane-derived vesicles and exosomes from blood plasma. J Immunol Methods. 2011;371:143–51.

214. Fernández-Llama P, Khositseth S, Gonzales PA, Star RA, Pisitkun T, Knepper MA. Tamm-Horsfall protein and urinary exosome isolation. Kidney Int. 2010;77:736–42.

215. Chen CY, Hogan MC, Ward CJ. Purification of exosome-like vesicles from urine. Methods Enzymol. 2013;524:225–41.

216. Duijvesz D, Luider T, Bangma CH, Jenster G. Exosomes as biomarker treasure chests for prostate cancer. Eur Urol. 2011;59:823–31.

217. Anderson NL, Anderson NG. The human plasma proteome: history, character, and diagnostic prospects. Mol Cell Proteomics MCP. 2002;1:845–67.

218. Edwards JJ, Tollaksen SL, Anderson NG. Proteins of human urine. III. Identification and two-dimensional electrophoretic map positions of some major urinary proteins. Clin Chem. 1982;28:941–8.

219. Castagna A, Cecconi D, Sennels L, Rappsilber J, Guerrier L, Fortis F, et al. Exploring the hidden human urinary proteome via ligand library beads. J Proteome Res. 2005;4:1917–30.

220. Giusti I, Dolo V. Extracellular Vesicles in Prostate Cancer: New Future Clinical Strategies? BioMed Res Int. 2014;2014:561571.

221. Keller S, Sanderson MP, Stoeck A, Altevogt P. Exosomes: from biogenesis and secretion to biological function. Immunol Lett. 2006;107:102–8.

222. Zhou H, Yuen PST, Pisitkun T, Gonzales PA, Yasuda H, Dear JW, et al. Collection, storage, preservation, and normalization of human urinary exosomes for biomarker discovery. Kidney Int. 2006;69:1471–6.

223. Decramer S, Gonzalez de Peredo A, Breuil B, Mischak H, Monsarrat B, Bascands J-L, et al. Urine in clinical proteomics. Mol Cell Proteomics MCP. 2008;7:1850–62.

224. Li J, Sherman-Baust CA, Tsai-Turton M, Bristow RE, Roden RB, Morin PJ. Claudin-containing exosomes in the peripheral circulation of women with ovarian cancer. BMC Cancer. 2009;9:244.

225. Skog J, Wurdinger T, van Rijn S, Meijer D, Gainche L, Sena-Esteves M, et al. Glioblastoma microvesicles transport RNA and protein that promote tumor growth and provide diagnostic biomarkers. Nat Cell Biol. 2008;10:1470–6.

226. Tesselaar MET, Romijn FPHTM, Van Der Linden IK, Prins FA, Bertina RM, Osanto S. Microparticle-associated tissue factor activity: a link between cancer and thrombosis? J Thromb Haemost JTH. 2007;5:520–7.

227. Perez A, Loizaga A, Arceo R, Lacasa I, Rabade A, Zorroza K, et al. A Pilot Study on the Potential of RNA-Associated to Urinary Vesicles as a Suitable Non-Invasive Source for Diagnostic Purposes in Bladder Cancer. Cancers. 2014;6:179–92.

228. Raimondo F, Morosi L, Corbetta S, Chinello C, Brambilla P, Della Mina P, et al. Differential protein profiling of renal cell carcinoma urinary exosomes. Mol Biosyst. 2013;9:1220–33.

229. Jansen FH, Krijgsveld J, van Rijswijk A, van den Bemd G-J, van den Berg MS, van Weerden WM, et al. Exosomal Secretion of Cytoplasmic Prostate Cancer Xenograft-derived Proteins. Mol Cell Proteomics MCP. 2009;8:1192–205.

230. Nilsson J, Skog J, Nordstrand A, Baranov V, Mincheva-Nilsson L, Breakefield XO, et al. Prostate cancer-derived urine exosomes: a novel approach to biomarkers for prostate cancer. Br J Cancer. 2009;100:1603–7.

231. Bijnsdorp IV, Geldof AA, Lavaei M, Piersma SR, van Moorselaar RJA, Jimenez CR. Exosomal ITGA3 interferes with non-cancerous prostate cell functions and is increased in urine exosomes of metastatic prostate cancer patients. J Extracell Vesicles. 2013;2:10.3402/jev.v2i0.22097.

232. Duijvesz D, Burnum-Johnson KE, Gritsenko MA, Hoogland AM, Vredenbregt-van den Berg MS, Willemsen R, et al. Proteomic profiling of exosomes leads to the identification of novel biomarkers for prostate cancer. PloS One. 2013;8:e82589.

233. Mitchell PJ, Welton J, Staffurth J, Court J, Mason MD, Tabi Z, et al. Can urinary exosomes act as treatment response markers in prostate cancer? J Transl Med. 2009;7:4.

234. Principe S, Jones EE, Kim Y, Sinha A, Nyalwidhe JO, Brooks J, et al. In-depth proteomic analyses of exosomes isolated from expressed prostatic secretions in urine. Proteomics. 2013;13(10-11):1667–71.

235. Inuzuka T, Inokawa A, Chen C, Kizu K, Narita H, Shibata H, et al. ALG-2-interacting Tubby-like protein superfamily member PLSCR3 is secreted by an exosomal pathway and taken up by recipient cultured cells. Biosci Rep. 2013;33:e00026.

236. Takagi J, Petre BM, Walz T, Springer TA. Global conformational rearrangements in integrin extracellular domains in outside-in and inside-out signaling. Cell. 2002;110:599–511.

237. Manza LL, Stamer SL, Ham A-JL, Codreanu SG, Liebler DC. Sample preparation and digestion for proteomic analyses using spin filters. Proteomics. 2005;5:1742–5.

238. Oliveros J. VENNY. An interactive tool for comparing lists with Venn Diagrams. http://bioinfogp.cnb.csic.es/tools/venny/index.html; 2007.

239. Clough T, Thaminy S, Ragg S, Aebersold R, Vitek O. Statistical protein quantification and significance analysis in label-free LC-MS experiments with complex designs. BMC Bioinformatics. 2012;13:S6.

240. Chambers MC, Maclean B, Burke R, Amodei D, Ruderman DL, Neumann S, et al. A cross-platform toolkit for mass spectrometry and proteomics. Nat Biotechnol. 2012;30:918–20.

241. Choi H, Nesvizhskii AI. Semisupervised model-based validation of peptide identifications in mass spectrometry-based proteomics. J Proteome Res. 2008;7:254–65.

242. Nahnsen S, Bielow C, Reinert K, Kohlbacher O. Tools for label-free peptide quantification. Mol Cell Proteomics MCP. 2013;12:549–56.

243. Taverner T, Karpievitch YV, Polpitiya AD, Brown JN, Dabney AR, Anderson GA, et al. DanteR: an extensible R-based tool for quantitative analysis of -omics data. Bioinforma Oxf Engl. 2012;28:2404–6.

244. Karpievitch Y, Stanley J, Taverner T, Huang J, Adkins JN, Ansong C, et al. A statistical framework for protein quantitation in bottom-up MS-based proteomics. Bioinforma Oxf Engl. 2009;25:2028–34.

245. Hochberg Y, Benjamini Y. More powerful procedures for multiple significance testing. Stat Med. 1990;9:811–8.

246. Schilling B, Rardin MJ, MacLean BX, Zawadzka AM, Frewen BE, Cusack MP, et al. Platform-independent and label-free quantitation of proteomic data using MS1 extracted ion chromatograms in skyline: application to protein acetylation and phosphorylation. Mol Cell Proteomics MCP. 2012;11:202–14.

247. Choi M, Chang C-Y, Clough T, Broudy D, Killeen T, MacLean B, et al. MSstats: an R package for statistical analysis of quantitative mass spectrometry-based proteomic experiments. Bioinforma Oxf Engl. 2014;pii.

248. Livak KJ, Schmittgen TD. Analysis of relative gene expression data using real-time quantitative PCR and the 2(-Delta Delta C(T)) Method. Methods. 2001;25:402–8.

249. Kılıç Y, Çelebiler AÇ, Sakızlı M. Selecting housekeeping genes as references for the normalization of quantitative PCR data in breast cancer. Clin Transl Oncol Off Publ Fed Span Oncol Soc Natl Cancer Inst Mex. 2014;16:184–90.

250. Boulesteix AL. WilcoxCV: an R package for fast variable selection in cross-validation. Bioinformatics. 2007;23:1702–4.

251. Slawski M, Daumer M, Boulesteix AL. CMA: a comprehensive Bioconductor package for supervised classification with high dimensional data. BMC Bioinformatics. 2008;9:439.

252. Akaike H. A new look at the statistical model identification. IEEE Trans Autom Control. 1974;19:716–23.

253. Venables WN, Ripley BD. Modern Applied Statistics with S. Springer; 2002.

254. R Development Core Team. R: A language and environment for statistical computing. [Internet]. Vienna, Austria: R Foundation for Statistical Computing; 2013. Available from: http://www.R-project.org

255. Hsu S-D, Tseng Y-T, Shrestha S, Lin Y-L, Khaleel A, Chou C-H, et al. miRTarBase update 2014: an information resource for experimentally validated miRNA-target interactions. Nucleic Acids Res. 2014;42:D78–85.

256. Franceschini A, Szklarczyk D, Frankild S, Kuhn M, Simonovic M, Roth A, et al. STRING v9.1: protein-protein interaction networks, with increased coverage and integration. Nucleic Acids Res. 2013;41:D808–815.

257. Jenjaroenpun P, Kremenska Y, Nair VM, Kremenskoy M, Joseph B, Kurochkin IV. Characterization of RNA in exosomes secreted by human breast cancer cell lines using next-generation sequencing. PeerJ. 2013;1:e201.

258. Gonzales PA, Pisitkun T, Hoffert JD, Tchapyjnikov D, Star RA, Kleta R, et al. Large-Scale Proteomics and Phosphoproteomics of Urinary Exosomes. J Am Soc Nephrol JASN. 2009;20:363–79.

259. Loeb S. Guideline of Guidelines: Prostate Cancer Screening. BJU Int. 2014;doi: 10.1111/bju.12854. [Epub ahead of print].

260. Makovey I, Stephenson AJ, Haywood S. Response to the U.S. Preventative Services Task Force decision on prostate cancer screening. Curr Urol Rep. 2013;14:168–73.

261. Brand TC, Thibault GP, Basler JW. Dealing with non-cancerous findings on prostate biopsy. Curr Urol Rep. 2006;7:186–92.

262. Montironi R, Mazzucchelli R, Lopez-Beltran A, Scarpelli M, Cheng L. Prostatic intraepithelial neoplasia: its morphological and molecular diagnosis and clinical significance. BJU Int. 2011;108:1394–401.

263. Descazeaud A, Rubin MA, Allory Y, Burchardt M, Salomon L, Chopin D, et al. What information are urologists extracting from prostate needle biopsy reports and what do they need for clinical management of prostate cancer? Eur Urol. 2005;48:911–5.

264. Hessels D, Schalken JA. The use of PCA3 in the diagnosis of prostate cancer. Nat Rev Urol. 2009;6:255–61.

265. Wood SL, Knowles MA, Thompson D, Selby PJ, Banks RE. Proteomic studies of urinary biomarkers for prostate, bladder and kidney cancers. Nat Rev Urol. 2013;10:206–18.

266. Moon P-G, You S, Lee J-E, Hwang D, Baek M-C. Urinary exosomes and proteomics. Mass Spectrom Rev. 2011;30:1185–202.

267. Principe S, Kim Y, Fontana S, Ignatchenko V, Nyalwidhe JO, Lance RS, et al. Identification of prostate-enriched proteins by in-depth proteomic analyses of expressed prostatic secretions in urine. J Proteome Res. 2012;11:2386–96.

268. Bologna M, Vicentini C, Festuccia C, Muzi P, Napolitano T, Biordi L, et al. Early diagnosis of prostatic carcinoma based on in vitro culture of viable tumor cells harvested by prostatic massage. Eur Urol. 1988;14:474–6.

269. Garret M, Jassie M. Cytologic examination of post prostatic massage specimens as an aid in diagnosis of carcinoma of the prostate. Acta Cytol. 1976;20:126–31.

270. Dijkstra S, Birker IL, Smit FP, Leyten GHJM, de Reijke TM, van Oort IM, et al. Prostate Cancer Biomarker Profiles in Urinary Sediments and Exosomes. J Urol. 2013;191(4):1132–8.

271. Gabriel K, Ingram A, Austin R, Kapoor A, Tang D, Majeed F, et al. Regulation of the Tumor Suppressor PTEN through Exosomes: A Diagnostic Potential for Prostate Cancer. PLoS ONE. 2013;8:e70047.

272. Lu J, Getz G, Miska EA, Alvarez-Saavedra E, Lamb J, Peck D, et al. MicroRNA expression profiles classify human cancers. Nature. 2005;435:834–8.

273. Neilson KA, Ali NA, Muralidharan S, Mirzaei M, Mariani M, Assadourian G, et al. Less label, more free: approaches in label-free quantitative mass spectrometry. Proteomics. 2011;11:535–53.

274. Rabinowits G, Gerçel-Taylor C, Day JM, Taylor DD, Kloecker GH. Exosomal microRNA: a diagnostic marker for lung cancer. Clin Lung Cancer. 2009;10:42–6.

275. Silva J, Garcia V, Rodriguez M, Compte M, Cisneros E, Veguillas P, et al. Analysis of exosome release and its prognostic value in human colorectal cancer. Genes Chromosomes Cancer. 2012;51:409–18.

276. Bolduc S, Lacombe L, Naud A, Grégoire M, Fradet Y, Tremblay RR. Urinary PSA: a potential useful marker when serum PSA is between 2.5 ng/mL and 10 ng/mL. Can Urol Assoc J J Assoc Urol Can. 2007;1:377–81.

277. Megger DA, Bracht T, Meyer HE, Sitek B. Label-Free Quantification in Clinical Proteomics. Biochim Biophys Acta. 2013;1834(8):1581–90.

278. Dumitrescu Pene T, Rosé SD, Lejen T, Marcu MG, Trifaró J-M. Expression of various scinderin domains in chromaffin cells indicates that this protein acts as a molecular switch in the control of actin filament dynamics and exocytosis. J Neurochem. 2005;92:780–9.

279. Trifaró JM. Scinderin and cortical F-actin are components of the secretory machinery. Can J Physiol Pharmacol. 1999;77:660–71.

280. Wang D, Sun S-Q, Yu Y-H, Wu W-Z, Yang S-L, Tan J-M. Suppression of SCIN inhibits human prostate cancer cell proliferation and induces G0/G1 phase arrest. Int J Oncol. 2014;44:161–6.

281. Dubbink HJ, de Waal L, van Haperen R, Verkaik NS, Trapman J, Romijn JC. The human prostate-specific transglutaminase gene (TGM4): genomic organization, tissue-specific expression, and promoter characterization. Genomics. 1998;51:434–44.

282. Shaikhibrahim Z, Lindstrot A, Buettner R, Wernert N. Analysis of laser-microdissected prostate cancer tissues reveals potential tumor markers. Int J Mol Med. 2011;28:605–11.

283. Oka K, Suzuki T, Onodera Y, Miki Y, Takagi K, Nagasaki S, et al. Nudix-type motif 2 in human breast carcinoma: a potent prognostic factor associated with cell proliferation. Int J Cancer J Int Cancer. 2011;128:1770–82.

284. Nakamura I, Duong LT, Rodan SB, Rodan GA. Involvement of alpha(v)beta3 integrins in osteoclast function. J Bone Miner Metab. 2007;25:337–44.

285. Brakebusch C, Bouvard D, Stanchi F, Sakai T, Fassler R. Integrins in invasive growth. J Clin Invest. 2002;109:999–1006.

286. Robinson SD, Hodivala-Dilke KM. The role of β3-integrins in tumor angiogenesis: context is everything. Curr Opin Cell Biol. 2011;23:630–7.

287. Zheng D-Q, Woodard AS, Fornaro M, Tallini G, Languino LR. Prostatic Carcinoma Cell Migration via αvβ3Integrin Is Modulated by a Focal Adhesion Kinase Pathway. Cancer Res. 1999;59:1655–64.

288. McCabe NP, De S, Vasanji A, Brainard J, Byzova TV. Prostate cancer specific integrin αvβ3 modulates bone metastatic growth and tissue remodeling. Oncogene. 2007;26:6238–43.

289. Pols MS, Klumperman J. Trafficking and function of the tetraspanin CD63. Exp Cell Res. 2009;315:1584–92.

290. Salih M, Zietse R, Hoorn EJ. Urinary extracellular vesicles and the kidney: biomarkers and beyond. Am J Physiol Renal Physiol. 2014;306:F1251–1259.

291. Ralla B, Stephan C, Meller S, Dietrich D, Kristiansen G, Jung K. Nucleic acid-based biomarkers in body fluids of patients with urologic malignancies. Crit Rev Clin Lab Sci. 2014;1–32.

292. Varambally S, Laxman B, Mehra R, Cao Q, Dhanasekaran SM, Tomlins SA, et al. Golgi protein GOLM1 is a tissue and urine biomarker of prostate cancer. Neoplasia N Y N. 2008;10:1285–94.

293. Fernández S, Mosquera JL, Alaña L, Sanchez-Pla A, Morote J, Ramón Y Cajal S, et al. PTOV1 is overexpressed in human high-grade malignant tumors. Virchows Arch Int J Pathol. 2011;458:323–30.

294. Gravdal K, Halvorsen OJ, Haukaas SA, Akslen LA. A switch from E-cadherin to N-cadherin expression indicates epithelial to mesenchymal transition and is of strong and independent importance for the progress of prostate cancer. Clin Cancer Res Off J Am Assoc Cancer Res. 2007;13:7003–11.

295. Bertilsson H, Tessem M-B, Flatberg A, Viset T, Gribbestad I, Angelsen A, et al. Changes in gene transcription underlying the aberrant citrate and choline metabolism in human prostate cancer samples. Clin Cancer Res Off J Am Assoc Cancer Res. 2012;18:3261–9.

296. Tidehag V, Hammarsten P, Egevad L, Granfors T, Stattin P, Leanderson T, et al. High density of S100A9 positive inflammatory cells in prostate cancer stroma is associated with poor outcome. Eur J Cancer Oxf Engl 1990. 2014;50:1829–35.

297. Lee S, Desai KK, Iczkowski KA, Newcomer RG, Wu KJ, Zhao Y-G, et al. Coordinated peak expression of MMP-26 and TIMP-4 in preinvasive human prostate tumor. Cell Res. 2006;16:750–8.

298. Harma V, Virtanen J, Makela R, Happonen A, Mpindi J-P, Knuuttila M, et al. A Comprehensive Panel of Three-Dimensional Models for Studies of Prostate Cancer Growth, Invasion and Drug Responses. PLoS ONE. 2010;5:e10431.

299. Barbera M, Pepe P, Paola Q, Aragona F. PCA3 score accuracy in diagnosing prostate cancer at repeat biopsy: our experience in 177 patients. Arch Ital Urol Androl Organo Uff Soc Ital Ecogr Urol E Nefrol Assoc Ric Urol. 2012;84:227–9.

300. Etzioni R, Kooperberg C, Pepe M, Smith R, Gann PH. Combining biomarkers to detect disease with application to prostate cancer. Biostat Oxf Engl. 2003;4:523–38.

301. Yacoub JH, Verma S, Moulton JS, Eggener S, Aytekin O. Imaging-guided prostate biopsy: conventional and emerging techniques. Radiogr Rev Publ Radiol Soc N Am Inc. 2012;32:819–37.

302. Loeb S, Catalona WJ. The Prostate Health Index: a new test for the detection of prostate cancer. Ther Adv Urol. 2014;6:74–7.

303. Catalona WJ, Partin AW, Sanda MG, Wei JT, Klee GG, Bangma CH, et al. A multicenter study of [-2]pro-prostate specific antigen combined with prostate specific antigen and free prostate specific antigen for prostate cancer detection in the 2.0 to 10.0 ng/ml prostate specific antigen range. J Urol. 2011;185:1650–5.

304. Ferro M, Bruzzese D, Perdonà S, Marino A, Mazzarella C, Perruolo G, et al. Prostate Health Index (Phi) and Prostate Cancer Antigen 3 (PCA3) significantly improve prostate cancer detection at initial biopsy in a total PSA range of 2-10 ng/ml. PloS One. 2013;8:e67687.

305. Lughezzani G, Lazzeri M, Haese A, McNicholas T, de la Taille A, Buffi NM, et al. Multicenter European External Validation of a Prostate Health Index-based Nomogram for Predicting Prostate Cancer at Extended Biopsy. Eur Urol. 2013;doi: 10.1016/j.eururo.2013.12.005. [Epub ahead of print].

306. Scattoni V, Lazzeri M, Lughezzani G, De Luca S, Passera R, Bollito E, et al. Head-to-head comparison of prostate health index and urinary PCA3 for predicting cancer at initial or repeat biopsy. J Urol. 2013;190:496–501.

307. Stephan C, Vincendeau S, Houlgatte A, Cammann H, Jung K, Semjonow A. Multicenter Evaluation of [–2]Proprostate-Specific Antigen and the Prostate Health Index for Detecting Prostate Cancer. Clin Chem. 2013;59:306–14.

308. Stephan C, Jung K, Semjonow A, Schulze-Forster K, Cammann H, Hu X, et al. Comparative assessment of urinary prostate cancer antigen 3 and TMPRSS2:ERG gene fusion with the serum [-2]proprostate-specific antigen-based prostate health index for detection of prostate cancer. Clin Chem. 2013;59:280–8.

309. Porpiglia F, Russo F, Manfredi M, Mele F, Fiori C, Bollito E, et al. The Roles of Multiparametric Magnetic Resonance Imaging, PCA3 and Prostate Health Index-Which is the Best Predictor of Prostate Cancer after a Negative Biopsy? J Urol. 2014;60–6.

ANNEX

Annex I. Supplementary data for Objective 2

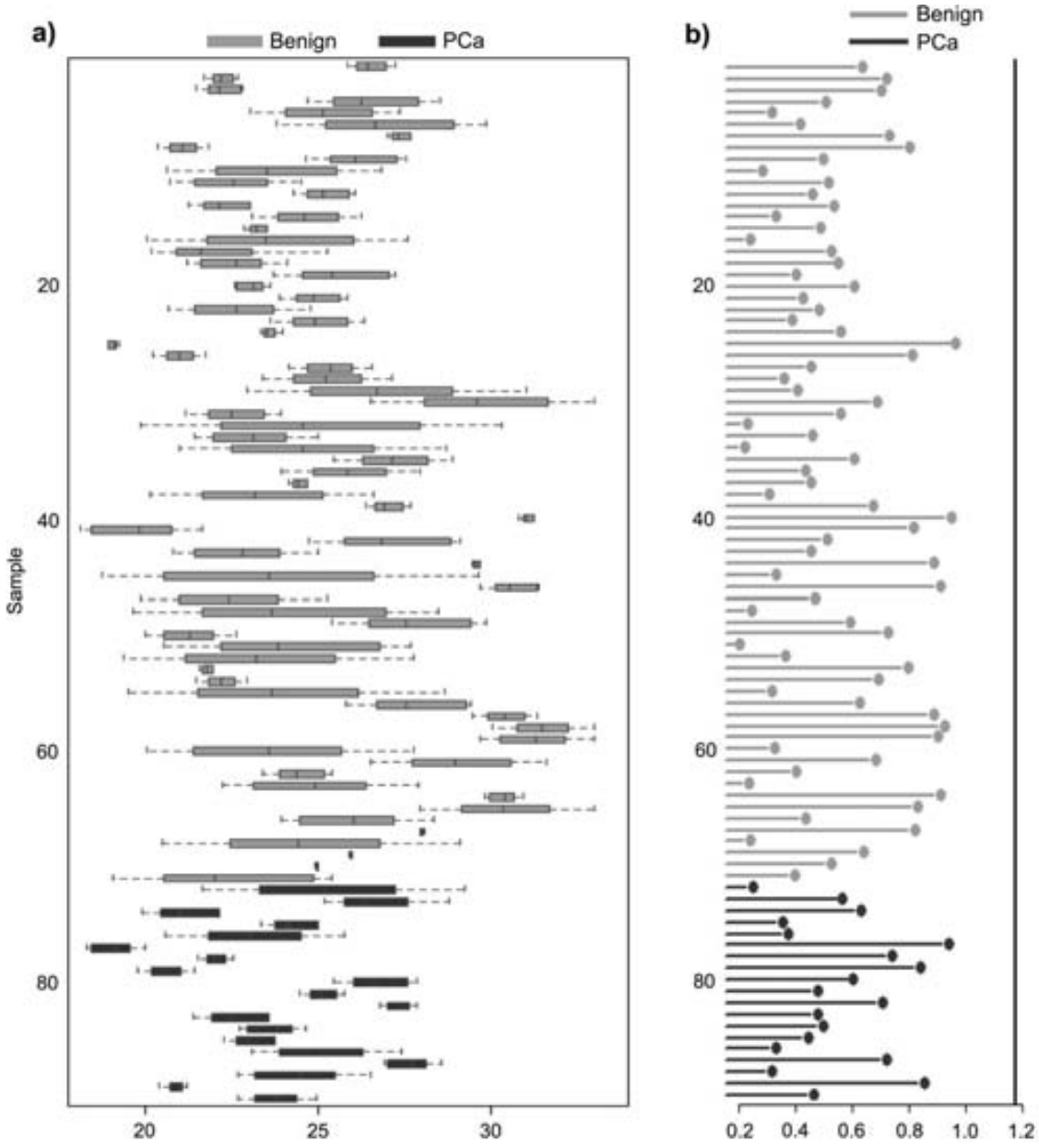

Supplementary Figure 1. Outliers detection for the 90 urine sediment samples. (a) Boxplots representing summaries of the signal intensity distributions of the samples. Typically, boxes are expected to have similar positions and widths. If the distribution of a sample is very different from the others, this may indicate an experimental problem. Outlier detection was performed by computing the Kolmogorov-Smirnov statistic Ka between each sample"s distribution and the distribution of the pooled data. **(b)** Bar chart of the Kolmogorov-Smirnov statistic Ka, the outlier detection criterion from (a). Based on the distribution of the values across all samples, a threshold of 1.18 was determined, which is indicated by the vertical line in the right. None of the arrays exceeded the threshold and was considered an outlier.

Supplementary Table 1. Parameters calculated for all 36 multiplex models in predicting PCa in patients referred for a repeat PB due to a previous diagnosis of HGPIN.

Model	AUC	PPV	NPV	Specificity			Estimated TRUS-PB avoided
				Sens. 100%	Sens. 95%	Sens. 90%	
KLK3 + *PSMA* (Iso. 1, 2, 3, 4, 5) + *PSMA* (Iso. 1, 2, 3, 4) + *PSGR* + *CDH1*	0,86	31%	97%	28%	44%	70%	36%
KLK3 + *PSMA* (Iso. 1, 2, 3, 4, 5) + *PSMA* (Iso. 3, 4) + *PSMA* (Iso. 1, 2, 3, 4) + *PSGR* + *CDH1*	0,88	49%	98%	28%	73%	73%	59%
KLK3 + *PSMA* (Iso. 1, 2, 3, 4, 5) + *PSMA* (Iso. 1, 2, 3, 4) + *PSGR*	0,85	42%	98%	28%	65%	68%	52%
KLK3 + *PSMA* (Iso. 1, 2, 3, 4, 5) + *PSMA* (Iso. 3, 4) + *PSGR* + *CDH1*	0,85	36%	98%	32%	55%	58%	44%
KLK3 + *PSMA* (Iso. 3, 4) + *PSMA* (Iso. 1, 3, 5) + *PSGR* + *CDH1*	0,85	38%	98%	38%	58%	59%	48%
KLK3 + *PSMA* (Iso. 3, 4) + *PSMA* (Iso. 1, 3, 5) + *PSGR* + *GOLM1*	0,84	37%	98%	37%	56%	56%	45%
KLK3 + *PSMA* (Iso. 3, 4) + *PSMA* (ISO. 1, 3, 5) + *PSGR*	0,84	32%	97%	38%	47%	63%	38%
KLK3 + *PSGR* + *CDH1*	0,81	29%	96%	32%	37%	41%	30%
KLK3 + *PSMA* (Iso. 3, 4) + *PSGR* + *CDH1*	0,84	30%	97%	34%	41%	48%	33%
KLK3 + *PSMA* (Iso. 3, 4) + *PSGR*	0,82	30%	97%	37%	39%	39%	32%
KLK3 + *PSMA* (Iso. 1, 2, 3, 4) + *PSMA* (Iso. 1, 3, 5) + *PSGR*	0,82	29%	96%	27%	37%	70%	30%
KLK3 + *PSGR*	0,80	31%	97%	38%	42%	42%	34%
PSMA (Iso. 1, 2, 3, 4, 5) + *PSMA* (Iso. 3, 4) + *PSGR* + *CDH1*	0,82	39%	98%	25%	61%	62%	49%
PSMA (Iso. 1, 2, 3, 4, 5) + *PSMA* (Iso. 1, 2, 3, 4) + *PSGR* + *CDH1*	0,81	26%	95%	20%	28%	56%	23%
PSMA (Iso. 1, 3, 5) + *PSGR* + *CDH1*	0,80	28%	96%	6%	34%	47%	28%
PSMA (Iso. 1, 2, 3, 4, 5) + *PSGR* + *CDH1*	0,79	26%	95%	16%	28%	50%	23%
PSGR + *CDH1*	0,78	26%	95%	24%	28%	48%	23%
PSMA (Iso. 1, 3, 5) + *PSGR*	0,77	29%	97%	11%	38%	61%	31%
PSMA (Iso. 1, 2, 3, 4, 5) + *PSMA* (Iso. 1, 2, 3, 4) + *PSMA* (Iso. 1, 3, 5) + *PSGR*	0,80	28%	96%	18%	34%	52%	28%
PSMA (Iso. 3, 4) + *PSMA* (Iso. 1, 3, 5) + *GOLM1* + *CDH1*	0,80	29%	96%	34%	37%	54%	30%
PSMA (Iso. 3, 4) + *PSMA* (Iso. 1, 3, 5) + *PSGR* + *GOLM1*	0,81	31%	97%	37%	42%	59%	34%
KLK3 + *PSMA* (Iso. 3, 4) + *GOLM1* + *CDH1*	0,81	29%	96%	34%	37%	41%	30%
GOLM1 + *CDH1*	0,77	27%	96%	32%	32%	39%	27%

PSMA (Iso. 1, 3, 5) + *PSGR* + *GOLM1*	0,78	29%	97%	38%	38%	38%	31%
PSMA (Iso. 1, 2, 3, 4, 5) + *PSMA* (Iso. 1, 2, 3, 4) + *PSMA* (Iso. 1, 3, 5) + *PSGR* + *GOLM1*	0,81	36%	98%	32%	55%	58%	44%
PSMA (Iso. 3, 4) + *PSMA* (Iso. 1, 3, 5) + *PCA3* + *CDH1*	0,81	31%	97%	31%	44%	66%	36%
PSMA (Iso. 1, 2, 3, 4, 5) + *PSGR*	0,76	27%	96%	24%	30%	54%	24%
PSMA (Iso. 1, 2, 3, 4, 5) + *PSMA* (Iso. 1, 2, 3, 4) + *GOLM1* + *CDH1*	0,79	31%	97%	23%	42%	56%	34%
KLK3 + *PSMA* (Iso. 3, 4) + *PCA3* + *CDH1*	0,81	30%	97%	35%	39%	48%	32%
PSMA (Iso. 1, 2, 3, 4, 5) + *PSMA* (Iso. 3, 4) + *PCA3* + *CDH1*	0,79	27%	96%	32%	32%	50%	27%
PSMA (Iso. 1, 2, 3, 4) + *PSMA* (Iso. 1, 3, 5) + *GOLM1* + *CDH1*	0,79	30%	97%	34%	39%	41%	32%
PSMA (Iso. 1, 2, 3, 4) + *PSMA* (Iso. 1, 3, 5) + *GOLM1*	0,77	29%	97%	35%	38%	42%	31%
PSMA (Iso. 3, 4) + *PSMA* (Iso. 1, 3, 5) + *GOLM1*	0,74	29%	97%	31%	38%	42%	31%
PSMA (Iso. 1, 2, 3, 4, 5) + *PSMA* (Iso. 1, 3, 5) + *GOLM1*	0,75	31%	97%	25%	42%	42%	34%
PSMA (Iso. 1, 2, 3, 4) + *PSMA* (Iso. 1, 3, 5)	0,73	29%	97%	27%	38%	38%	31%
PSMA (Iso. 3, 4) + *PSMA* (Iso. 1, 3, 5) + *PCA3*	0,73	26%	95%	24%	27%	31%	22%